Cape Peninsula
University of Technology

The production of hydrogen from the Water Gas Shift Reaction through the use of a Palladium-Silver membrane reactor

By

LIBERTY NTSHUXEKO BALOYI

Dissertation submitted in fulfilment of the requirements for the degree Masters of Technology: Chemical Engineering, in the Faculty of Engineering and Built Environment at the Cape Peninsula University of Technology

Supervisor: Prof T.V. Ojumu
Co-supervisor: Dr B North

Cape Town Campus
Date submitted (January-2016)

DECLARATION

I LIBERTY NTSHUXEKO BALOYI declare that the contents of this dissertation represent my own unaided work, and that the dissertation has not previously been submitted for academic examination towards any qualification. Furthermore, it represents my own opinions and not necessarily those of the Cape Peninsula University of Technology nor those of the Council for Scientific and Industrial Research.

_____ _____

Signed Date

ABSTRACT

The Water Gas Shift (WGS) reaction describes the reaction between carbon monoxide and water vapour to produce carbon monoxide and hydrogen. This work describes the application of a Palladium-Silver (Pd-Ag)-based membrane film reactor, wherein the Pd-Ag film was supported by porous stainless steel (PSS), for the potential replacement of the current multi-stage WGS reaction. The objective of this work was to develop a better understanding of impediments which are relevant to the application of Pd-Ag membrane reactor for the WGSR. The long term behaviour (hydrogen permeability and selectivity) of Pd-Ag membrane under hydrogen exposure was studied, and the use of the Pd-Ag membrane reactor to produce hydrogen through the WGSR was also performed.

A detailed literature review was conducted, based on the information gathered from literature. A Permeability and WGS reaction testing stations was designed and built. A thin (20µm) 77%wtPd-23%wtAg film was purchased from Takanaka Company in Japan. The membrane film was enclosed between two stainless steel plates to form a membrane reactor. The membrane reactor was fitted at the two different testing stations. The permeability of the Pd-Ag film membrane was tested at different temperatures (320°C, 380°C and 430°C). A long term test of the thermal stability of the Pd-Ag membrane under hydrogen exposure was conducted at high temperature (450°C) and low temperature (300°C) for 250 hours. The thermal cyclibility of the Pd-Ag membrane was also conducted under hydrogen and nitrogen exposure. The effect of non-permeating species (CO, N_2, CO_2 and H_2O) was conducted to investigate the effect on hydrogen permeation rate. A Pd-Ag membrane reactor was loaded with Ferrochrome catalyst and tested under different process variables for WGS reaction in pressures of 2 to 8 bars and temperatures of (300 to 450°C) regime. The membrane film was characterised by SEM, EDS and XRD after hydrogen exposure.

The membrane showed infinite selectivity towards hydrogen before defects (cracks and pinholes) developed. The permeability of hydrogen through the Pd-Ag membrane was found to be higher at higher temperatures. Bulk diffusion of hydrogen atoms and surface contamination were found to be the rate limiting steps for hydrogen transportation through the metal membrane. The membrane showed poor thermal cyclibility under hydrogen, as it failed within 10 cycles. The membrane showed unsteady state permeation of Hydrogen permeation at high temperatures (450°C) after 150 hours of continuous operation, after which the selectivity of the membrane declined due to cracks. Steady state hydrogen permeation was observed at low temperatures (300°C). The membrane showed poor durability under different process conditions over time.

The membrane showed the ability to produce high purity hydrogen through the WGS Reaction in the presence of the catalyst. From the WGS reaction testing stations, the

highest conversion of carbon monoxide was 84% with hydrogen recovery of 82% with a steam ratio (CO/H_2O) of 2.5 at gas space velocity of 2530 $h^{-1}.g_{catalsyt}^{-1}$. The membrane has suffered from hydrogen attack due to the hydrogen atoms that interacted with the membrane during the process of desorption and absorption of hydrogen on the membrane surface. SEM results revealed surface defects on the membrane film after hydrogen exposure. Lastly, the XRD results revealed peak shifting, peaks broadening and lattice expansion on the analysed membrane film due to hydrogen atoms which have caused crystal lattice distortion. Therefore, it can be suggested that the membrane failed due to phase transition from α phase to β phase which caused lattice expansion and crystal distortion which caused defects in the membrane and allowed non-permeable species (N_2, CO and CO_2) to pass through the membrane.

ACKNOWLEDGEMENTS

I wish to thank

- Dr Brian North for his endless support and believing in me through my Masters studies
- Prof Tunde Victor Ojumu for his support and making sure that all administrative work is done at the university and his academic input towards my studies
- Prof Bernard Bladergroen for allowing me to work at his lab at the University of the Western Cape and his expertise in the field of membrane science
- David Abrahams for assisting me in assembling the equipment's and building testing stations.

I remain grateful for the opportunity that I was given by the Council for Scientific and Industrial Research (CSIR) for funding my Mtech studies. I am grateful to Dr Mkhulu Mathe and Dr Henrietta Langmi for giving me the opportunity to develop my career and for their encouragement throughout my studies. I would also like to thank the whole Energy Materials team for their (direct and indirect) support.

Table of Contents

LIST OF FIGURES

LIST OF TABLES

GLOSSARY

LIST OF ABBREVIATIONS

BCC	Body Centered Cubic
DoE	Department of Energy
EDS	Energy Dispersive Spectroscopy
FCC	Face Centered Cubic
HTS	High Temperature Shift
HySA	Hydrogen South Africa
IGCC	Integrated Gasification Combined Cycle
LTS	Low Temperature Shift
Pd_{77}-Ag_{23}	77% Palladium weight and 23% Silver weight
PEMFCs	Proton Exchange Membrane Fuel Cells
PGMs	Platinum Group Metals
PSA	Pressure Swing Adsorption
SEM	Scanning Electron Microscopy
SMR	Steam Methane Reforming
WGS	Water Gas Shift
XRD	X-ray diffraction

LIST OF SYMBOLS

Å	Angstrom
A	Surface Area
α	Alpha (first phase for hydrogen hydride)
β	Beta (second phase for hydrogen hydride)
E	Activation Energy
ΔH	Enthalpy

H_{rec}	Hydrogen recovery
J	Hydrogen flux
P_{fee}	Pressure of feed
P_{reje}	Pressure of reject stream
Q	flow rate
R	Universal gas constant
X_{co}	Conversion of Carbon monoxide

CHAPTER ONE

1 INTRODUCTION

1.1.1 Background and motivation

The current use of fossil fuels as a primary source of energy has led to severe environmental impact. According to the US energy information administration report for2015, in 2013, 72% of South African primary energy was derived from coal. The overall energy sector, ranging from household applications, transportation system and industrial plant uses 90% carbon intense material as the energy source (Gallucci *et al*. 2013). The future generation will be facing critical irreversible environmental challenges, such as climate change and global warming. These consequences are the results of human activities such as the use of carbon intense materials like coal, oil and coke as a source of energy. In order to conserve the environment and minimize climate change, major steps should be taken to address these issues, because energy and waste management issues are a global crisis (Basile *et al*. 1996). The demand for cleaner energy sources has increased, because the use of cleaner fuels could also help in a slow atmospheric build-up of carbon dioxide (Abdollahi *et al*. 2012).

Extensive research for alternative energy sources has increased internationally. Within this context, the Department of Energy (DoE) in South Africa initiated a long term program to resolve these energy-related issues, which is called the Integrated Resource Plan (IRP). The goal of the IRP is to create a reliable, resilient electricity supply infrastructure in South Africa whilst reducing the carbon footprint in the energy sector through the use of renewable and environmentally friendly energy resources. The South African Department of Science and Technology (DST) were tasked to evaluate the Hydrogen society in South Africa for the potential adoption of Hydrogen technologies application such as Hydrogen cars. Thereafter, Hydrogen South Africa (HySA) was launched in 2007. The key goals for the HySA program are the production of hydrogen from renewable energy resources and the use of Platinum Group Metals (PGMs) to promote the beneficiation of our mineral resources. South Africa is the largest producer of platinum in the world and holds a large percentage of global reserves. According to the US Geological Survey, South Africa produced 140 000 kg of platinum and 79 000 kg of Palladium in 2010. Value addition to PGMs will benefit the South African mineral industry and will create jobs and wealth in South Africa. This research presented here is fully aligned with HySA's goals, and adds value in this specific scientific research area.

There is various sources of energy that are promising to address the current energy crisis whilst simultaneously dealing with the waste management issues. Wind and solar energy are some of the alternative energy sources that are being proposed for a green economy. However, they have certain drawbacks in terms of availability and applicability. Alternatively, there have been developments in the energy sector attempting to shift toward the cleaner fuels that are less carbon intense or carbon free to generate energy. Figure 1.1 represents the energy consumptions from the early 1990s until 2012.

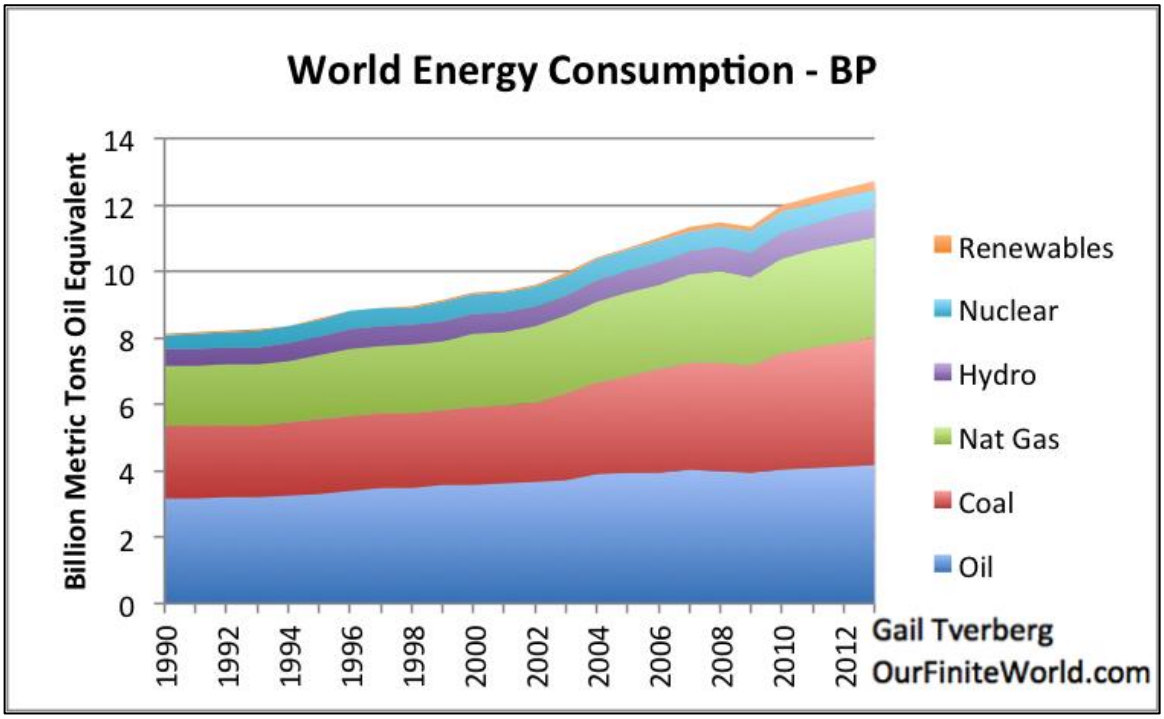

Figure 1.1 World energy consumption

Sourced from (Davidson, 2011)

Figure 1.1 represents world energy consumption from different energy sources since from 1990 until 2012; the data were adapted from the world energy summit report. In 1990, the energy consumption rate of gases has always been high relative to coal. However, the production of energy from gases has been growing until 2012; this is an indication of an evolution in the energy sector: Cleaner fuels renewed interest over from fossil fuels, especially coal, due to their high carbon footprint and they are getting depleted. Countries like China use biogas as a substitute for fossil fuels. The drawback pertaining to biogas is the fact that the initial investment is very expensive. However, Brown *et al*. (2007) argued that the use of biogas is cost effective in the long term**.**

The use of hydrogen has been explored recently. Hydrogen is considered to be a promising alternative energy carrier for addressing the environmental concerns associated with the use

of fossil fuels. The advantage of using hydrogen is that it has zero harmful emissions when burned; hydrogen is environmental friendly (non-toxic). Yet there are advantages of using hydrogen as an energy carrier, hydrogen has a problem of a low energy density, storage problems and it is expensive since it has to be extracted from other elements.

Figure 1.2 depicts the energy profile for South Africa in 2010.

The major energy supply in South Africa is derived from coal, followed by oil, (National treasury, 2013). However, various industries and scholars plan to revolutionize the energy society in South Africa by increasing the use of cleaner fuels technologies such as fuel cells and promotion of production of cleaner fuels as an energy carrier. Figure 1.2 shows the energy supply in South Africa in 2010. It can be observed from figure 1.2 that coal is major source of energy supply in South Africa. The current technologies for generating energy from coal are not environmental friendly. However, clean coal technologies are under research at CSIR to improve the current use of coal.

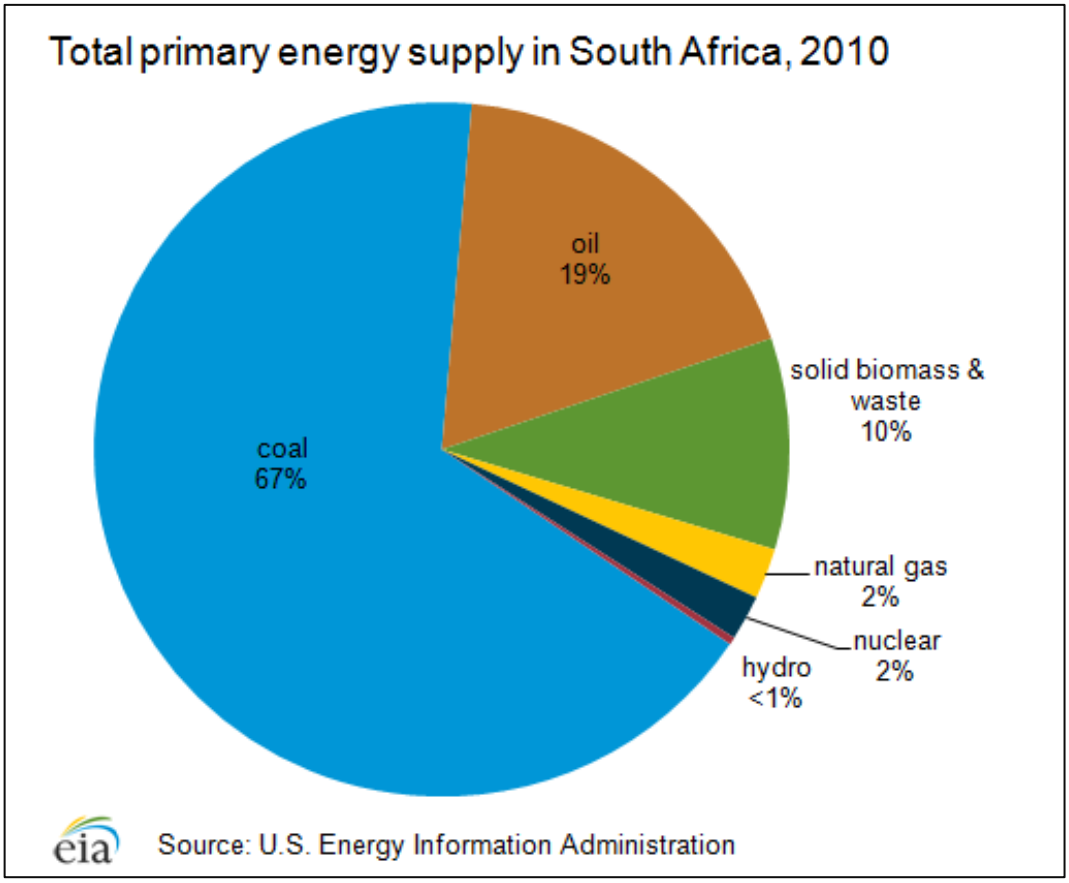

Figure 1.2 South African primary energy profile supply in 2010

Sourced from (Daviddon , 2012)

Reported by the US energy information administration 2015, South Africa has limited proven reserves of oil and natural gas and uses its large coal deposits to meet most of its energy needs, particularly in the electricity sector. However, research on cleaner fuel devices such as fuel cells is currently underway to reduce the use of coal and to improve the current coal utilisation technologies.

Currently, fuel cells are the leading choice for the generation of clean electricity, owing to their high efficiency and low pollution (Baschuk & Li , 2001). A fuel cell is an electrochemical device which directly converts the chemical energy stored in a fuel (hydrogen, ethanol or methanol) into electricity. Hydrogen is the most commonly used fuel. The hydrogen dissociates over a platinum catalyst at the anode into protons and electrons to generate electricity (Ford, 1981). The performance of a fuel cell heavily depends on the quality (degree of purity) of the hydrogen. Reported by Callaghan (2006), the hydrogen produced from steam methane reforming (SMR) is not 100% pure, it contains 25-35%traces of carbon monoxide (CO) which is not suitable for fuel cell applications. The amount of CO contained in the feed for a hydrogen fuel cell should not exceed 10 ppm because the platinum anode is intolerant of CO. Damage caused to the anode adversely affects the performance of the fuel cell over time (Baschuk & Li , 2001)**.** Therefore, there is a need to improve methods of producing high purity hydrogen on an industrial scale**.**

Currently, the global production of hydrogen mainly depends on processes which extract hydrogen from fossil fuel feedstock. 96% of Hydrogen is produced directly from fossil fuel and only about 4% is indirectly produced by the use of renewable resources that are carbon free (Abdollahi *et al*. 2012). The production of hydrogen is expected to increase in the future as the world moves toward the greater use of hydrogen as an energy carrier. The main challenge for the upcoming generation is to increase the percentage of hydrogen produced from biomass or through electrolysis based on Renewable Energy. There are a variety of techniques being used to produce hydrogen, which depend on the feedstock; hydrogen can be produced from different sources such as water, biomass, hydrogen sulfide, hydrocarbons, boron hydrides and chemical compounds with hydrogen (Iyoha *et al.* 2007). The methods for hydrogen production include High Temperature Steam Electrolysis, Partial Oxidation, Bio-photolysis, Photo-catalysis, Thermo-Chemical Process, Electrolysis, Dark fermentation, Coal Gasification and steam reforming of natural gas (Drnevich & Papavassiliou, 2006). At present, the dominant technology for direct production of hydrogen is steam reforming of natural gas because it is more economically viable relative to other emerging technologies (Drnevich & Papavassiliou, 2006)

The focus of this work was on the intermediate stage of reforming natural gas. Figure 1.3 represents the convictional process flow diagram of SMR.

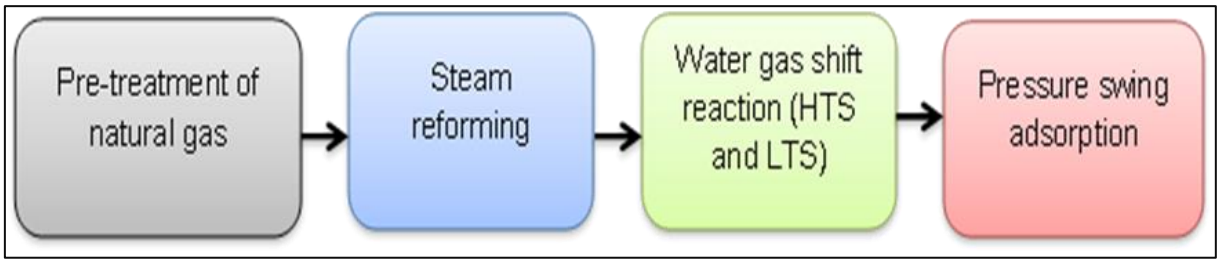

Figure 1.3 Convictional process flow diagram for steam reforming of methane

The production of hydrogen from natural gas comprises of four major stages as shown in Figure 1.3. Pre-treatment of gases removes impurities. The second stage is reforming; steam is mixed with the natural gas and heated up to 1500^{o}C under the presence of a nickel catalyst. Equation 1.1 represents the reforming reaction

$$\mathbf{CH_4 + H_2 \leftrightharpoons 3H_2 + CO} \qquad \mathbf{\Delta H\ 45\ kJ/mol} \quad \text{Equation…….. (1.1)}$$

The reaction is endothermic; the composition of the product depends on operating conditions such as catalyst type, temperature and other process variables (Drnevich & Papavassiliou, 2006).

The third stage of the process is the two stage WGS reaction. This converts Carbon Monoxide (CO) produced from the reforming stage into Carbon Dioxide (CO_2); furthermore, it also produces more hydrogen. The WGS reaction is represented by equation 1.2 below where the enthalpy is -41.2 KJ/mol (exothermic).

$$\mathbf{CO + H_2O \leftrightharpoons H_2 + CO_2} \qquad \mathbf{: \Delta H - 41.2\ kJ/mol} \quad \text{Equation …… (1.2)}$$

The WGS reaction is the upgrading stage in the cycle of hydrogen production from SMR. WGS reaction plays an important role in the production of hydrogen, by allowing the conversion of CO when mixed with steam in the presence of a catalyst to produce CO_2. This process was pioneered in 1780 by an Italian physicist Felice Fontana (Ford, 1981). The process of WGSR is characterized by a multiple stage process with an intercooler between these two stages. These stages include high temperature shift (HTS) to attain faster reaction kinetics and low temperature shift (LTS) to increase hydrogen yield and improve the degree of purity. Selective catalytic membranes are promising devices to reduce the process

complexity of WGSR, and enhance a high yield of hydrogen; Selective membranes combine the reaction and separation into a single unit.

Palladium (Pd) based membrane reactor has been identified as a promising alternative solution for producing ultra-pure hydrogen in industrial processes. Pd based membrane reactors combines the reaction and separation steps into a single unit, which offers more advantages when compared with the traditional process of WGSR. From open literature, replacement of the current multi-stage water gas shift reaction by a Pd based membrane, has the potential to improve the overall efficiency of the process by 3.2 % (Augustine *et al*. 2011; Pinacci *et al.* 2010; Pinacci *et al*. 2010; Amadeo & Laborde , 1995) From equation 1.2, if the reaction is equilibrium, the continuous removal of hydrogen will cause the reaction to shift towards the right in accordance with Le Chatelier's principle (Amadeo & Laborde ,1995). Therefore, more hydrogen is produced due to shift effect.

Palladium based catalytic membrane reactors have demonstrated a wide range of applicability towards the hydrogen production processes; Pd based membrane produces high degree purity of hydrogen, ability to increase the store hydrogen when incorporated with metal-organic framework (Abdollahi *et al*. 2012). One of the most fundamental requirements for palladium based membrane reactors is to produce a robust, defect free, uniform and thin metallic membrane which will exhibit long term selectivity and permeability towards hydrogen. The fabrication techniques for producing a uniform and dense Pd defect free film remain a challenge

Numerous studies have been conducted to test the selectivity towards and permeability of hydrogen through these membranes. Promising results were attained by some researchers (Pan *et al*. 2003; Ciocco *et al*. 2005). However; several gaps still exist in the relevant literature regarding the design of a palladium membrane reactor. The irreversibility of coke formation and membrane durability has not yet been fully documented in literature. Additionally, the long term permeability and selectivity of the palladium membrane has not yet been fully demonstrated. These technical drawbacks pertaining the Palladium membrane reactor make it difficult for the membrane to be applied in industry.

The core purpose of this study is to produce high degree of purity for hydrogen and to test the long term selectivity and permeability of hydrogen through the porous supported membrane, in order to build a benchmark in terms of the life span of the membrane. If a Pd-membrane WGS reactor is to be applied on an industrial scale, an estimate in terms of life span of the membrane will be required to project the frequency and cost of membrane maintenance or replacement.

One of the key performance requirements for Pd-membrane, which is yet to be thoroughly demonstrated, is long-term permanence and selectivity stability of hydrogen through the membrane. Relatively few studies have investigated the robustness of membrane stability towards hydrogen separation. For example, a porous stainless steel supported Pd-membrane has been tested for 190h at 400 ^{o}C at a maximum pressure of 7 bars; conversion and recovery of 97% and 88% respectively were achieved. However, leakages were experienced during experiments due to the welding technique (Augustine *et al*. , 2012). Furthermore, it has been shown in several studies (Abdollahi *et al.* , 2012; Peters *et al*. , 2009; Iyoha *et al.* , 2007; Hou& Hughes , 2003) that the Pd membrane is capable of achieving higher conversion in membrane reactors compared to traditional packed bed WGS reactors. Peter *et al.* (2008) studied the long term stability of a Pd_{77}-Ag_{23} membrane reactor for 100 days at 400°C during continuous operation, the membrane suffered from pinholes formations and a decline in hydrogen selectivity. Surface changes were observed from SEM analysis. Despite the formation of pinhole Peter and his co-workers estimated the life span of a membrane to be 2-3 years.

According to studies by different scholars (Augustine *et al*. 2012; Edlund & McCarthy , 1995; Okazaki *et al*. 2011), it has been noticed that the hydrogen flux permeating through the palladium membrane does not remain constant over a long period of time, the hydrogen flux declines as time elapses at elevated temperatures. It is of practical importance to establish the challenges that inhibit the industrial application of Pd membrane reactors with respect to carrying out separation and reaction functions. Within this context, this research will in part provide an understanding in terms of which aspects need to be addressed in order to make membrane reactors economically and technically feasible for industrial applications. However, this study will not be looking at economic feasibility of Pd based membrane reactors.

1.2 **Problem statement**

The Department of Science and Technology (DST) of South Africa developed the National Hydrogen and Fuel Cells Technologies, Research, Development and Innovation Strategy. The national strategy was branded Hydrogen South Africa (HySA).The overall goal of HySA is to develop and guide innovation along the value chain of hydrogen and fuel cell technologies in South Africa. HySA has been established consisting of three Centres of Competence, namely HySA Infrastructure, HySA Catalysis and HySA Systems. HySA Infrastructure focusses on hydrogen production, storage and distribution. A key aim is to promote the incorporation of Platinum Group Metals (PGMs) as part of the national mineral beneficiation strategy.

The use of Palladium as a membrane reactor for producing hydrogen through WGS reaction is part of mineral and within the scope of DST.

The purpose of this research is to produce high degree purity of hydrogen through WGS reaction and to develop a fundamental understanding of the operating principles and impediments which are relevant to the application of Palladium membrane reactors in the water gas shift reaction. The study will help in establishing how far (technical aspects to be addressed) palladium membrane reactors are from being implemented in industry for carrying out separation and reaction in a single unit.

1.3 **Study objectives**

1. To study the permeability, selectivity and long term stability of Palladium-Silver membrane towards hydrogen exposure.
2. To study the thermal cycle and stability of a Palladium-Silver membrane under hydrogen exposure.
3. To produce high degree purity of hydrogen by the water gas shift reaction through the use of a Pd-Ag membrane reactor.
4. To investigate the effect of process variables (pressure, flow rate, temperature, steam to carbon monoxide ratio, and different feed composition) on the membrane performance towards hydrogen recovery and carbon monoxide conversion.
5. To investigate the effect of hydrogen permeance and WGS reaction on the palladium membrane degradation.

1.4 **Dissertation outline**

This dissertation is divided into five (5) chapters as outlined below:

Chapter 1:

This chapter gives the reader a brief research background and motivation for why the research was conducted. It has clearly showed the research gap in literature and identified relevant problems within the field of hydrogen production using membrane reactors. It outlined the significance of the current work and the end goal of this research.

Chapter 2:

The chapter entails a comprehensive literature study of WGSR, starting from the traditional method of using multiple reactors, catalyst types and the kinetics of the reaction. Furthermore, it gives an overview of palladium based membrane reactors, ranging from membrane preparation methods and membrane classification. A special focus on Pd-based membrane reactor towards hydrogen separation is provided. This chapter also gives a detailed description of relevant parameters affecting the WGS reaction in membrane reactors such as membrane stability, deactivation and durability of membranes and problems associated with palladium membrane towards hydrogen selectivity.

Chapter 3:

This chapter outlines the experimental procedures that were followed from literature, and also explains the apparatus used for this work with their manufactures specification standards. All assumptions made during the experiments and how the research was executed in order to address the problem statement is detailed in this chapter.

Chapter 4

The chapter reports and discusses the results obtained in this work. The chapter is divided into four sections. The first, **Section A,** revises the project objectives of this work. **Section B** discusses the permeability of pure hydrogen through the Pd-Ag membrane reactor and evaluates the effect of process variables on the membrane durability and hydrogen permeation stability. **Section C** discusses the production and performance of a membrane water gas shift WGS reactor. **Section D,** discusses the post characterisation of the membranes used for hydrogen production various analytical techniques.

Chapter 5

This chapter concludes and makes recommendations for future work to be conducted to further enhance the operability and durability of Pd- membrane for WGS reactors.

CHAPTER TWO:

2 LITERATURE REVIEW

2.1 Chapter outline

The current environmental and energy concerns about the burning of fossil fuels have demonstrated a renewed interest in processes that produce clean energy carriers, especially hydrogen processes. The water-gas-shift reaction (WGSR) is among industrial reactions studied in conjunction with the palladium membrane for hydrogen production. This chapter reviews the most relevant topics of WGSR membrane technology, in order to establish the state-of-the-art for a palladium based membrane reactor which has the potential to replace the current multi-stage process for WGSR.

This chapter starts with a detailed introduction of the current multistage process of WGSR and catalysts that are currently commercially used for both high temperature shift (HTS) and low temperature shift (LTS). Furthermore, a discussion of recent studies on the synthesis of appropriate catalysts and an overview of literature for membrane technology is outlined. A detailed review of the key concepts that govern the industrial adoption of Pd-based membrane reactors is outlined; parameters such as hydrogen permeability stability, membrane durability (life span), the deactivation of the membrane and the current problems associated with the permeability of palladium membrane, are fully detailed in this chapter.

.

2.2 **Hydrogen as future energy carrier**

For many centuries the global energy economy was built on a notion that cheap, abundant fossil fuels will forever be available as a primary source of energy. However, if the dependence on fossil fuel as a primary source of energy continues, the current environmental and energy crisis will not be easily addressed. Currently, there is an expected increase in energy demand as well as carbon taxes (National Treasury, 2013). According to the National Treasury of the Republic of South Africa, carbon taxes are expected to increase to 34% in 2020 and 42% by 2025. High quality fossil fuels are reportedly becoming depleted**.** Within this context, there is a need to move towards the development of clean energy carriers in order to address the current environmental crisis associated with fossil fuels. Therefore, it is critically important to urgently develop sustainable energy carriers that are free of carbon dioxide emissions. In a prior study by Mendes *et al*. (2010) hydrogen was pointed out as a potential energy carrier among other candidates, because the combustion of hydrogen liberates heat and produces only water vapour as a bi-product which does not contribute to greenhouse gases. The utilization of hydrogen in fuel cells as energy carrier is represented by Equation 2.2

$$\boldsymbol{2H_2 + O_2 \leftrightharpoons 2H_2O} \qquad \boldsymbol{\Delta H} > 0 \ldots\ldots\ldots\ldots\ldots \text{Equation 2.1}$$

Hydrogen has the potential to revolutionize the energy sector from household application, transportation and all the way through to industrial processes. Hydrogen combined with air (oxygen) at elevated temperatures produces water vapour which does not add to greenhouse gases (GHGs). Despite these potential benefits, however, the production of pure hydrogen also has substantial problems (Tong *et al.* 2004). For hydrogen as an energy carrier to successfully replace the fossil fuel production and distribution channel, it must make economic and environmental sense.

Hydrogen stands as a potential energy carrier for transportation, stationary application and most importantly for electricity generation. There is also a vast need to improve the production yield of hydrogen, since it is also used in food production processes such as hydrogenation. Hydrogen plays a vital role in the fertilizer industries, especially the production of ammonia through the Haber process.

2.3 **Routes for hydrogen production**

According to Tong *et al*. (2004) the production, purification, and storage of hydrogen represents a significant technological obstacle for the realization of a hydrogen economy. Historically, almost all hydrogen produced is based on fossil fuels as a raw material; coal and natural gas are the primary sources. Furthermore, renewable and non-renewable material can be used to produce hydrogen. Hydrogen production technologies fall into four general categories: thermal, electrolytic, biochemical and photolytic processes. Table 2.1 indicates different methods for producing hydrogen from different feedstock.

Table 2.1 Different methods for hydrogen production

Primary source of hydrogen	Production method	Comments	Reference
Water	Electrolysis	Electrolyzes have limited life time	(Harada *et al*. 1997)
Water	Thermo-lysis	High temperatures dependent , expensive	(Baykara , 2004)
Hydrogen sulphide	Thermo-catalysis	Toxic process	(Adesina *et al*. 1995)
Biomass	Dark fermentation	Availability of feed is a problem	(Nakamura *et al*. 1990)
Water	High temperature electrolysis	Energy intense	(Koc *et al*. 2011)
Natural gas	Steam methane reforming	Currently used process, but there is room for improvement	(Laurendeau , 1978)

An electrolytic process includes water electrolysis, whereby electricity is used to split water into hydrogen and oxygen. The electrolysis of water is a typical example of an electrolytic process. A photolytic process uses light energy and a catalyst to split water into hydrogen and oxygen. Currently this method is still at an early stage of research (Holladay *et al*. 2009). Among these technological processes, the thermal process is the most researched and industrially utilised methods for hydrogen production. From literature, steam methane reforming is the most energy efficient and the most commercialized process for the production of hydrogen, accounting for 48% of the total hydrogen produced (Ciocco *et al*. 2005).

Traditionally, steam methane reforming primarily consists of three major processes as represented by Figure 2.1, which include steam reforming of natural gases, water gas shift (WGS) reaction and pressure swing adsorption (PSA).The initial stage of pre-treatment is to remove impurities from the feed. The key process step is the reforming of the carbonaceous material with steam over an appropriate catalyst to produce hydrogen and carbon monoxide, carbon dioxide and traces of methane.

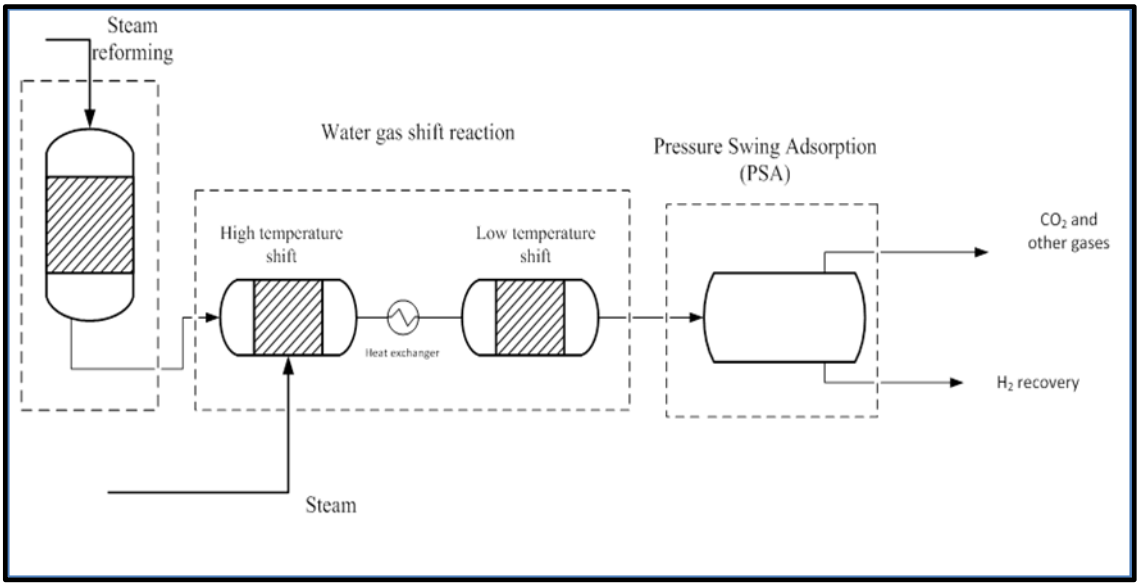

Figure 2.1 Convectional process flow diagram for steam methane reforming

Reforming hydrocarbons with steam produces significant amounts of carbon monoxide, which contaminates hydrogen as a fuel for fuel cells. Within this context, fuel cells are important for hydrogen economy and have the potential to revolutionize the power generation scenario, providing cleaner and more efficient alternatives for producing cleaner energy. Proton Exchange Membrane Fuel Cells (PEMFCs) require a high degree of purity of hydrogen as fuel, as the anode of a PEMFC is coated with platinum which is CO intolerant (Zhang *et al*. 2007). Therefore, it is critical to minimize the percentage of CO in order to have a stable fuel cell. To minimize the content of CO, WGSR is used to convert CO into CO_2 and additional hydrogen. This research was focused on this stage of converting CO into CO_2 while increasing and producing a high degree purity of hydrogen through the use of a palladium based membrane reactor.

2.4 **Water Gas Shift Reaction**

The water gas shift reaction (WGS) reaction was first discovered by an Italian physicist Felice Fontana towards the end of the 19th century (Smith *et al*. 2010) **.** The WGSR is an important step in carbon based hydrogen production processes. The water gas shift reaction is used for downgrading CO produced from SMR into CO_2 while increasing the percentage yield of hydrogen. Traditional process such as coal gasification, hydro-treating of petroleum feed stock and the Haber process employs WGSR to reduce the CO content from prior stages. Most importantly, WGSR is the preferred reaction when removal of CO feed is needed and high purity hydrogen is desired. Historically, the first industrial application of the WGSR was a single stage process in the early 20th century, since the production of synthetic gas was primarily from coal and coke. Therefore, the need to reduce CO and enhance hydrogen production was important. The WGSR is moderately exothermic and reversible at equilibrium; it is expressed by Equation 2.2

$$\boldsymbol{CO + H_2O \leftrightharpoons H_2 + CO_2 :} \quad \boldsymbol{\Delta H - 41\ kJ/mol} \quad \text{……Eequation 2.2}$$

The process is carried at a temperature between 400^{o}C-600^{o}C under the presence of a catalyst (Byron *et al*. 2011; Rossi *et al*. 2012; Romero & Wilhite, 2012). Iron (III) oxide (Fe_2O_3) was used and continues to be used today as a catalyst for high temperature shift (HTS). Chromium (III) oxide (Cr_2O_3) is used together with the Fe_2O_3 as stabilizers to prevent catalyst sintering (Mendes *et al*. 2010)**.** In order to improve equilibrium conversion of the process, a two stage process configuration was adopted with an inter cooler between the two steps. From Equation 2.1, the CO conversion at equilibrium is favored by low temperatures, however the kinetics of the reaction are slow at low temperatures. In order to achieve faster kinetics and higher equilibrium conversion at equilibrium, the reaction is carried by a two stage process.

Figure 2.2 represents the current industrial process of WGS reaction. The first stage is known as high temperature shift (HTS) and the second stage is known as low temperature shift (LTS).

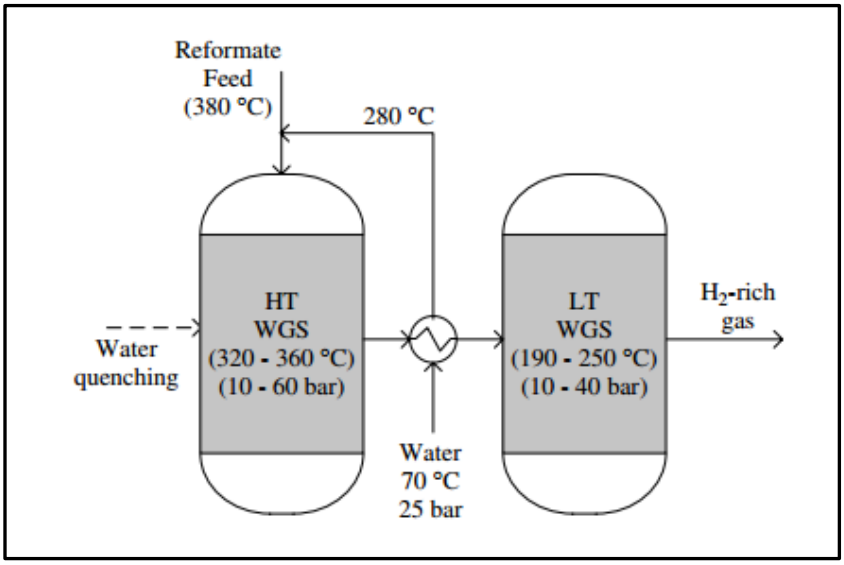

Figure 2.2 Multi-stage water gas shift reaction process flow diagram

Sourced from (Smith *et al*. 2010)

According to Ciocco *et al*. (2005) the conversion of CO at equilibrium is limited at high temperatures, because the forward reaction is exothermic. Therefore, to overcome equilibrium limitations the reaction is carried by two stages. From Figure 2.2, the first step involves a high temperature shift (HTS) step operating between 320-360 °C, which reduces the CO content to 2-3%, while the second stage is low temperature shift (LTS) which is conducted at a temperature range of 190-250^{o} C and reduces the concentration of CO content to 1-0.5% (Yun , 2005) . Different catalysts are employed in the two different stages. The iron oxide/chromium based catalysts are applicable at HTS and Copper-zinc based catalysts are employed at LTS.

2.5 Thermodynamics of water gas shift reaction

The WGS reaction is characterized by two important parameters; it is moderately exothermic and reversible at equilibrium. The first property implies that WGS reaction is favored by low temperatures; under these conditions it renders a high equilibrium conversion of CO to CO_2. The equilibrium constant (K_p) is generally expressed by Equation 2.3.

$$\boldsymbol{K_p = Exp\left(\frac{4577.8}{T(K)} - 4.33\right)} \quad \text{.....Equation 2.3}$$

As the temperature increases (T in kelvins), the equilibrium conversion of CO and equilibrium constant (K_p) inherently decreases. However, at low temperatures the reaction rate is

kinetically limited. On the other hand, at high temperatures the WGS reaction is kinetically fast, but thermodynamically limited because the reverse reaction is favored, while consuming some of the hydrogen that has already been produced. As mentioned before, the WGSR is thermodynamically unfavorable at high temperatures as shown by Equation 2.2 and as reported on by other scholars (Ciocco *et al*. 2005; Smith *et al.*2010; Diogo , 2010; Pinacci *et al*. 2010). According to Le-Chatelier's principle, "When equilibrium is reached by a reversible reaction, if the equilibrium is disturbed by any change in temperature, concentration or pressure, the system will react to establish a new equilibrium." The WGS reaction is an equilibrium-limited industrial reaction process; the pressure does not affect the equilibrium conversion, since moles are equal both sides. Only the concentration and temperature of the reactant will affect the value of K_p. However, for membrane reactors, pressure plays an important role since it increases the driving force for hydrogen diffusion.

2.6 **Catalyst for water gas shift reaction**

Catalysts have been used over the past 2000 years (Scott, 2005). However, there has been on-going research aiming at developing the most efficient commercial catalyst for WGSR for both the high and low temperature shift reactions. According to Scott (2005) catalysts do not maintain their activity at the same level indefinitely, they are subjected to deactivation, which refers to the decline in catalyst activity as time progresses due to various reasons such as aging, poisoning and coking. Within such context, the likely encountered phenomena in WGS is catalyst aging and coking due to low steam carbon ratio.

Currently, both high and low temperature shifts were and still are catalysed by metal oxides. Iron oxide, supported by chromium oxide, is the most researched and applied catalyst for high temperature shift (HTS) in WGS reaction. It was first applied in an ammonia plant. Since the current WGSR is carried in a two stage process as outlined earlier, namely a high and a low temperature shift, the development of a catalyst that would be suitable and optimal for both stages is needed. However, this work will use the current developed catalyst for WGSR.

2.6.1 Low Temperature Shift Catalyst

The most widely used industrial catalyst for LTS is a copper based catalyst with a typical composition of 32.7% CuO, 47% ZnO, and 11% Al_2O_3. The catalyst has a surface area of 42 m^2/g and a copper metallic surface area of 13 m^2/g, with a pore volume of 0.11cm^3/g (Amadeo & Laborde,1995). Copper oxide is the active catalyst, zinc oxide is a structural promoter and aluminium oxide is a chemical promoter. The Cu-based catalyst is subjected to

deactivation due to thermal sintering. Therefore, research to improve the catalyst activity, stability and resistance to poisoning is being conducted.

Outlined by Callaghan (2006) the copper and zinc oxide forms are stable under reaction conditions. Copper, the active species, remains active at temperatures as low as 200^{o}C. The zinc oxide provides some protection of the copper from sulphur poisoning by reacting with adsorbed sulphur compounds while acting partially as a support for the copper (Callaghan, 2006). Due to the relatively low melting point of zinc, the commercial LTS catalyst is more sensitive to deactivation caused by sintering than the HTS catalyst. This causes the maximum operating temperature to be limited to around 250^{o}C

2.6.2 High Temperature Shift Catalyst

It is well known that the WGSR proceeds very slowly at “low temperatures”. As reported in literature by (Ciocco *et al*. 2005; Bi *et al*. 2009; Basile *et al.* 1996) HTS is the first catalytic stage in the commercial WGSR which is responsible for faster kinetics, and the major conversion of CO into CO_2 occurs at this stage. The reaction is operated adiabatically between temperatures of 320-450^{o}C; it is responsible for reducing the CO content from 25% to 2-3% under the presence of a Ferro chrome base catalyst (Diogo , 2010). The reaction is carried out by using iron oxide as a catalyst which is structurally promoted by chromium oxide. It is reported that chromium oxide (Cr_2O_3) retards the thermal sintering of magnetite and it also prevents the loss of active surface area of the catalyst at high temperatures (Diogo, 2010).

The Cr_2O_3 content is generally less than 14 wt%, which is the maximum amount of Cr_2O_3 that will form a homogeneous solid solution with ferric oxide (Ciocco *et al.* 2005). The composition of a catalyst varies according to manufacturers, with the typical composition falling within the range of 70-74.2 %Fe_2O_3, 8-10% Cr_2O_3 and 0.2%MgO balance volatiles. In the HTS reaction, the ratio of steam to CO is an important parameter, as operating the reaction at low ratios could lead to methanation, carbon deposition, the Fischer Tropsh reaction or formation of metallic iron (Smith *et al*. 2010) .

A prior study by Xue *et al*. (1996) conducted a HTS-WGSR using a membrane rector while incorporating a commercial Fe-Cr catalyst. The catalyst sample was crushed into particle sizes of 0.212 to 0.425 mm and the catalyst loading for the experiments was 200 mg. 80% CO conversion, which is higher compared to normal packed reactors for WGRS, was reported. Furthermore, Zhao *et al*. (1999) also studied the WGS reaction at a constant temperature of 390^{o}C and a pressure range of 0.1 – 1.4 MPa while maintaining a constant conversion at a space velocity of 1000 h^{-1} on a commercial iron oxide-based catalyst with a

specific surface area of 45 m^2/g catalyst. The composition of the catalyst was reported to be 63- 75% Fe_2O_3, 12-14% Cr_2O_3 and 3.5-4.5% MgO. The size of the catalyst particles was estimated at 0.2-0.3 mm. The amount of catalyst in the reactor was 0.2g. From several studies; it can be observed that the composition falls within the same range, even though some studies did not narrate the operating conditions. Regarding the catalysts, strong efforts are being devoted to the development of more active, non-pyrophoric and poison-resistant catalysts (Iyoha *et al.* 2007b).

2.7 **Palladium metal as a membrane material**

In 1866, Sir Thomas Graham pioneered research into the ability of Palladium (Pd) to have high selectivity and permeability properties towards hydrogen gas (Tong *et al.* 2004). However; little attention was paid towards the use of palladium for hydrogen applications until the recent increase in demand for and use of hydrogen. The high demand of this clean energy carrier has led scientists and engineers to search for alternative processes to produce hydrogen in order to increase the yield and meet the global demand for energy.

Palladium metal has numerous advantages over other materials that permeate hydrogen. Firstly, it has a good catalytic surface, high hydrogen permeability, infinite hydrogen selectivity, temperature stability and corrosion resistance (Morreale *et al*. 2003). The catalytic surface of the palladium membrane refers to the ability of a Pd surface to dissociate hydrogen molecules into atoms without an external agent to catalyse the process. Figure 2.3 represents the permeability of hydrogen through different metals.

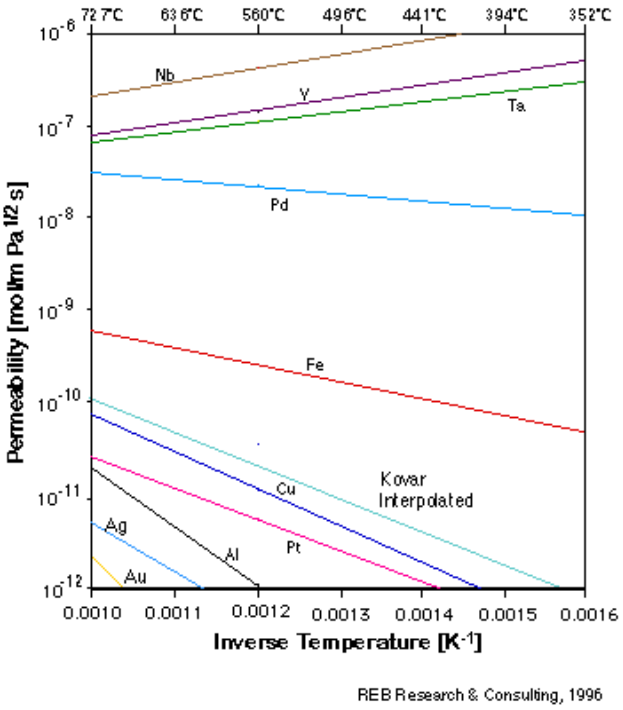

Figure 2.3 Permeability of hydrogen through different metallic membranes

Sourced from (Basile *et al*. 2011)

It can be observed from the graph in Figure 2.3 that Niobium (Nb), Tantalum (Ta) and Vanadium (V) have higher permeability towards hydrogen at different temperatures. These metals (Nb, Ta and V) have bigger BCC pores opening compared to palladium. However, these bigger pores also lead to material failure. Pd stands before these other metals for hydrogen due to its ability to dissociate hydrogen molecules (Nakamura *et al*. 1990)**.** Further reported by Morreale *et al*. (2003), Pd exhibits high catalytic activity for the adsorption and dissociation of hydrogen into atoms entering the membrane and recombination of the atoms into molecular hydrogen exiting the membrane.

2.8 General classifications of membrane

In the field of material science and chemical processes, membrane technology is an important field to be explored. It aims at discovering and improving materials that possess special morphological and structural properties to obtain higher permeations and infinite selectivity. Membranes can be broadly classified into four categories such as polymeric, metallic, carbonaceous and ceramic. A detailed summary of classifying Pd-based membranes is represented by Figure 2.4.

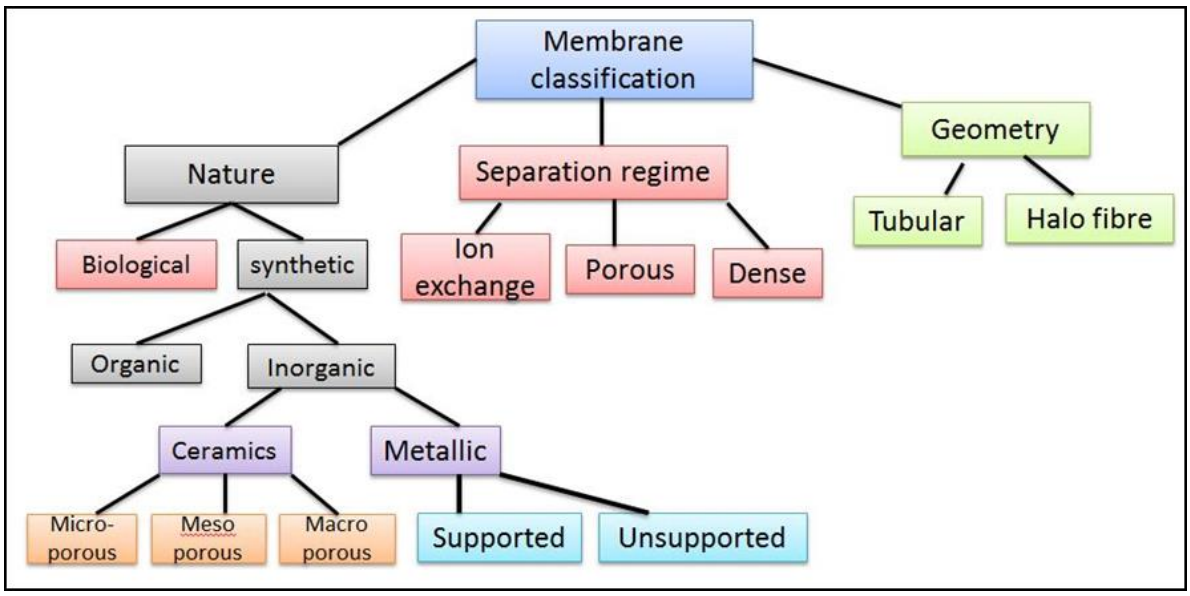

Figure 2.4 Classifications of palladium based membranes

Sourced from (Basile *et al*. 2011)

A classical representation of how a membrane can be classified is represented by Figure 2.4.The art work of Basile *et al*. (2011) reviewed the state of art of palladium membrane reactors. Figure 2.4 shows that the biological membranes face several disadvantages compared to metal membranes, such as restrictions in operating temperatures, limitation of biological functions to certain pH conditions, increasing operational costs due to the pre-cleaning processes, low selectivity, and susceptibility to microbial degradation (Chicas, 2013).

From a geometrical point of view, the membrane can be plain tubular or hollow fibre as shown in figure 2.4. Currently, the most commonly used geometrical shape for gas separation is a plain tubular shape. In the industry, the choice of the geometry of a palladium membrane is driven by the technique used for depositing palladium on a support or a substrate material. According to Straczewski *et al*. (2001) tubular shape can accommodate most deposition techniques.The most successfully reported synthesis method for deposition of palladium on complicated structures is electro-less plating, which is capable of achieving uniform layers (Augustine *et al*.2011).

There are three classes of separation techniques that a membrane uses to separate the desired products from unwanted products. Firstly, based on the chemistry of the material being separated, membranes can be considered porous, dense or ionic. Palladium membranes are considered to be dense membranes based on the transportation of

hydrogen through the membrane. Ionic membranes are used for reverse osmosis in water purification.

Both organic and inorganic membranes can be used for H_2 separation. Polymeric membranes constitute the most traditionally known types, because they have been used since the early 1980´s in the ammonia industry for H_2 recovery. More recently, refineries and integrated gasification combined cycle (IGCC) processes have shown explicit interest in using them, but the operating conditions (temperature, pressure, etc.) limit the applicability of polymeric membrane modules that can only operate at temperatures up to 100 ºC (Gallucci *et al*. 2013).

2.9 **Palladium membrane reactor system**

Membrane reactors can be broadly defined as an integrated device where a reaction and separation can simultaneously take place (Rossi *et al.* 2012). Reported by *Marín et al*. (2012) the use of membrane in WGSR reduces process complexity by eliminating PSA and the LTS and the intercooler between the stages. Membranes are known as a multifunctional reactor, combining separation and a chemical reaction in one single unit. Therefore, membrane reactors become more attractive compared to traditional reactors for WGSR owing to their characteristics of being able to separate the final product from the reaction stream. From an economic feasibility study by Crisuoli *et al*. (2001) the use of membrane reactor reduces the capital cost of producing hydrogen through the SMR (due to reduction in size of the process unit), improves yield and selectivity (due to equilibrium shift) and finally reduces the downstream separation cost (eliminating PSA or a Cryogenic process). Substantial interest exists today in the development of high-performance membranes for hydrogen separation (Morreale *et al*. 2003). Figure 2.5 shows the schematic drawing of the membrane reactor, which consists of a tube (where the catalyst is located) and the shell. It is a similar design to a shell and tube heat exchanger. This kind of configuration is used if sweep gas is to be applied.

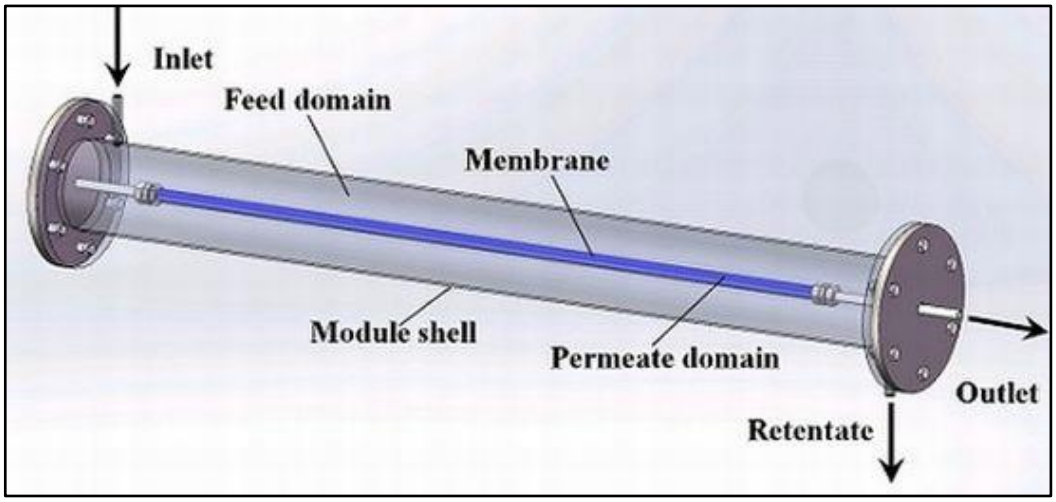

Figure 2.5 Palladium based membrane shell and tube configuration

Sourced from (Basile *et al.* 2011)

Figure 2.5 shows the hydrogen gas being supplied into the shell part of the reactor; the hydrogen will permeate from the shell side through the membrane into the tubular side of the reactor. Sweep gas is often employed to recover the desired gas at higher rates.

From the reaction point of view, when products are continuously removed during the course of the reaction, the shift effect of Le Chatelier's principle applies. In the event of a continuous removal of hydrogen during the course of the reaction which is at equilibrium, the system will respond to re-establish new equilibrium.

A prior study by Zhang *et al*. (2012) tested the permeability of a Pd-Ag membrane with a thickness of 25 µm. The membrane was tested at 300^{o}C and at pressure ranging between 6.9-690 kPa. No sweep gas was used during the experiments. A hydrogen flux of1.25 mol/m^2.s was reported. However, the surface morphology analysis of SEM images showed that air oxidation causes surface roughness and forms protruding grains. These surface changes provide a pathway for inert gas N_2 to pass through the membrane.

Furthermore, a study by Hawa *et al.* (2015) tested the permeability of hydrogen through the Pd membrane at high temperatures – a membrane with a thickness of 5µm and with an effective surface area of 13.3 cm^2. The membrane was also tested for WGSR. A nickel catalyst was used and the membrane was operated at 580°C and 2.9 MPa. A conversion of 98% was achieved with a hydrogen recovery of 85%. The failure mode of the reactor was not discussed. A study by Cooney *et al.* (2014) investigated the effect of hydrogen exposure on a Pd based membrane for 40 hours at 500^{o}C and 10 psi. The membrane failed to show durability over timeafter 23 hours of continuous hydrogen exposure the membrane failed due to the occurrence of pinhole and leak growth.

2.10 **Hydrogen transport mechanism**

The diffusion of hydrogen though a metallic palladium membrane occurs in a series of steps, of which any can be a potential rate limiting step for hydrogen transport through the metal membrane. Figure 2.6 represents the transport mechanisms.

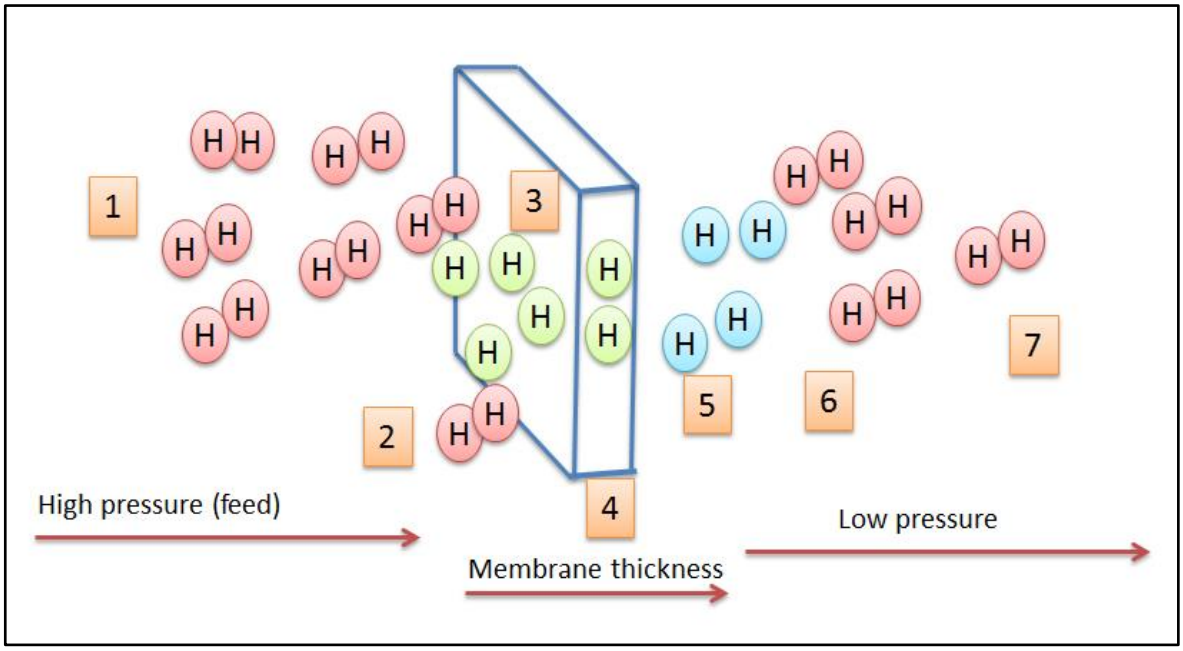

Figure 2.6 Hydrogen transportation mechanism through the palladium based membrane

Sourced from (Ward & Dao, 1999)

From literature (Rossi *et al*. 2012; Ward &Dao, 1999) the transport mechanism follows the series of steps as represented by Figure 2.6. These are, in order from the high partial pressure side to the low partial pressure side:

1. Molecular transport from the bulk gas to the gas layer adjacent to the surface,
2. Dissociative adsorption onto the surface,
3. Transition of atomic H from the surface into the bulk metal,
4. Atomic diffusion through the bulk metal,
5. Transition from the bulk metal to the surface to the low partial pressure side,
6. Re-combinative desorption from the surface, and
7. Gas transports away from the surface to the bulk gas

2.11 **Permeability of hydrogen**

Permeability and perm-selectivity are the most imperative concepts when dealing with membrane reactors. According to Lester (2009) perm-selectivity is the membrane's capability of separating permeates from non-permeates, which is also known as the retentate. Within this context, palladium membranes have the ability of being selective towards hydrogen atoms to diffuse through the membrane while retaining other gases on the feed side, while the retained gases will leave the system through the reject stream. The membrane can be considered to have an ideal selectivity if it does not permeate inert gases (N_2 & He) given that the membrane is defect free. To determine the selectivity of the membrane, Equation 2.4 is applicable.α is a dimensionless value which is the selectivity of the membrane between hydrogen flux (J_{H2}) and nitrogen flux (J_{N2}), and $\alpha_{H2/N2}$ the selectivity of the membrane.

$$\alpha_{\frac{H_2}{N_2}} = \frac{J_{H2}}{J_{N2}} \text{..... Equation 2.4}$$

From Equation 2.4, if the nitrogen flux (J_{N2}) is zero, the membrane is considered to have infinite selectivity towards hydrogen. However, infinite selectivity only occurs when the membrane is defect free. On the other hand, the permeability of a membrane is used to identify whether a membrane has the ability of processing a large or small quantity of permeate per unit area at particular operating temperatures and pressures. According to Morreale *et al*. (2003), the ability to transport hydrogen through palladium membranes is typically quantified in terms of permeability, permeance or flux.

There are various equations in literature which propose to describe the hydrogen flux through the membrane. Fick's and Sievert's law explain the diffusion rate of hydrogen atoms on an ideal basis. Firstly, diffusion is defined as the movement of molecules from higher concentration into lower concentration through a random motion. Mostly, diffusion is always related to mass transfer principles which are governed by concentration gradient; however diffusion can occur without concentration gradient. According to Fick's law, "the net diffusion rate of a gas across the membrane surface is proportional to the difference in partial pressure, proportional to the area of the membrane and inversely proportional to the thickness," as represented in Equation 2.5. J_{H2} represents the hydrogen flux, Q represents the flow rate of the gas, μ represent the membrane thickness, P_{feed} pressure on the feed side, P_{rej} pressure on the reject stream and n is the pressure exponent

$$J_{H2} = \frac{Q}{\mu}\left({P_{feed}}^{n} - {P_{rej}}^{n}\right) \text{..... Equation 2.5}$$

A prior study by Charudatta (2005) found that the transport mechanism of hydrogen through the metal membrane follows the solution-diffusion mechanism which is broadly defined by the elementary steps for hydrogen transportation. These series of elementary steps for

hydrogen diffusion can be expressed mathematically to estimate the hydrogen flux as represented by Equation 2.5. The hydrogen flux (J_{H2}) is the function of material permeability which is the product of solubility and diffusivity of the material which are temperature dependent. The pressure exponent “n” value ranges from 0-1. The “n” value determines the rate limiting step for hydrogen transport. A value closer to 1 indicates that the surface adoption is the rate limiting for hydrogen transport through the material. A value close to 0.5 indicates that the diffusion of bulk hydrogen atoms is the rate limiting step.

Reported by Chiappetta *et al.* (2008), n = 0.5 suggests that the diffusion of hydrogen atoms is the rate limiting step. Further reported, an “n” value less than 0.5 suggests that adsorption and desorption processes are accruing at an equal rate. When the “n” value is equal to 1, it is suggested that each process occurs independently. However, a study by McLeod *et al*. (2009) argued that Sievert’s law is only valid for specific temperature and pressure ranges, and it only describes the ideal behavior of hydrogen in a metal lattice at infinite dilution. The ideal model for hydrogen permeability has been pointed out to be inadequate as they fail to predict the performance of a thicker membrane in the region of 125-250µm (McLeod *et al*. 2009).

2.12 **Membrane durability**

Fundamental engineering principles dictate that “material of construction for products should be durable”, in order to have an economically viable product (Xue *et al* .1996). Membrane durability is defined as the ability of the membrane to withstand several process operating conditions such as different feed composition, high pressure and temperature, while being able to perform a desired reaction and separation over a long period (Okazaki *et al*. 2011). Apart from the ideal selectivity of the palladium membrane, durability is an integral part for membrane reactors to be adopted industrially. A durable material can be considered as a material that maintains its performance over a long period of time at a minimal cost of maintenance.

According to Ma *et al*. (2003) many technical issues, such as producing thin membranes with good separation characteristics, and long term thermal and mechanical stability, remain to be solved. A study by Hani *et al*. (2014) investigated the thermal stability of Pd-Ag composite membranes for high temperature; the thermal stability was investigated in the temperature range of 773K-873K. The study revealed that coating or doping the Pd with Pt or Ru reduces the nitrogen leaks, but the hydrogen stability in terms of permeability was not observed over a period of 120 hours. Furthermore, a study by Gade *et al*. (2008) investigated the durability

of unsupported Pd- foil membrane fabricated from electroless plating methods, and found that the membrane suffered from mechanical strength since the membrane was thin (7.5µm).

According to Augustine *et al*. (2011), a key requirement in membrane applications is to synthesize a robust dense membrane that will exhibit a high permeation rate of hydrogen as well as long term selectivity and permeability. Several studies (Chiappetta *et al*. 2008; Peters *et al*. 2009;) were conducted to reduce the cost of membrane synthesis, which tested the expected life span of the membrane with the aim of optimising process variables involved during membrane operations. These studies highlighted the fact that increasing the thickness increases the membrane life span, but were not cost effective.

2.13 **Membrane stability toward hydrogen permeation**

One of the key performance requirements for Pd membrane, which is yet to be thoroughly demonstrated, is the long term permeance and hydrogen selectivity stability. A few studies (Basile *et al.* 2011; Hawa *et al*. 2015; Augustine *et al.* 2012; Augustine *et al*.2011; Edlund & McCarthy, 1995) have unambiguously demonstrated the robustness of membrane stability after a continuous exposure of hydrogen. A prior study by Augustine *et al.* (2012) investigated the durability of Pd membrane. A palladium based membrane supported by porous stainless steel was operated for 1000 hours at the pressure and temperature range of 2.6-6.1 bar 400-450^{o}C respectively. 98% and 88% CO conversion and hydrogen recovery were achieved respectively. It was observed from the study that the selectivity starting decreasing after 900 hours; this was due to pinhole formation on the membrane surface. Table 2.2 summaries some of the studies which tested the membrane stability towards hydrogen permeation for longer periods under various operating conditions.

Table 2.2 long term tested permeability

Membrane type	Thickness of membrane	Tested time	comments	Operating conditions	Reference
PdComposite **Pd-v** **Pd-Nb**	100nm	20 h 148 h 160 h	The flux declined	10-15 psig and 500^{o}C. No sweep gas	(Cooney *et al*. 2014)
Pd-Ag With PSS	25µm	25 h	Steady state permeation	6.9kPa-690kPa and 300^{o}C. sweep	(Zhang *et al*. 2012)

				gas	
Pd-Ru With PSS	5µm	50 h	Steady state permeation	2.9Mpa and 580^{o}C	(Hawa *et al*. 2015)
Pd-pure unsupported	7.2µm	50h	Selectivity declined	No sweep gas, 350^{o}C and 4 bar	

From table 2.2 it can be deduced that the permeation of hydrogen through composite and pure palladium based membrane reactors doesn't remain stable over time. The selectivity and permeability ability of the membranes mostly decline due to different failure modes of the membranes.

2.14 **Challenges associated with palladium membrane**

2.14.1 Hydrogen embrittlement

Defined by Louthan *et al*. (1972) embrittlement is a process of loss in ductility of materials (especially metals) which results in brittleness of a material. Defined by Wikipedia, hydrogen embrittlement, also known as hydrogen attack, is a process whereby metal becomes brittle or fractures due to exposure and diffusion of hydrogen though the metal. Hydrogen embrittlement is reported to cause lattice expansion (3.4%) and results in internal stress, which generates defects (Okazaki *et al*. 2006). It has been submitted by various scholars that the phase change can be suppressed by alloying palladium with other transition metals (Uemiya *et al*.1991; Okazaki *et al*. 2011; Armor, 1989) Reported by Okazaki *et al.*(2006) thin palladium membranes easily suffer from hydrogen embrittlement due to phase change α-β. This phenomenon occurs when a pure palladium metal is exposed to hydrogen at temperatures below 293^{o}C. At low temperatures the diffusion of hydrogen through the metal causes crystallographic defects.

Pd-Ag alloys have been studied by different researchers (Augustine *et al.* 2012; Okazaki *et al*. 2006; Mendes *et al.* 2011) and it has been shown that hydrogen embrittlement can occur through aqueous solution or gaseous phases. The mechanism for hydrogen embrittlement follows different processes. For instance, as suggested by Chotirach *et al.* (2012), on non-hydride forming materials such as Fe and Zn where hydrogen does not form, they fail because hydrogen absorption decreases the atomic bond. However, materials such as Pd, V, Zn and Tt do form hydrides. They fracture due to stress induced hydride formation and cleavage mechanism. A study by Okazaki *et al.* (2006) investigated the effect of silver (Ag) incorporated in pure Pd. It was highlighted in that study that an improved durability in terms

of phase change was achieved. When hydrogen is exposed to palladium metal, it dissociates and diffuses in the metal. The dissolved hydrogen resides on the octahedral site of the palladium structure and, once the hydrogen is released, the crystals do not return to their original position. This causes overall expansion of the lattice by a small percentage. The dissolved hydrogen has been reported to cause a local strain gradient on the metal (Holleck, 1970).

2.14.2 Intermetallic diffusion

Intermetallic diffusion is defined as the migration of elements from the porous metal support material (mostly Fe, Cr, and Ni) into the Pd layer, which affects the hydrogen permeance of the membrane (Edlund & McCarthy, 1995). The rate of diffusion of Fe, Cr and Ni into Pd has been reported to be a slow process (Augustine *et al.* 2012). The intermetallic diffusion is temperature dependent: the lower the melting point of a support material, the higher the chance that intermetallic diffusion will occur. According to Chotirach *et al*. (2012) intermetallic diffusion is governed by the tamman temperature, which is the temperature half the melting point of the support material. The atoms' mobility of support material starts when the operating conditions are above the tamman temperature. Figure 2.7 represents the schematic process for intermetallic diffusion between the support and the membrane layer.

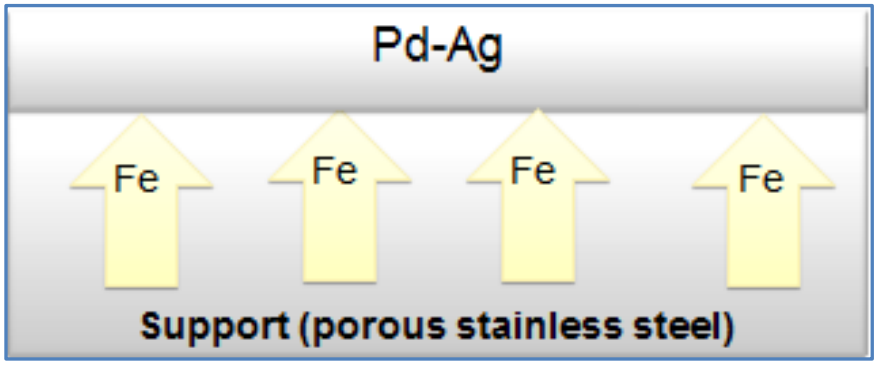

Figure 2.7 Intermetallic diffusion between the support and membrane

Sourced from (Chotirach *et al*.2012)

Metallic atoms start to acquire mobility at temperatures close to the melting point of the support material. As outlined by Gauzzone *et al*. (2006) metallic atoms of porous stainless steel at 500-550^{o}C start to acquire mobility to diffuse into Pd layer. Intermetallic diffusion can be prevented by forming or depositing an oxide between the support material and the membrane. An alternative is to use a material with a high melting point. Previously reported by Edlund & McCarthy (1995) incorporating an interior oxide layer resulted in a stable

hydrogen flux at temperatures greater than 500^{o}C. A study by Edlund & McCarthy (1995) investigated the relationship between intermetallic diffusion and the hydrogen flux decline within a composite palladium membrane. It was highlighted from the study that “the flux decline correlates to the degree of intermetallic diffusion.” A study by Basile *et al*. (2001) investigated the high flux of Pd-Au composite membranes for hydrogen separation. The study highlighted that the use of Pd-alloys reduces cost and improves the hydrogen embrittlement threshold temperature; also Pd-Cu has higher permeability properties than pure Pd membranes.

2.14.3 Membrane deactivation

Membrane deactivation is associated with the continuous decline in the membrane’s ability to separate permeate from the non-permeate. Several studies (Romero & Wilhite, 2012; Shaw ; Augustine *et al*. 2011; Kajiwara *et al.* 1999) have been directed to identify alloys or composite materials that can potentially minimize the membrane deactivation. There are various factors that can lead to membrane deactivation. According to (Kajiwara *et al*. 1999) deactivation by sulfur compounds lead to a rapid decline in hydrogen permeability.

A study by Iyoha *et al.* (2007) investigated the influence of hydrogen sulfide (H_2S) on the permeation rate of hydrogen through the Pd-Cu membranes. These membranes were studied at 900^{o}C using 1,000 ppm H_2S-10% He-H_2, 2,000 ppm H_2S-in-H_2 and 5,000 ppm H_2S-in-H_2 gas mixtures. It was observed from the experimental data that the hydrogen flux was reduced by 25% when exposed to H_2S above 1500 ppm. The desire to enhance H_2 generation and separation from mixed gas streams that may contain varying concentrations of H_2S has led to numerous studies on the effect of H_2S on H_2 permeability of dense Pd-based membrane (Peters *et al.* 2009; Iyoha *et al*. 2007; Kulprathipanja *et al*. 2004). Furthermore, apart from coke formation it has also been pointed out that the pure Pd membrane reactors are not tolerant to hydrogen sulfide, since it can lead to deactivation of the Pd membrane.

Furthermore, the exposure of H_2S on the membrane has additional effects such as morphological changes, including pitting of Pd-based membranes within seconds of contact with a high concentration of hydrogen sulfide. Coke formation has not typically been a concern in the traditional WGS reactor system, but it has a potential of deactivating the catalyst. However, coke formation can be a significant problem in the Pd-WGS membrane. The coke formation in the Pd-catalytic membrane has the potential to block the active hydrogen adsorption site on the Pd surface over time, which will limit the long term performance of the reactor. In contrast, to attain a higher driving force for hydrogen

permeation, a low ratio of H_2O/CO needs to be used which also leads to coke formation. To be specific it is reported in literature (Chiappetta *et al*. 2008) that a ratio of less than 2,5:1 of H_2O/CO has the potential of causing the formation of coke. Therefore, a better understanding of coke formation thermodynamics and kinetics in WGS reaction Pd membrane opens other research areas within the scope of a catalytic membrane reactor. However, the focus of this study is to produce hydrogen through the use of Pd-Ag membrane based reactor

CHAPTER THREE:

3 EXPERIMENTAL METHODS

3.1 Chapter outline

This chapter systematically outlines the experimental procedures and apparatus used in this work. This chapter consists of five major sections: **Section 3.2** outlines the preparation technique used to build the membrane reactor; **Section 3.3** presents the leak test setup and procedure; S**ection 3.4** discusses the experimental set-up for the permeation test unit; **Section 3.5** presents the water gas shift reaction setup and procedure; and finally, **Section 3.6** discusses the characterization techniques used by the membrane reactor.

3.2 Membrane reactor preparation

An alloy of Pd-Ag film was purchased from a Japanese company called Tanaka Kikinzoku group. According to the manufacturer's specifications, the alloy is a mixture of 77wt% Pd and 23wt% Ag with a thickness of 20µm. Two stainless steel plates, shown in figure 3.1, were purchased from thermodynamic fluid design (TFD). Plate A is punched with a single outlet for permeate products. Plate B has two holes punched within the plate, one for the feed supply and the other for reject stream. Plate B also has a catalyst channel volume as represented in figure 3.1.

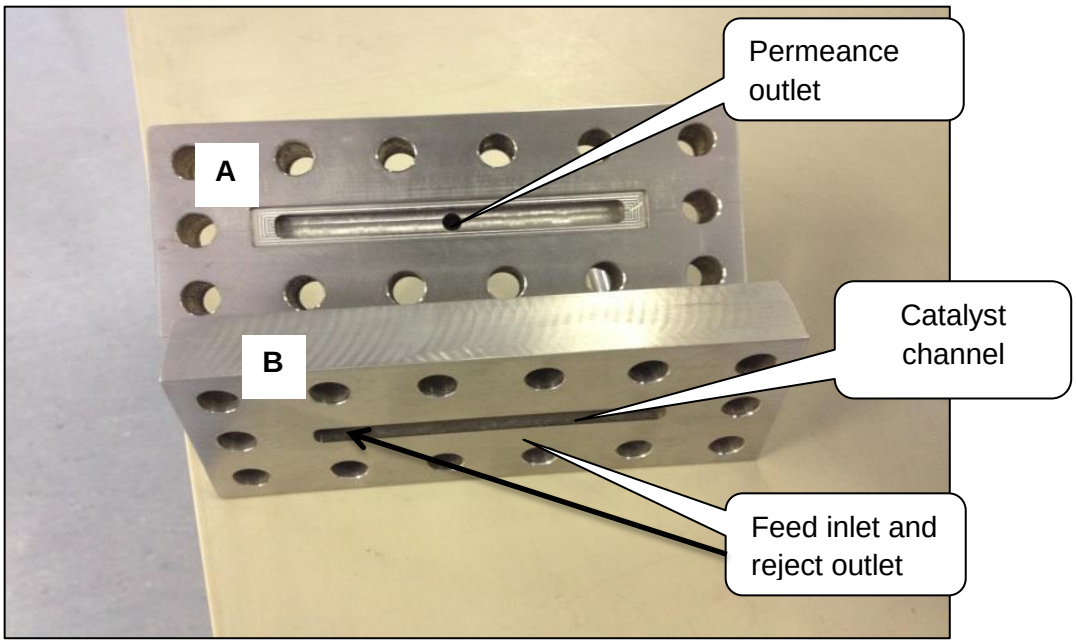

Figure 3.1 Stainless steel plate for membrane reactor

Plate A was fitted with a support of porous stainless steel metal which acts as support material for the Pd-Ag film, shown in figure 3.2. Figure 3.2 represents all the necessary major components before they are assembled to form a membrane reactor. The graphite is used to seal the two plates to ensure there is no gas escaping on the edges of the plates. Bolts and nuts have been used to tighten the plate while enclosing the membrane film and the graphite between them. The Pd-Ag film was placed in between the two plates on the side of porous stainless steel in order to be supported.

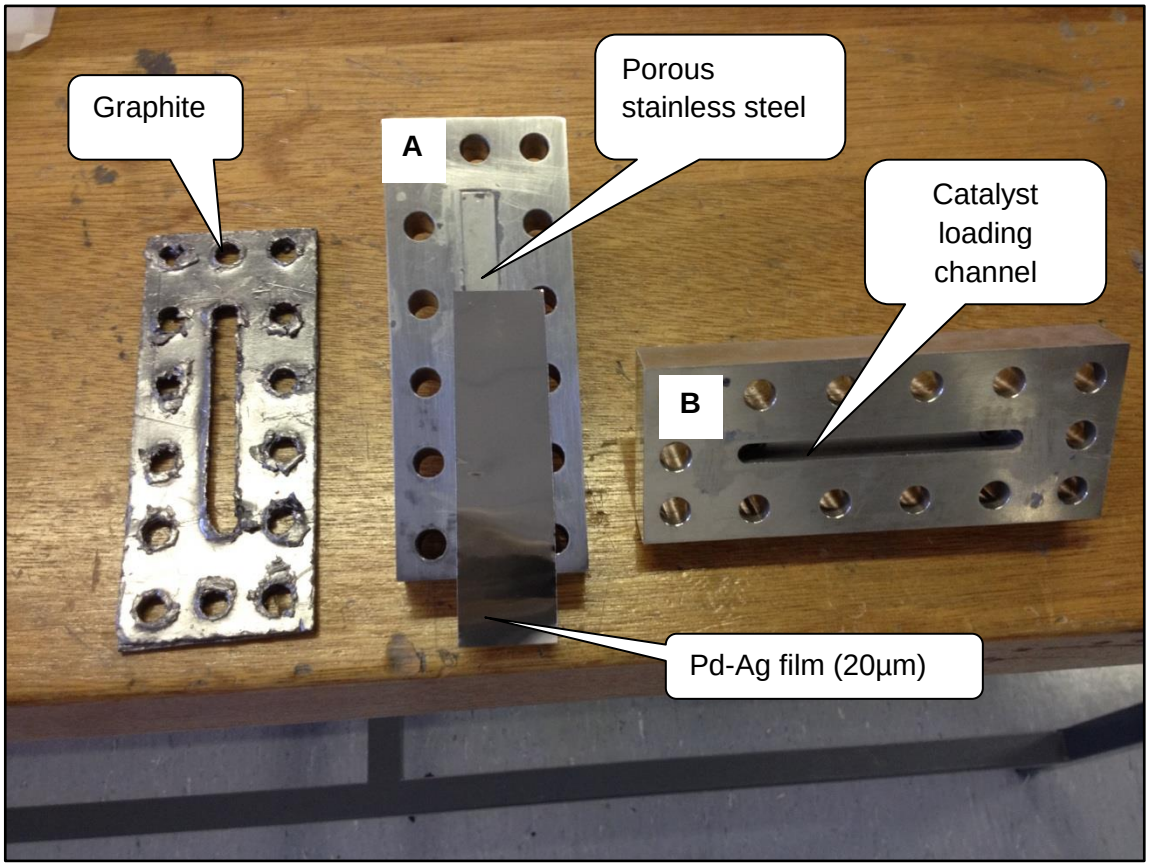

Figure 3.2 stainless steel plate with porous stainless steel as support material

Plate A was fitted with a porous stainless steel (PSS) support which is a 98 % grade, with an active surface area of 5.6 cm^2 (8cm*0.7cm). Plate B has a catalyst channel with a volume of 2.88 cm^3 (8cm*0.7cm*0.7cm). Different amounts of catalyst were loaded into the catalyst channel during the water gas shift reaction experiments. After assembling all components of the membrane reactor, the reactor was leak resistant.

3.3 **Membrane bubbles leak test**

The reactor was leak tested with nitrogen at room temperature and at a maximum pressure of 10 bars. The leak test was done by monitoring the pressure of nitrogen applied to the membrane reactor. A bubble leak test was also done in order to increase the confidence level of leak free reactor

In order to locate the defects within the assembled membrane reactor, the water bubble leak test was done on the membrane. The membrane reactor was submerged into a bucket filled with water as shown in figure 3.3. Defects were identified by the formation of bubbles around the plate. The test was conducted at a pressure range of 0-10 bar with the use of nitrogen gas at room temperature.

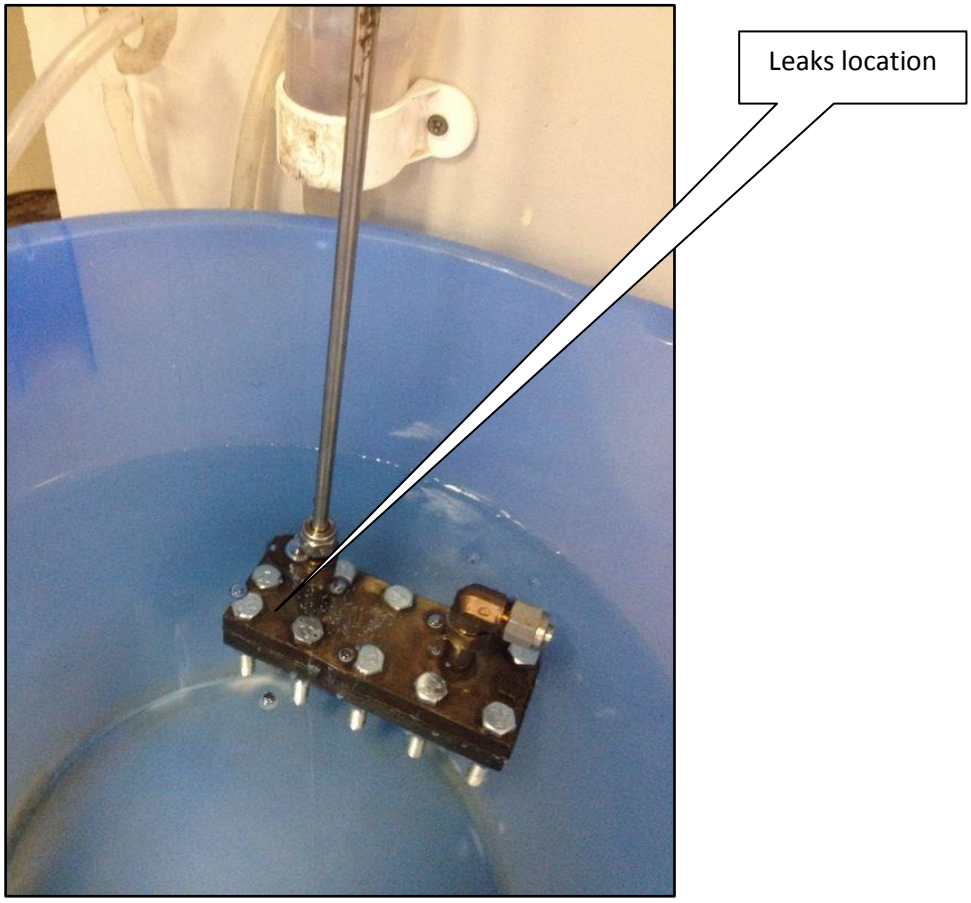

Figure 3.3 bubbles leak test at room temperature

If leaks were observed, the bolts and nuts were tightened until a leak free membrane was achieved. A defect free membrane reactor was then moved from the leak testing station into the permeance testing station which is discussed in section 3.4 for permeance measurements.

3.4 **Permeance testing unit**

3.4.1 Process Set-up description and equipment specifications

The experimental setup has been designed and constructed at the University of Western Cape (UWC) specifically for the measurement of hydrogen permeability (flux rate) through composite membrane reactors. The system has been designed to handle a pressure up to 10 bar and with a furnace that can heat up the system to 600^{o}C maximum. A schematic overview of the setup is given in figure 3.4

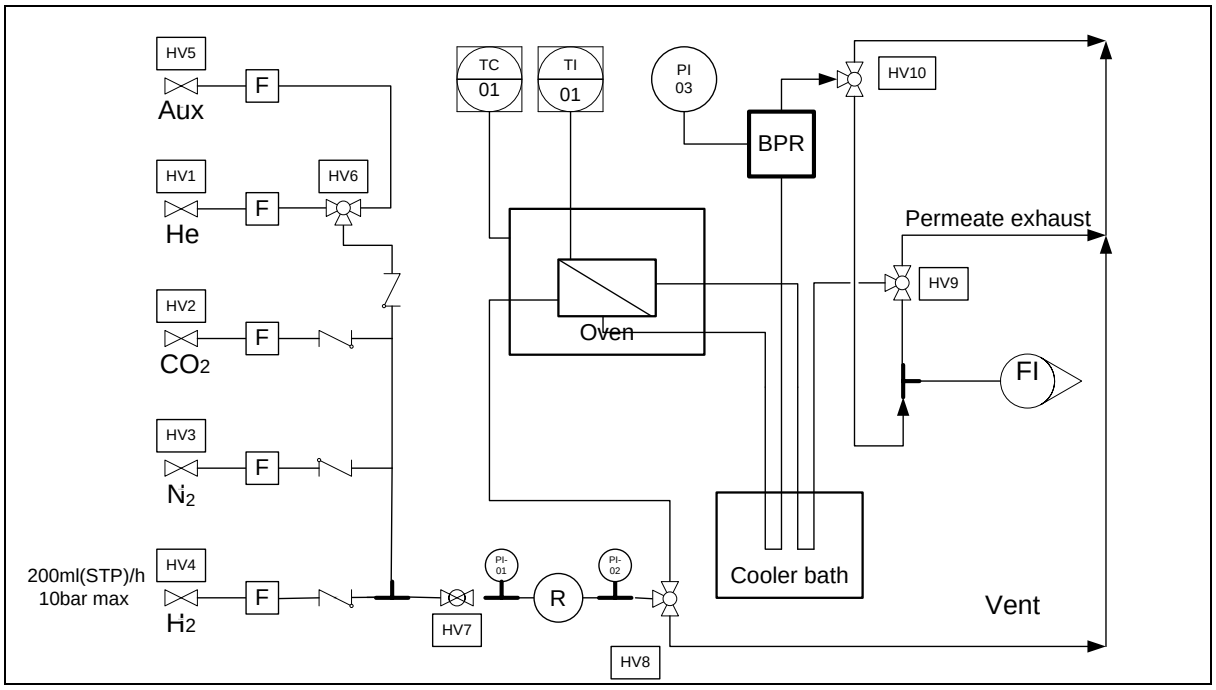

Figure 3.4 Process flow diagram for hydrogen permeance testing unit

The set-up consists of a feed section, membrane reactor section, cooling section and the measurement section. The feed section consists of different gas lines (He, H_2, CO_2 and N_2) which supply the gases into the system at a pressure of 20 bars from cylinders. A pressure regulator R (0-20 bar) and back pressure regulator BPR (0-7 bar) from Swagelok are used to control the pressure of the gases supplied into the system. The BPR is used to regulate the system pressure of permeate and non-permeate, it also acts as a relief valve, if the system pressure builds over the operating specification. The membrane section consists of a membrane reactor, as shown in **section 3.2** encapsulated inside a furnace**.** The membrane and a pre-heater are encased within the oven. This is equipped with two thermocouples (K-type thermocouple). One of these measures the temperature of the furnace and the other measures the gas temperature entering the membrane from the pre-heater. The cooling system consists of a water bath filled with water and a coiled tube within the bath to cool

permeates from the membrane reactor before the flux measurement section. After the cooling section, the gas can be directed to the soap flow meter or exhaust stream. Figure 3.5 represents a cross section of the equipment encased inside the furnace.

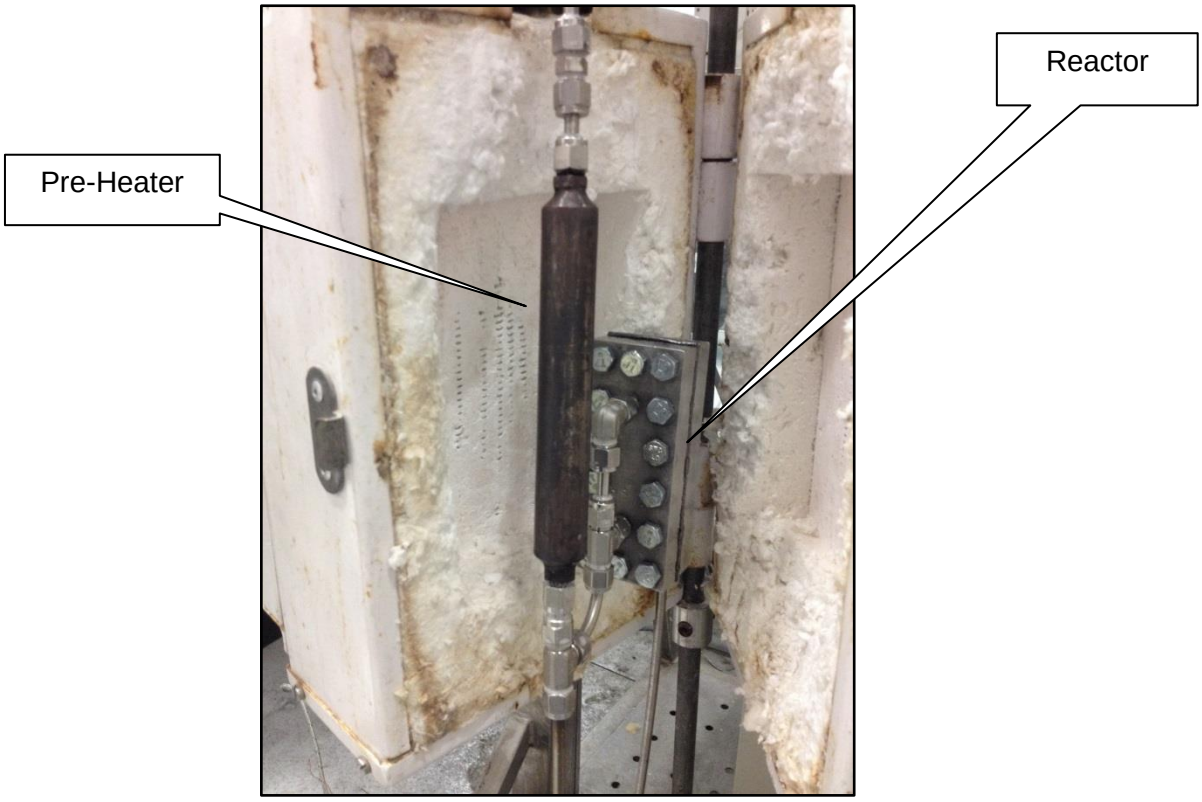

Figure 3.5 Cross section views of a furnace with a pre-heater and a membrane reactor

3.4.2 Experimental procedure

The assembled reactor shown in **section 3.2** which is encased within the furnace in figure 3.5 was first tested for leaks at room temperature by using nitrogen. Ideally, nitrogen does not permeate through palladium silver alloy provided the membrane film is defect free, therefore it was used for checking for leaks on the membrane. Subsequently, the leak free membrane was attached to the permeance setup represented by figure 3.4. After this the entire setup was tested for leaks by nitrogen gas at room temperature. Thereafter, the membrane reactor was heated by the furnace to the desired temperature (300-450^{o}C). Once the system had reached a steady state at desired temperatures, nitrogen was further used for leak testing of the membrane reactor and system before hydrogen exposure. The permeability of hydrogen was measured at different temperatures as a function of system pressure. The objective of this study was to benchmark the hydrogen flux before the water gas shift reaction, in order to

correctly select the right size of mass flow controllers and investigate the hydrogen exposure behaviour on the membrane film.

3.4.3 Thermal cycling of the membrane

In order to investigate the proposed objectives in chapter one, the thermal stability test was conducted. The membrane was cycled under nitrogen and hydrogen in order to evaluate the heat effect on the membrane. The membrane was also exposed to a higher temperature for a long period of time until the membrane failed. Nitrogen was used to test the failure mode of the membrane reactor, since a defect free membrane will not permeate any gas through other than hydrogen at elevated temperatures.

3.4.4 Permeability tests

The permeability of Pd-Ag was tested on the station described section in 3.2 represented by figure 3.4. A series of experiments were conducted at different temperatures and pressure in order to benchmark the permeability of the film. The long term permeability of the membrane was also investigated for a period of 250 hours. The durability of the membrane under different process conditions was also investigated using the permeance testing station.

3.5 Water gas shift experimental set-up

3.5.1 Process set up description and equipment specifications

The water gas shift reaction set-up was designed and built based on the permeability of the membrane reactor, which was tested as described earlier in **section 3.3**. The purpose of this unit is to produce ultra-pure hydrogen through the use of a palladium based reactor, which was built as explained in section 3.2. A process flow diagram for WGSR is represented in figures 3.6 and 3.7. The set up consisted of four major sections feed sections, heating section, cooling system and analysis.

Figure 3.6 Water gas shift testing station pictorial overview

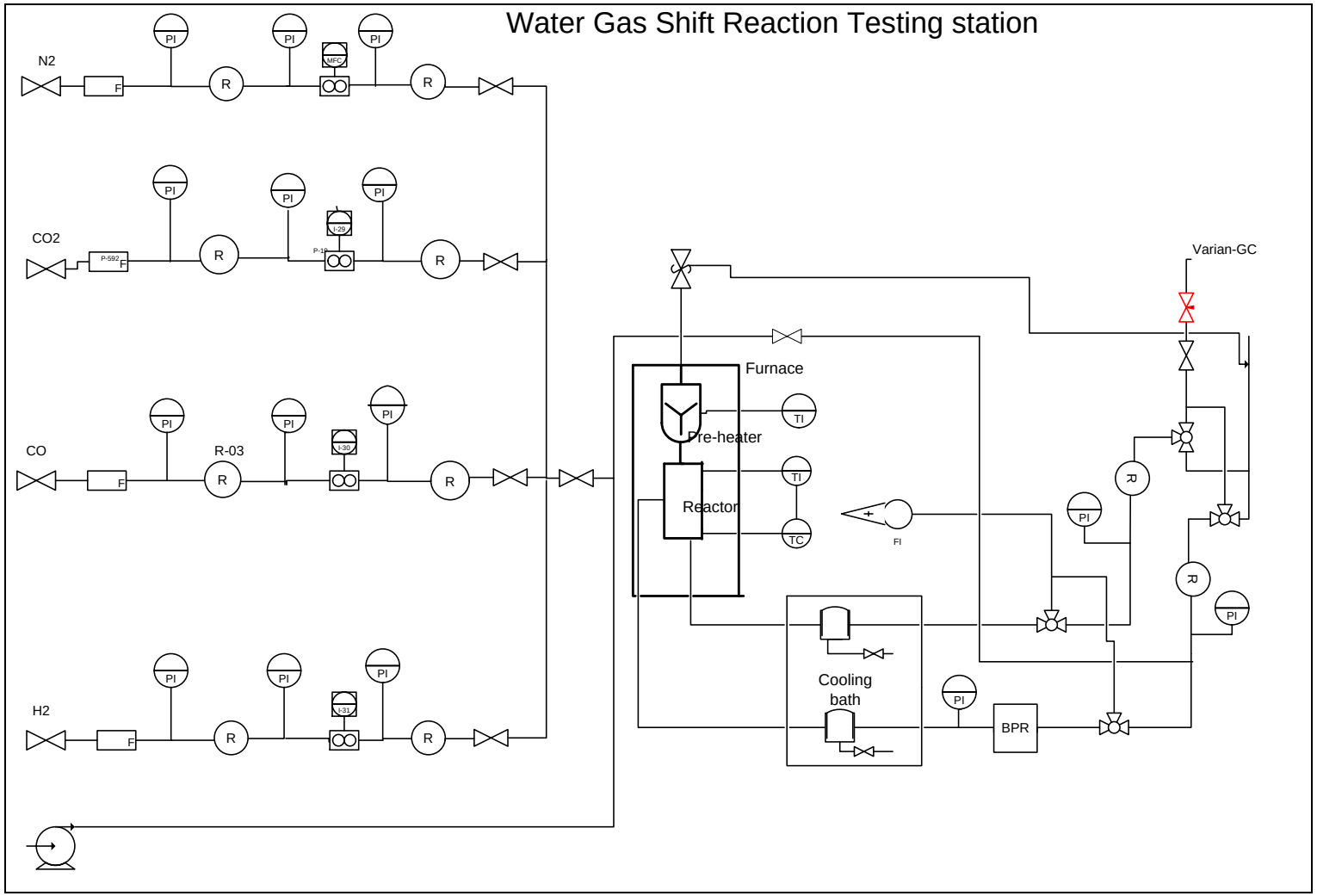

Figure 3.7 Convectional process flow diagram for water gas shift reaction

Figures 3.6 and 3.7 represent the water gas shift reaction testing station. The feed section consists of four different gas lines (N_2, H_2, CO_2 and CO) supplying the gases at different pressures. The gases were supplied at 80 bars from different gas cylinders, pressure regulators (403 bar-103 bar) fitted with pressure indicators from Swagelok to reduce the pressure to the desired pressure. An HPLC pump (A series (II) pump) with a flow range of (0. 001-5ml/min) self-flush, pulse damper SS was purchased from SMI-Labhut Ltd. The pump was used to supply distilled water at the desired flow rate at room temperature. The mass flow controllers were purchased from Bronkhorst High-Tech 15ml/min CO and with pressure up to 20 bar to control the feed rate of the gases. The heating section consists of a pre-heater filled with silica beads; the pre-heater was connected in series to the membrane reactor**.** A relief valve (20 bars) was purchased from Swagelok and connected to the system for safety reasons.

The feed stream is also connected to the reject stream and exhaust stream, the feed stream connected to the exhaust is controlled by the pressure relief valve to avoid excess pressure built up in the system in relation to figure 3.7. Back pressure regulator BPR up to 20 bars was purchased from Air Liquide to control the system pressure. The membrane reactor encased within the furnace was loaded with an Iron-chrome based high temperate catalyst. The catalyst was supplied by HiFUEL. Table 3.1 shows the catalyst properties

Table 3.1 Catalyst specifications

Name	**Ferro-chrome**
Phase	Solid
Load density	1260kg/m3
Shape	Pellets, 5.4mm*3.6mm
Recommended GHSV	<7500 hr^{-1}
Recommended temperature	320-500 ^oC

The other major section of the water gas shift reaction set-up is the gas analysis; a micro Varian gas chromatography which is a two channel base was used. A CP-4900 Micro Gas Chromatograph that uses two gases as carrier gas N_2 and H_2 was used for the analysis of gas compositions. Firstly, the GC was calibrated with pure gases (N2, H2, CO and CO2) in order to develop different retention time for the gases. The injection temperature was set to 100^{o}C to ensure there is no moisture entering the system. The column temperature and pressure was set at 100^{o}C and 50 kPa respectively. The injection volume ranges from 1-10µL.

3.5.2 Experimental procedure

The system represented by figure 3.6 and 3.7 was also tested for leaks before experiments took place for safety reasons; nitrogen at room temperature was used. The membrane was kept under N_2 atmosphere during heating. The system was flushed with N_2. Relative to the P&ID represented by figure 3.7, the direction of the product was directed either to the soap meter, GC or exhaust gas depending on the desired results. Lab - View was used to set the mass flow controllers to the desired flow rate. The system was then heated to the desired temperature. A minimum time of 30 minutes was given for the system to reach a steady state (stabilise) after any change of a process variable. A series of experiments were conducted varying the process variables in order to fulfil the proposed primary objectives of the research.

3.6 Membrane characterization

In order to fulfil objective 4 described in chapter 1 of this research, different analytical techniques were used to characterize the membrane after being exposed to different process conditions

3.6.1 Scanning electron microscopy and Energy dispersive spectroscopy

The scanning electron microscope (SEM) is a type of electron microscope that is used to image the surface of material by scanning it with focused high energy electron beam in a raster pattern. The Pd-Ag foil was analysed for surface change before and after hydrogen exposure, in order to develop a better understanding of surface changes. The samples were coated with carbon and fitted with an aluminium sample holder. Energy dispersive spectroscopy is an analytical technique used in the elemental analysis of samples. EDS was carried out to identify if intermetallic diffusion occurred between the Pd-Ag and the PSS support material. The optimized setting for both EDS and SEM are tabulated in Table 3.1.

Table 3.2 Operating condition for SEM and EDS

Optimized SEM operating conditions	Energy	3 kV
	Spot size	9
	Working distance	15
	Tilt	0^o
Optimized EDS analysis conditions	Energy	5kV
	Spot size	10
	Working distance	30
	Tilt	33°

3.6.2 X-ray Diffraction

X-ray diffraction is an analytical tool used for identifying the atomic and molecular structure of a crystal, in order to provide information crystal parameters and identification of unknown crystalline materials. The membrane crystallinity was analysed using PAN analytical X'pert pro diffractometer with CuKα radiation, with a wavelength of 1.54 as a radiation source of operating at 45kV and 40mA. The XRD diffractometric pattern was observed between 0-90^{o}.

Summary

This chapter had outlined the preparation methods for Pd-Ag membrane reactor for the production of hydrogen from WGSR. The process flow diagram below summarises the method used to address the problem statement from chapter one.

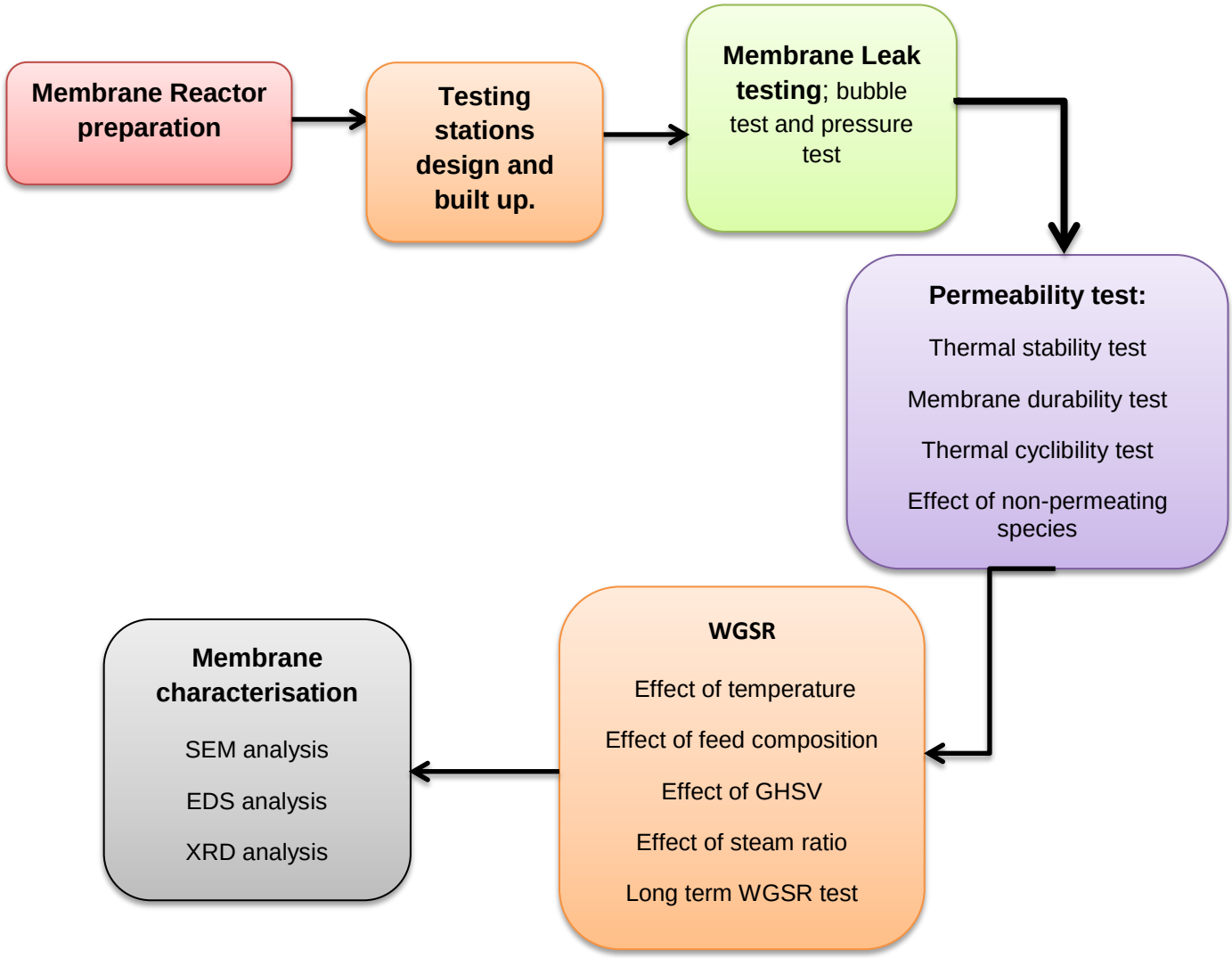

Figure 3.8. Process flow diagram for the entire experimental process procedure

CHAPTER FOUR:

4 RESULTS AND DISCUSSION

4.1 Chapter outline

This chapter reports and discusses the results obtained in this work. The chapter is divided into four major sections. The first **Section A,** revises the project objectives of this work, **section B** discusses the permeability of pure hydrogen through the Pd-Ag membrane and evaluates the effect of process variables on the membrane durability and hydrogen permeation stability. **Section C** discusses the production and performance of a membrane reactor for the Water Gas Shift (WGS) reaction. The last **section D,** discusses the post surface characterisation of the membranes using XRD, SEM and EDS.

Section A

The following objectives were derived to address the problem statement discussed in chapter one:

- To study the permeability, selectivity and long term stability of palladium-Silver membranes towards hydrogen exposure.
- To study the thermal cycling and thermal stability of a Pd-Ag membrane under hydrogen exposure.
- To produce high purity hydrogen through the WGS reaction through the use of a Pd-Ag membrane reactor.
- To investigate the effect of process variables (pressure, flow rate, temperature, steam to carbon monoxide ratio and different feed compositions) on the membrane stability and permeability towards hydrogen.
- To investigate the effect of hydrogen permeance and WGS reaction on the degradation of the palladium-silver membrane.

Section B

This section discusses the permeability of pure hydrogen through the Pd-Ag membrane reactor. The ideal selectivity of the Pd-Ag membrane and the effect of non-permeating species on hydrogen permeation rate were investigated. The permeability of hydrogen at different temperatures was measured. Lastly, the thermal stability and membrane durability under hydrogen exposure is discussed.

4.2 The selectivity of Pd-Ag membrane

The Perm-selectivity of a Pd based membrane is its ability to only allow certain gases to diffuse through the membrane (permeate) and not allowing other gases to diffuse through it (the non-permeate). In this work, hydrogen is the only gas that is supposed to diffuse through the Pd-based membrane. From literature (Amandusson *et al.* 2001; Basile *et al*. 1996a; Caravella *et al.* ,2010), nitrogen and helium are gases mostly used as a reference point to quantify the selectivity of a perm-selective membrane. Nitrogen was used to check for defects (pinholes, cracks and sealing problems) in this work. A series of experiments were conducted to leak test the Pd-Ag plate membrane reactor as detailed in chapter 3. To investigate the ideal selectivity of the prepared membrane reactor, N_2 gas was supplied in the system and the pressure of the system was monitored for 6 hours at 25°C and 320°C as shown in figure 4.1. The Knudsen diffusion equation for binary mixtures was used to calculate the perm-selectivity of the membrane.

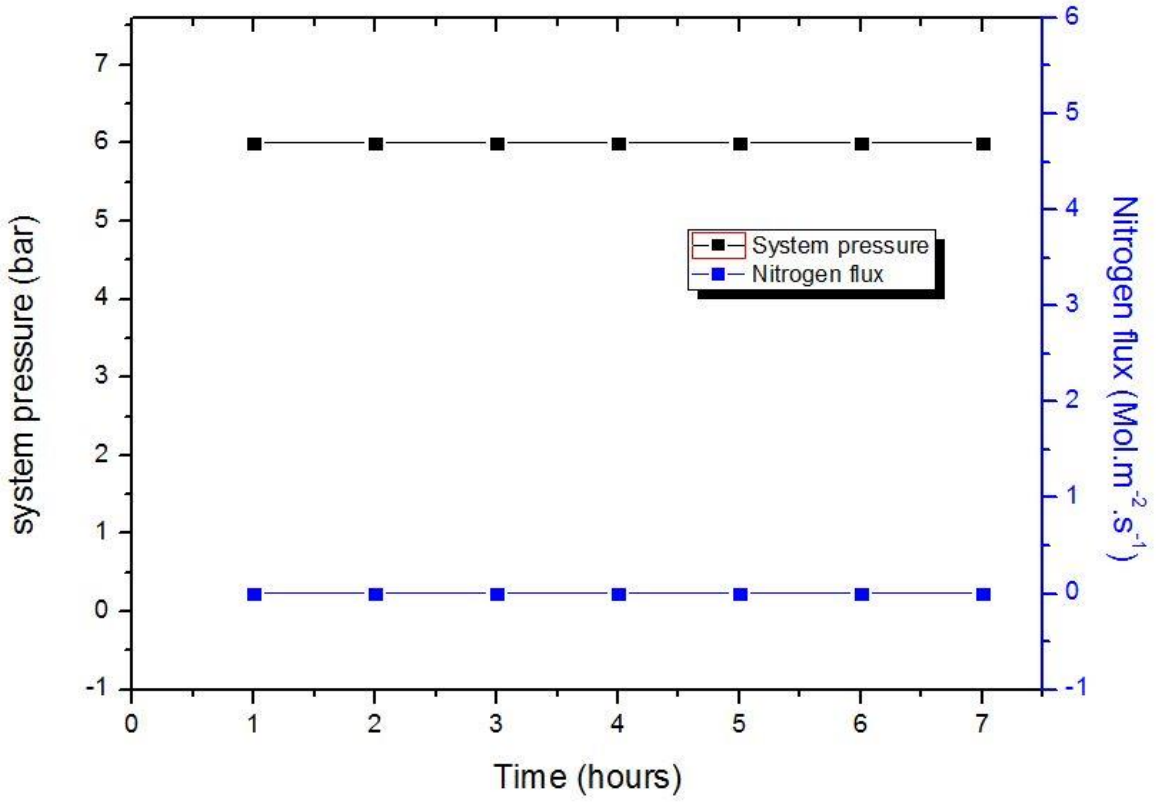

Figure 4.1 Perm-selectivity of Pd-Ag membrane reactor at 25°C and 320°C

Nitrogen gas was supplied into the system at 6 bars, the feed valve was then closed, and the system pressure was monitored. The pressure remained at 6 bars at both temperatures of 25°C and 320°C. The system pressure was monitored for 6 hours to check for leaks and to measure for nitrogen flux. The pressure remained unchanged for 6 hours both at 320 °C and at room temperature. The flux of nitrogen was found to be zero. This was an indication that the membrane reactor was free from defects such as pinholes, and the entire system was leak free. According to the Knudsen equation for binary mixture diffusion, represented by equation 4.1. The Knudsen number represents the selectivity of the membrane between permeable species and none-permeable species. The equation expresses the ratio of permeate to non-permeate. K_n represents the Knudsen number, and J_{H2} and J_{N2} represent the hydrogen and nitrogen flux respectively.

$$Kn = \sqrt{\frac{J_{H_2}}{J_{N_2}}} \quad \text{..... Equation 4.1}$$

The fact that zero nitrogen gas permeated through the Pd-Ag membrane reactor shows that the membrane has infinite selectivity towards hydrogen, since no defects were detected. Therefore, K_n as calculated by equation 4.1 is infinite. Some studies (Mardilovich *et al.* 1998; Guazzone *et al*. 2006; Tosti , 2015) also reported a defect free membrane reactor. A study by Morreale *et al*. , (2003) used helium gas for leak testing the membrane, since helium cannot automatically permeate the membrane unless there are defects in the membrane. Both gases (N_2 and He) are inert gases can be used for benchmarking the selectivity of a membrane. A study Morreale *et al*. (2003) reported an infinite selectivity at room temperature; however, the performance of the membrane did not continuously show infinite selectivity at elevated temperatures, because the membrane was damaged at higher temperatures, allowing helium gas to pass through. In the work presented in this thesis, nitrogen did not permeate through the membrane prior to hydrogen exposure. The permeability of hydrogen through the membrane was tested at different process conditions. As soon as hydrogen is exposed to the membrane, defects were only observed after hydrogen exposure on the membrane.

4.3 The permeability of hydrogen through the Pd-Ag membrane at different temperatures

Membrane permeability refers to the ability of a gas to diffuse through a solid material due to partial pressure difference. This work evaluates diffusive flow. Gas permeability is the volume of gas passing through a material of unit thickness per unit are and unit time under unit partial pressure difference between two sides of material. To determine the permeability of a Pd-Ag membrane supported by porous stainless steel (PSS), a series of experiments for pure gas (H_2) and binary mixtures (H_2 and N_2) were conducted. The permeability of hydrogen was investigated at different temperatures as shown in figure 4.2. The permeability of hydrogen was calculated based on Sieverts equation (equation 4.2) for ideal gas diffusion. Assuming the Sievert ideal gas diffusion, the “n” value was assumed to be 0.5, which suggested that bulk diffusion was the rate limiting step for hydrogen transport through the metal membrane. Figure 4.2 represents the permeability of hydrogen at 320°C, 380°C and 430°C.

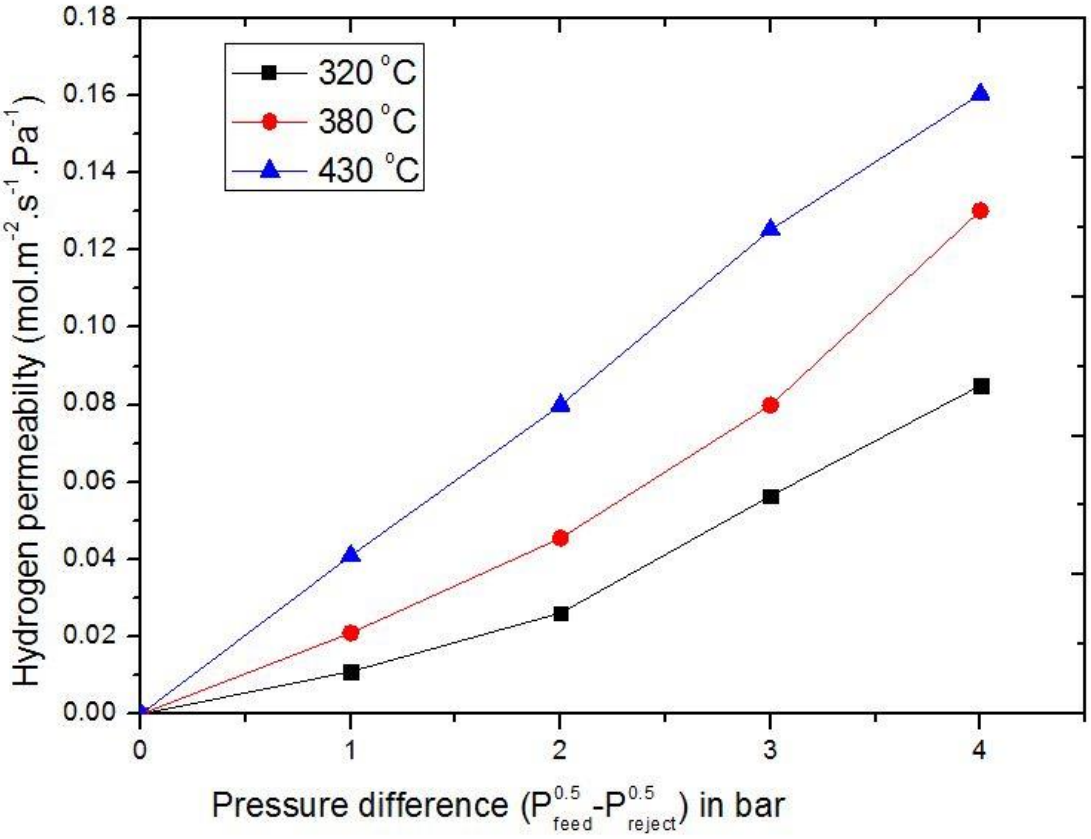

Figure 4.2 Permeability of hydrogen at different temperatures

Figure 4.2 represents the permeability of pure hydrogen as a function of pressure difference (P^n_{feed}- P^n_{reject}). Upon exposing the membrane to hydrogen at different temperatures, hydrogen started permeating through the membrane within 2 minutes. The hydrogen flux was measured after a steady state of permeation was achieved. The hydrogen permeability was calculated based on Sieverts law represented by equation 4.2 J_{H2} represents the hydrogen flux (mol.s^{-2}.m^{-2}) P_{feed} represent the pressure of the feed, P_{rej} represent the pressure of reject stream (Pa), µ represent the membrane thickness (micro meters).

$$J_{H2} = \frac{Q}{\mu}({P_{feed}}^n - {P_{rej}}^n) \quad \text{..... Equation 4.2}$$

The permeability of hydrogen through the Pd-Ag membrane was found to be 0.0021 mol. m^{-2} s^{-1}. Pa $^{0.5}$ at 320°C and 1 bar, and the maximum permeability of 0.165 mol.m^{-2}.s^{-1}.$Pa^{0.5}$ at 480°C and 4 bars attained. A partially linear relationship can be observed between hydrogen flux and pressure difference in figure 4.2. A study by Osemwengie (2007) measured the permeability of

pure Pd and Pd-Cu based membrane at same temperatures as for current studies, the study showed low permeability relative to the obtained permeability's for Pd-Ag at same conditions.

Indeed, the Pd-Ag membrane based membrane has shown again to have a higher permeability in comparison to pure Pd based membrane reactors for same process conditions. As the pressure of the feed (P^n_{feed}) increases, the driving force which is the pressure difference (P^n_{feed}-P^n_{reject}) also increases, which results in higher hydrogen flux. An increase in temperature also induces a positive effect on the permeation rate of hydrogen through the membrane at a constant pressure. From Sievert's equation which represented by figure 4.2, for equal driving force which is (P^n_{feed} -$P^n_{recj)}$, but at different temperatures, the permeability is greater at higher temperatures.

The reason why the permeability of hydrogen through the membrane increases as the temperature increases is that the adsorption energy for diffusion dominates the exothermic energy for adsorption of hydrogen through the membrane. Therefore, at a higher temperature, the diffusion rate of hydrogen is also higher. Similar results were reported by other Researchers (Morreale *et al*. 2003; Hara *et al*. 2012; Okazaki *et al.* 2006; Uemiya *et al.* 1991) . The permeability of hydrogen through the metal is also dependent on the solubility and diffusion coefficient of the gas through the membrane. Therefore, it is desirable to have a higher diffusion coefficient together with the larger value of solubility in order to achieve higher permeability. The permeability of hydrogen increases as the temperature increases as shown in figure 4.2. But for ceramic membrane normally used for hydrogen purification, permeability of hydrogen decreases as the temperature increases (Chein *et al.* 2013).

It is widely accepted and detailed in the literature that hydrogen permeation through the membrane is limited by a series of steps which are involved in the process of transporting hydrogen molecules through the membrane. Since Sievert plot assumed an ideal behaviour and diffusion of a gas, a linear relationship was not observed. From figure 4.2, the "n" value was assumed to be 0.5, which suggested that the rate limiting step for hydrogen transportation through the membrane is bulk diffusion of hydrogen atoms. However, a linear relationship did not occur as expected based on the calculated correlation of regression factor R^2<0.8. Therefore, the "n" was iterated for predicting the rate limiting step of hydrogen. This process is detailed in section 4.3.1.

4.3.1 The rate limiting step for hydrogen transportation through Pd-Ag membrane

There are a series of steps which are involved during the transportation of hydrogen through the metal membrane. The rate limiting step can be predicted based on the "n" value from the

Sievert's equation. The "n" value was obtained for each temperature by iteration methods. The value of "n" was iterated between "0-1". Figure 4.3 represents the fitted "n" value to result in a linear relationship for Sievert's plot. If "n" =0. 5 the bulk diffusion of hydrogen is the rate limiting step. If "n"=1 the surface contaminations is the limiting step for hydrogen transport. If "n">0.5 it is likely there is surface contamination which can be the rate limiting step.The "n'' value was found to be 0.523 at 320°C and 0.65 at 380°C and 0.62 at 450°C. This suggests that at 320°C the bulk diffusion of hydrogen can be the potential rate limiting step for hydrogen permeability, since the value is close to 0.5. A study by Thoen *et al*. (2006) investigated the permeability of hydrogen through a Pd-Cu membrane with a thickness less than 20μm reported an "n" value of 0.533 at 320°C. This value is closer to the obtained value for this current work. For different alloy composition of Pd membrane, but for same temperature, the "n" value are comparable.

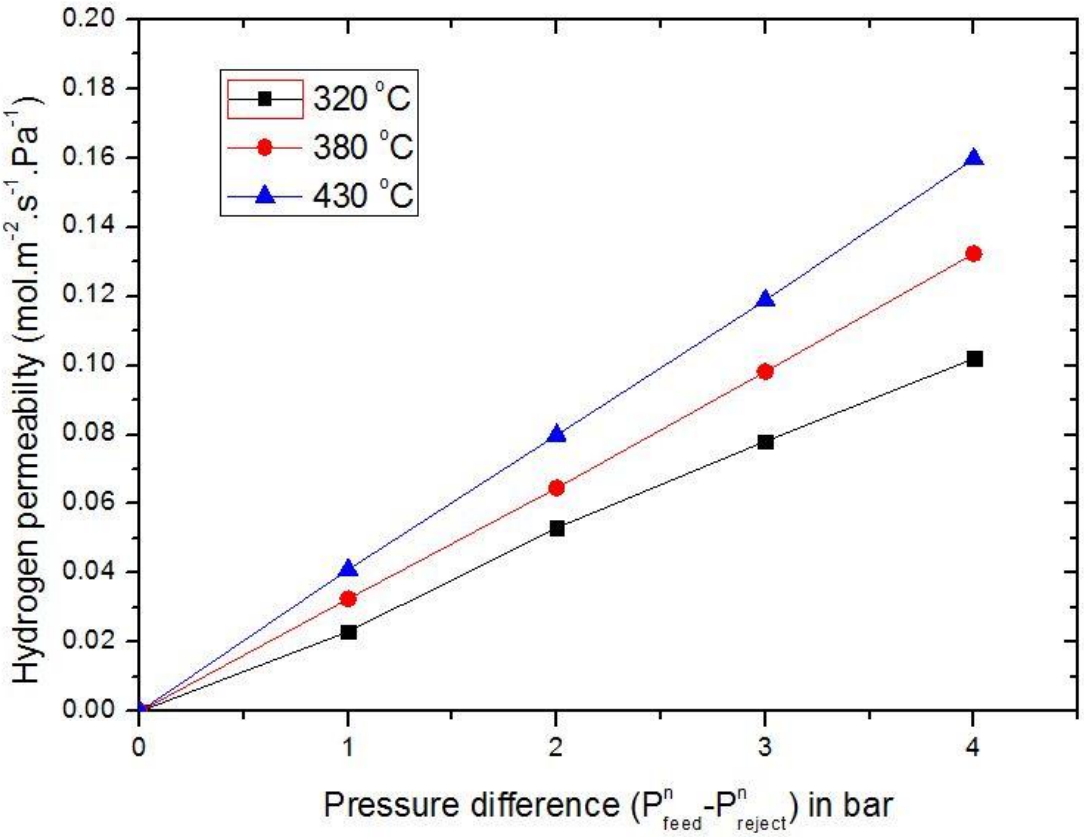

Figure 4.3 fitted with n value for Sievert plot

At 380°C and 450°C, the "n" value was iterated to fit a linear relationship, the "n values" were found to be 065 and 0.62 respectively. Therefore, bulk diffusion was the rate limiting step only

for 320°C. At 380°C and 450°C surface contamination can possibly be the rate limiting step for hydrogen permeating through the metal membrane.

There is no proper correlation reported in literature between the temperature and “n” values. A study by Basile *et al*. (2011) reported a different rate limiting step for hydrogen transportation with similar process conditions as for this current work, with different the membrane alloy compositions. Table 4.1 lists different “n” values obtained by other researchers with different process parameters from to this current wok. It has been observed that the “n-values” deviate from Sievert’s law of ideal diffusion. Hydrogen dissociation at the membrane surface is also outlined in literature as part of the rate limiting step, and the “n” value ranges from 0.55 to 1. Only a single study with a value less than of 0.5 was reported in relation to table 4.1. A value less than 0.5 suggest that the rate limiting step controlling the permeation rate is difficult to predict.

Table 4. 1 Different types of n values for obtained by other researchers

Membrane thickness	Temperature	N value	Regression coefficient	Permeance $mol.m^{-2}.S^{-1}.Pa^{-1}$	Reference
20µm	320	0.523	0.99864	$5.45*10^{-7}$	**Current work**
Pd-Ag	380	0.651	0.99548	$7.45*10^{-6}$	
	430	0.632	0.9941	$8.23*10^{-6}$	
8µm	350	0.5	0.9991	$7.93*10^{-10}$	(Mardilovich *et al*. , 1998)
Pd	470	0.646	0.9999	$5.03*10^{-7}$	
	500	0.434	0.9998	$1.169*10^{-5}$	
2 µm	300	0.5	Not specified	$2*10^{-9}$	(Bernard , 1996)
Pd-Cu	350	0.5			
19 µm	250	0.58	Not specified	$6.18*10^{-9}$	(Guazzone *et al*. , 2006)
Pd-Ag	250	0.64			
10 µm	380	0.5	Not specified	$3.43*10^{-9}$	155
Pd/V	480	0.5		$4.9*10^{-9}$	
11.4 µm	450	0.6	Not specified	$3.32*10^{-9}$	(Li *et al*. 2000b)
	500	0.57		$5.84*10^{-9}$	
1mm	765	0.62	0.963	$6.14*10^{-12}$	(Morreale *et al*. , 2003)
Pd-alloy	900	0.62		$1.05*10^{-11}$	

A study by Morreale *et al.* (2003) showed that “n” values greater than 0.5 are commonly reported for ultra-thin supported palladium membrane. The “n” value of 0.5 indicates the ideal solution diffusion of hydrogen atoms through the palladium membrane is governed by bulk diffusion of hydrogen atoms. Only 3 studies from table 4.1 reported n=0.5 with different membrane thickness, different alloy compositions and operating at different temperatures, but the bulk diffusion of hydrogen was reported as the rate limiting step for all studies. Therefore, it can be suggested that there is no particular order or concrete process parameter which can be suggested as the controlling factor for rate limiting step during hydrogen diffusion through the membrane. According to Basile *et al*. (2001) the thickness of the Pd-foil, than the support material only affect the rate at which hydrogen is diffusing through the membrane, it does not add to the factor for rate limiting step for hydrogen transport.

4.4 The activation energy for hydrogen permeation

The Permeability of hydrogen through a Pd-Ag membrane is temperature dependent from collisions theory. As the temperature increases, the molecules tend to move faster, their average kinetic energy has been increased, and the molecules tend to break their inter-molecular bond quicker at higher temperatures, which results in a higher permeation rate. This process is better explained based on the Arrhenius equation for determining the activation energy. The Arrhenius plot is used to study the effect of temperature on reaction rates It is generally known that the permeability coefficient is temperature dependent; from prior studies by Adesina *et l.* (1995) relating the Sievert ideal gas law of diffusion with the Arrhenius equation for the rate of reaction, equation 4.3 is obtained. The activation energy E_a (KJ/mol) for a hydrogen atom through the membrane was related to the membrane performance through equation 4.3. The ratio (Q_o/μ) represents the pre-exponential factor. The product of (RT) represents the average kinetic energy, where (R) is the universal gas constant (8.314 J mol^{-1} K^{-1}) and (T) temperature in (K). Equation 4.3 was adopted from literature in order to estimate the activation energy.

$$J_{H_2} = \frac{Q_0}{\mu} EXP(-E_a/RT) \text{..... Equation 4.3}$$

Taking natural logarithms on both sides of equation 4.4, the Arrhenius equation is obtained.

$$\ln(J_{H2}) = \ln\left(\frac{Q_0}{\mu}\right) - \frac{E_a}{RT} \text{..... Equation 4.4}$$

The results obtained from the hydrogen flux on figure 4.5 for pure hydrogen permeability at different temperatures was used to compute figure 4.4

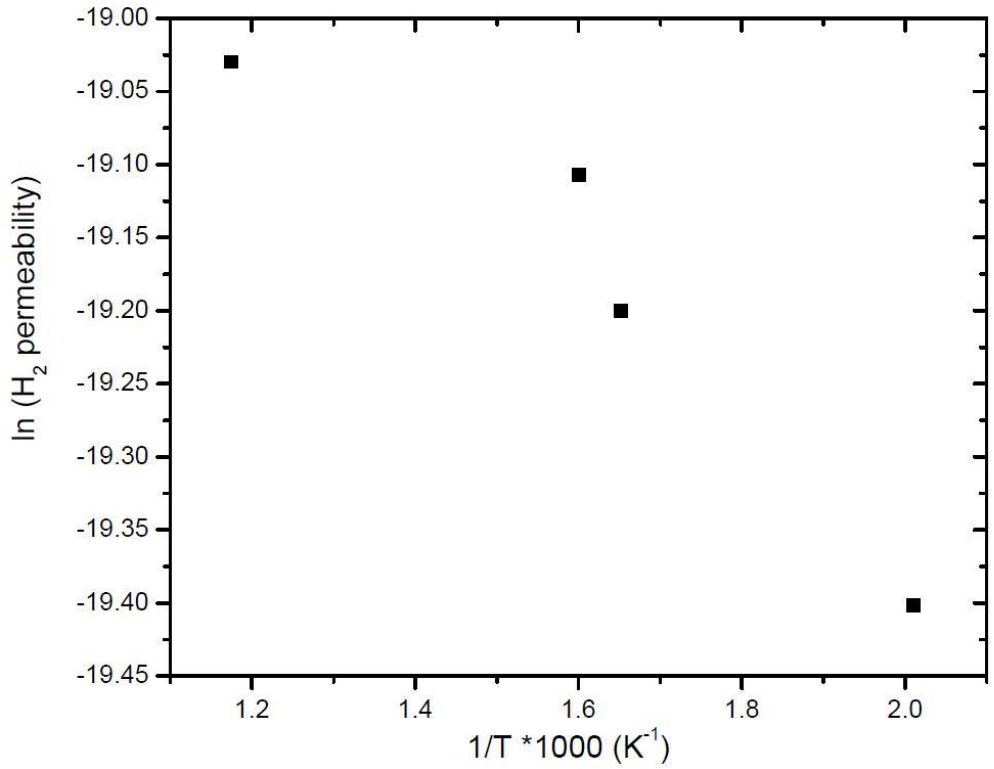

Figure 4.4 Arrhenius plot of the hydrogen permeability measured on the permeate side

Figure 4.4 represents the Arrhenius plot used to calculate the activation energy for hydrogen permeating through the membrane. It is known that the slope for the Arrhenius plot represent activation energy. A value of 10.543 KJ/Mol as the activation energy was obtained based on the slope of the graph in figure 4.4. The line of best fit with a regression correlation of R^2=0.9668 was used. The obtained activation energy is in line with what other researchers have reported by other . Table 4.1 gives different values for activation energy obtained by other researchers. It can be seen that the calculated value in this work is the lowest value in comparison to that obtained by other researchers. Therefore, a low value of the activation energy suggests that the rate of hydrogen permeation had occurred faster in comparison to other researchers.

There are a number of process variables which affect the value of the activation energy, since the value is calculated based on the hydrogen flux which is dependent upon process parameters such as support material, composition of the membrane and the thickness of the membrane.

Table 4. 2 the comparison of energy and permeability

Process parameters	E_p (KJ.mol^{-1})	Permeability Mol.m^{-2}.s^{-1}.Pa^n	Reference
Pd_{77}-Ag_{23}; supported on PSS,; 20µm	10.54	6.45*10^{-3}	**Current work**
Pd-Ag, supported on PSS, shell and tube design, with a sweep gas.	10.72	5.44*10^{-2}	(Diogo Manuel Pereira Mendes , 2010)
Pd/V. 20µm	16.38	8 .45*10^{-3}	(Mardilovich *et al*. , 1998)
Pd/ysz; 14.4µm Pd/Tio2: 25.3µm	15.67 29.2	0.0005 0.0026	(Straczewski *et al*. , 2014)
Pd, supported on PSS, 1000µm	13.81	1.92*10^{-9}	(Morreale *et al*. , 2003)
Pd-Ag, self-supported 800 µm	12.81	1.42*10^{-7}	(Holleck , 1970)
Pd/ V 70 µm	15.4	2.80*10^{-7}	Fletcher thesis
130-729 µm	18.56	2.20*10^{-7}	(Smithells&Ransley , 1935)

4.5 The effect of non-permeable species on hydrogen permeation rate

Perm-selectivity is defined as the ability of membrane to separate permeate from non-permeates (Yun , 2005). A series of experiments for a binary mixture with hydrogen as the key component species (permeable gas) were conducted to investigate the effect of external species (non-permeable) on the permeation rate of hydrogen at different temperatures. The flux of hydrogen was measured at different temperatures for different binary mixtures at constant pressure of 2 bars. Figure 4.5 represents the hydrogen flux as a function of temperature with different binary mixtures.

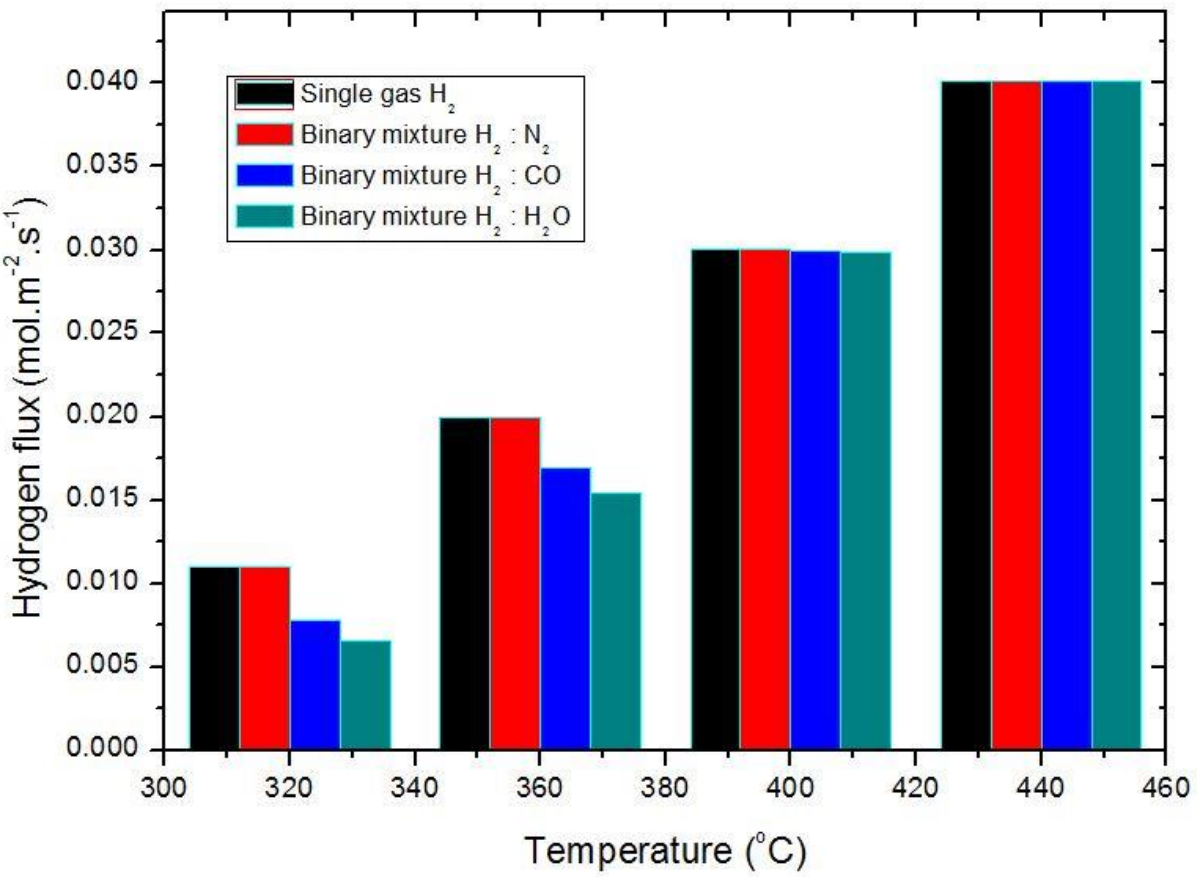

Figure 4.5 the Effect of binary mixture on Pd-Ag

The effect of non-permeable (N_2, CO, and H_2O) species on hydrogen flux was examined between 320-440°C at a constant pressure. Firstly, the permeation rate of pure hydrogen was measured at different temperatures. As expected the flux of hydrogen increased as the temperature increases because the average kinetic energy for hydrogen molecules is enhanced at higher temperatures. Furthermore, the solubility of hydrogen through the Pd-Ag membrane increases with an increase in temperature (Basile *et al.* 1996b). The composition of all mixtures investigated was 30% volume of non-permeable species and 70% volume of hydrogen was fed into a membrane reactor at different temperatures. For the H_2 and N_2 binary mixture, there was no significant effect of N_2 on the permeation rate of hydrogen at different temperatures, since N_2 is an inert gas, Therefore, the membrane showed infinite selectivity, since the measured flux of N_2 was found to be zero on the permeate side. The permeation rate of H_2 was not affected by the presence of N_2.

Similar results for infinite selectivity between H_2 and N_2 were also reported by Basile *et al*. (2001) for a defect free membrane at different process conditions .The effect of CO and steam was also investigated as shown in figure 4.5. A detailed summary of the observed effect of non-permeable species is given in table 4.3.

Table 4. 3 Effect of non-permeable species on the permeation rate of hydrogen

Components	320 ^{o}C and 2 bar	360 ^{o}C and 2 bar	400 ^{o}C and 2 bar	450 ^{o}C and 2 bar
H_2/N2	A negligible decrease on hydrogen permeation was observed.	No effect was observed	No effect was observed	No effect was observed
H_2/CO	The permeation rate decreased about 7%, due to competitive adsorption, between H_2 and CO	The permeation was also affected by the presence of CO about 2% - 5% decrease	No effect was further observed	No effect was observed. The competitive adsorption was suppressed by the increased temperature.
H_2/H2O	The permeation rate declined by 10%, a greater negative effect relative to CO at the same temperatures.	Same effect as the presence of CO, but steam showed more negative effect the permeation rate	Minor (0.1-0.9%) negative effect was observed relative to previous binary mixtures	No effect was observed

From figure 4.5 and table 4.2, it can be suggested that increasing temperature suppresses the negative effect of CO and H_2O on permeation rate, even though this is not fully supported by literature. A study by Amandusson *et al*. (2001) argued that the presence of CO in feedstock does not affect the permeation rate of hydrogen through a membrane. However, a study by Abdollahi *et al*. (2012) outlined that the presence of CO reduces the permeation rate of hydrogen on Pd-Ag membrane due to competitive adsorption, especially at low temperatures. Currently, there is no coherence in literature relative to the effect of CO on the permeation rate of hydrogen. For the present work, the presence of CO and H_2O has shown to reduce the hydrogen flux through the membrane. However, this negative effect towards hydrogen permeation was observed to be significant at temperatures below 360^oC. The presence of H_2O on a binary mixture has shown to have a stronger negative impact on the permeation rate of hydrogen in comparison to CO as shown by figure 4.5.

A study by Charudatta & Subhash (2006) investigated the effect of CO exposure on Pd metal membrane. The flux of pure hydrogen was measured before and after CO exposure on the membrane. This was not a binary mixture study which was conducted by Charudatta & Subhash (2006) revealed that the exposure to CO hardly influences the permeation rate of hydrogen at temperatures above 400°C. Furthermore, a study by Israni & Harold(2010) showed that there is a significant negative effect on hydrogen permeation when non permeable species are present due to competitive adsorption; the study revealed a decline in hydrogen flux due to CO. A study by Hou & Hughes (2002) reported that there is a potential for coke formation when there is an excess supply of CO on the membrane. The presence of coke will hinder the active surface site for hydrogen to dissociate and permeate through the membrane. The present work, confirmed the work conducted by (Amandusson *et al.* 2001; Israni & Harold , 2010; Hou & Hughes, 2002), that there is a significant impact on hydrogen permeation rate due to the presence of external species (non-permeable species). However, the effect was suppressed by increasing temperature; coke formation was not observed during the binary mixture tests in this work.

4.6 **The thermal cycling of Pd-Ag under hydrogen exposure**

The ability of a membrane to be heated and cooled without a change in structure and performance shows thermal cyclibility of a material. It is well established that heating and cooling of thin materials, tends to expand or contracts during the process. Few studies have shown robustness of the Pd-Ag membrane thermal cyclibility under exposure of hydrogen. In this work, the membrane was heated to 320^oC for 6 times at a constant heating rate of 7^oC/min, with

hydrogen exposure at each cycle. The membrane was cooled after 3 hours and other cycle was started again. Figure 4.7 represents the 6 cycles of heating and cooling the membrane under hydrogen exposure.

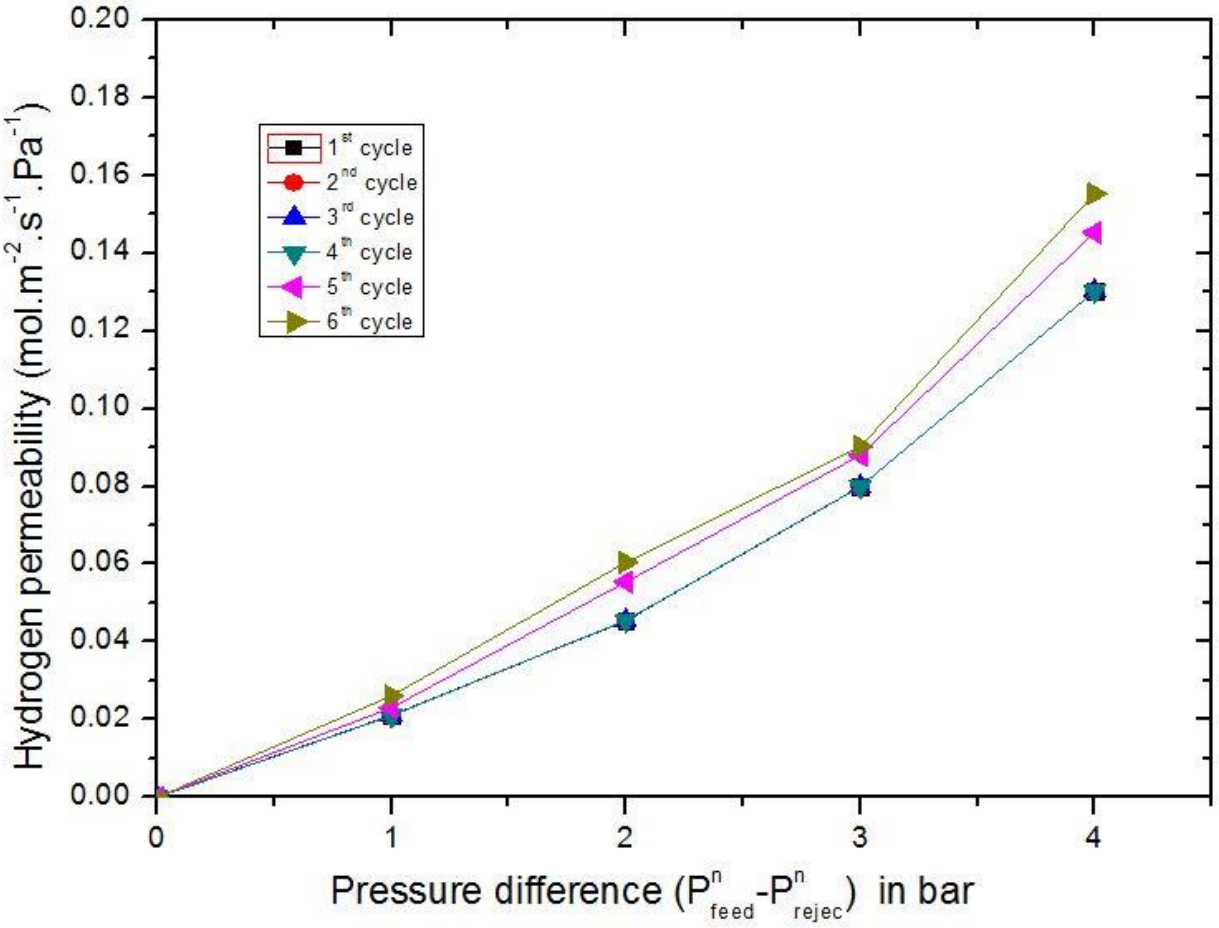

Figure 4.6 Thermal cycling of Pd-Ag at 350 degrees

From figure 4.6, Sievert plot was observed for the first four cycles, with consistent permeation results. During the first four cycles, the membrane did not allow nitrogen to permeate through the membrane, which was an indication that the membrane was defect free. However, on the 5th and 6th cycle, the membrane showed results which deviated from the first 4 cycles. The flux increased gradually from the initial results, and nitrogen started permeating through the membrane. Nitrogen was detected on the permeate side by the GC analysis. The membrane was dis-assembled and the structure of the membrane was seen to have changed significantly compared to the initial condition. Figure 4.7 shows the membrane before hydrogen exposure (A) and after thermal cycling under hydrogen exposure (B). The membrane had a uniform surface before the thermal cycling and hydrogen exposer. However, after thermal cycling and hydrogen

exposure the surface structure of the membrane changed significantly due to hydrogen atoms which remains stored within the membrane. In order to verify that indeed hydrogen was responsible for surface change, the membrane was also heated for 6 times under nitrogen exposure (no hydrogen present), and no surface changes were observed except a colour change due to heat. A study by Straczewski *et al*. (2014) investigated the thermal cyclibility of a membrane under nitrogen at different heating rates; the study reported no significant changes in membrane performance, except a continuous leak growth which was observed in the support material, the nitrogen flux increased slightly as reported due to mechanical failure of the membrane. Within this work, the membrane did not fail mechanically under nitrogen cycling, therefore it can be suggested that the membrane failed due to hydrogen.

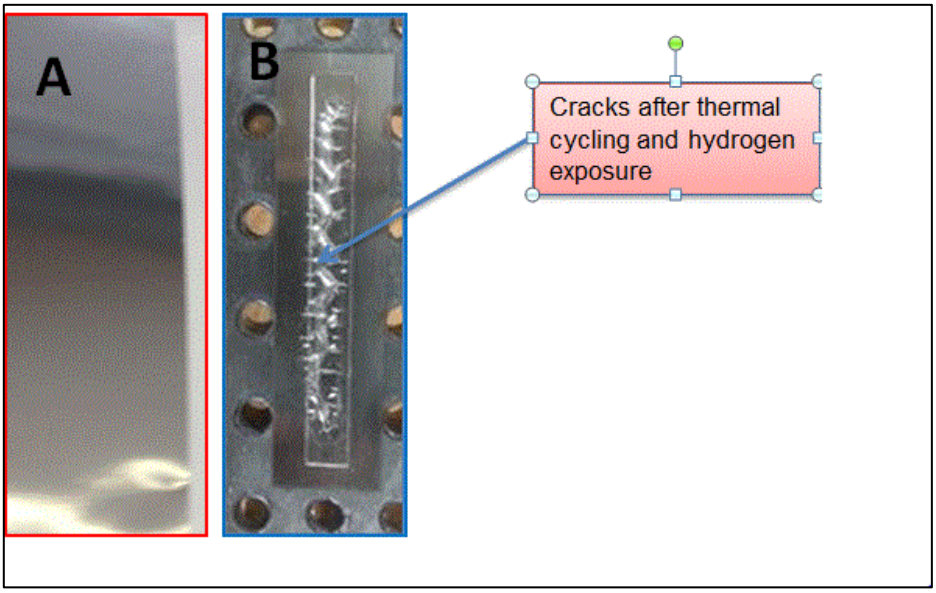

Figure 4.7 A) membrane before thermal treatment; B) membrane after thermal treatment under hydrogen exposure

The effect of thermal cycling on materials cannot be left unattended, since when thin materials are subjected to the temperature difference, the material tends to expand differential during the heating process. From Figure 4.7 a structural change on the membrane surface can be seen to have occurred due to hydrogen transport through the membrane (adsorption and desorption), not as a result of induced thermal stress. The material changed colour from silver to dark grey after thermal treatment and hydrogen exposure. The permeate side was darker grey in comparison to the feed side of the membrane. There evidence shows that the cracks were formed due to hydrogen loading, since the membrane under nitrogen cycling did not change structure nor formed any cracks; there was only a colour change under nitrogen due to heat.

Thoen *et al*. (2006) argued that palladium alloy does not suffer from thermal cycling problems. The study of Theon and co-workers carried out thermal cycling under nitrogen gas, and a similar effect was also observed under nitrogen cycling. But, a continuous loading of hydrogen in a metal, will cause variation in the concentration across the membrane thickness, which can result on concentration polarization of the membrane. Once hydrogen concentration polarization occurs, there is a possibility for a membrane to form cracks due to hydrogen stress on the surface of membrane (Shau *et al*. 2010). Furthermore, there is a high chance of metal hydride formation during a continuous loading of H_2 which can lead to a membrane failure. The membrane fails when a metal hydride is formed, due to volumetric expansion in the metal lattice. A detailed discussion on lattice expansion is given later in this chapter under post characterization (XRD). Logan (2001) explained the solubility process of hydrogen in metals, there is a high chance for a membrane failure under exposure of hydrogen due to the dissolving of hydrogen through the membrane. A 20µm thick Pd_{77}-Ag_{23} membrane used in this work suffered from thermal fatigue and concentration polarization due to continuous loading of hydrogen.

4.7 **Thermal stability of the Pd-Ag membrane under hydrogen**

A distinct difference exists between thermal stability and thermal cycling; thermal stability refers to the ability of a material to be stable (mechanical and chemical) at high temperature without a molecular decomposition. The thermal stability of a membrane within this work, refers to the ability of the membrane to diffuse hydrogen (permeate) consistently over time at higher temperatures. The long term thermal stability of a membrane is important for a membrane to be adopted for industrial purposes. The thermal stability of a Pd-Ag membrane was studied at two different temperatures at a constant pressure for a period of 230 hours. Figure 4.8 represents the relationship between hydrogen exposure over time at 320°C and 430°C.

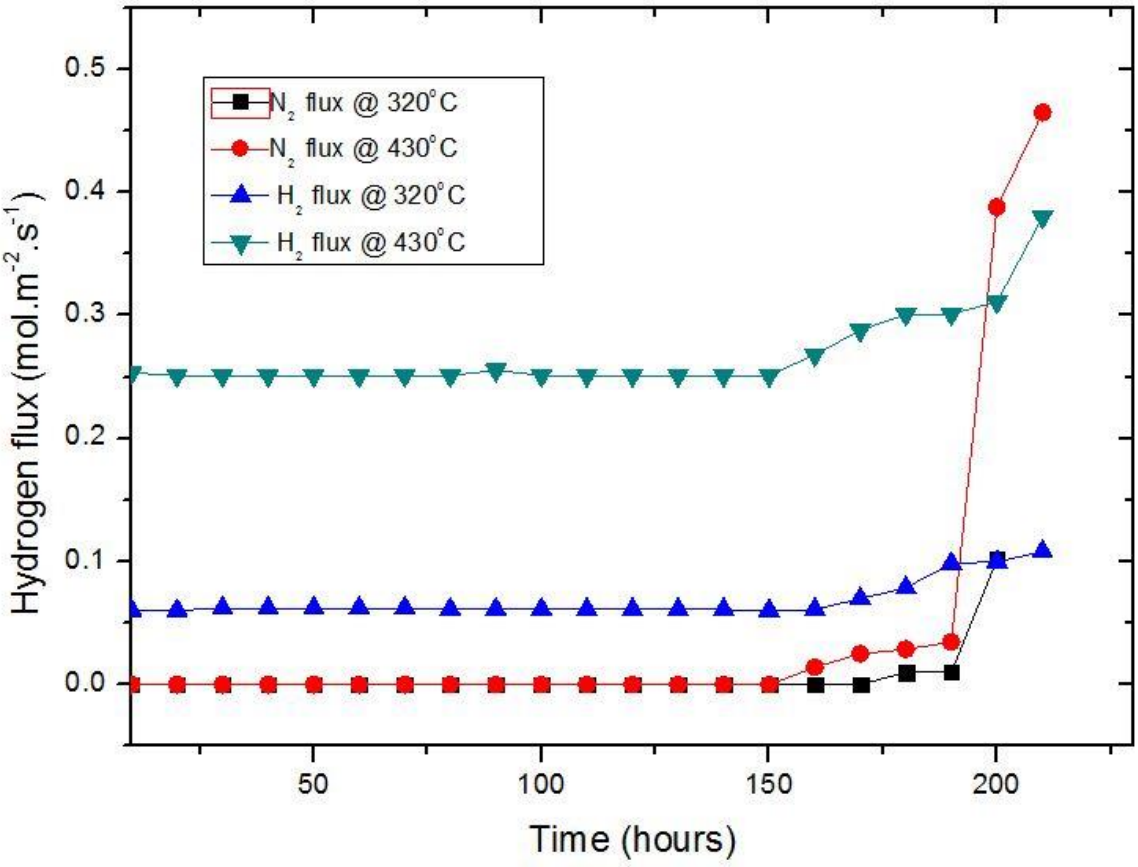

Figure 4.8 Thermal stability of a Pd-Ag membrane at a constant pressure

From Figure 4.8 the thermal stability was investigated for 230 hours at 320^{o}C and 3 bars. The membrane showed a stable permeation for the first 170 hours, with a minimal deviation. The membrane only allowed hydrogen to permeate through the Pd-Ag film. However, after a continuous exposure of hydrogen, at time equal 165 hours, the permeation rate of hydrogen started to increase, which suggested that there was a defect or a leak on the membrane. Nitrogen was used to check for defects. Nitrogen gas was observed on the permeate side of the membrane, which was an indication of the failure mode of the membrane at 320^{o}C. The passing of nitrogen through the metal membrane suggested that pinhole or cracks were formed after continuous exposure of hydrogen, as nitrogen cannot pass through a defect-free membrane. Furthermore, the thermal stability was also investigated at 430^{o}C as shown in figure 4.8. The permeation of hydrogen was initially stable for the first 30 hours, however, a minor decline of about 5% after 32 hours was observed. The observed declined persisted at a constant rate for 45 hours, then at time equals 84 hours the flux declined by 10-13% relative to the initial permeation rate. The decline was possibly due to intermetallic diffusion; EDS results showed

foreign atoms of iron (Fe) on the membrane. However, after 150 hours the permeation rate of hydrogen changed significantly, the permeation rate increased at fixed process parameters. The permeation rate increased due to defect formation at higher temperature after 150 hours.

A study by Cooney *et al*. (2014) investigated the thermal stability of palladium composites (Pd/V and Pd/Nb) at 500°C. The Pd/V composite failed within the first 20 hours, due to the Pd/V inter-diffusion between the support and metal membrane. The Pd/Nb failed after 48 hours due to poor mechanical strength and recrystallization process. For this work, the Pd-Ag has a face centred cubic (FCC) structure, which is more stable compared to the Pd/V which has a body centred cubic (BCC) structure. The BCC has a higher permeability in comparison to FCC but is less stable due to pore size. Cooney *et al*. (2014) also outlined that Pd/V suffers from hydrogen embrittlement quickly at temperatures below 350^{o}C which causes the membrane to break quickly. At temperatures above 350^{o}C Pd/V losses catalytic activity due to fragmentation. However, as outlined in literature, the threshold for pure Pd metal to encounter hydrogen embrittlement has been reported to be operating below 296^{o}C. So far, the longest reported defect-free membrane investigated for 1100 hours supported by PSS was tested at 450^{o}C for thermal stability (Mardilovich *et al.* 1998), however this membrane was continuously fixed during the operation. The membrane also failed after a period of time due to hydrogen adsorption on the metal which caused the lattice expansion by 3-4% (Mardilovich *et al.* 1998). In fact, during the 1100 hours of operation, the degree of hydrogen purity was compromised since non-permeable species were observed on the permeate side.

A study by Kajiwara *et al* (1999) suggested that the hydrogen stored in metals causes drastic microstructural changes in the host metallic matrix which can lead to undesirable changes in physical and mechanical properties of a material, such as hydrogen embrittlement. However, the failure mode which was encountered in this work was not due to hydrogen embrittlement, because the Pd-Ag was operated above the threshold for hydrogen embrittlement (296°C). Another study by Hawa, *et al*. (2014) also revealed that the Pd/Pt composite studied by them showed from poor thermal stability under hydrogen exposure. This was observed due to the continuous increase of nitrogen permeation through the membrane at 550^{o}C

In this work, higher and low temperature long-term exposure of hydrogen affected the stability of hydrogen permeation rate and the membrane life span. Major structural changes due to hydrogen adsorption and desorption (transportation mechanism) caused the membrane to have

surface cracks, which allowed non permeable species (nitrogen) to pass through the membrane. Lattice expansion was also observed from the XRD data. The XRD data is detailed in section D.

4.8 **Durability of the Pd-Ag membrane under hydrogen exposure**

The ability of membrane to withstand a variety of process conditions such as high pressures, high temperatures and poisonous compounds, while maintaining its performance over a long period of time without structural changes reflect durability (Augustine *et al*. 2012). Pd-Ag based membranes need to show long term stability and selectivity to be adopted for industrial process applications such as for a WGS reactor. An important factor highlighted by Alexander (2013) which literature has not robustly investigated is the leak growth mechanism of inert gases. However, this work focuses on the long term hydrogen exposure at different process conditions. Figure 4.9 represents the hydrogen permeation stability over 200 hours at different process conditions continuously.

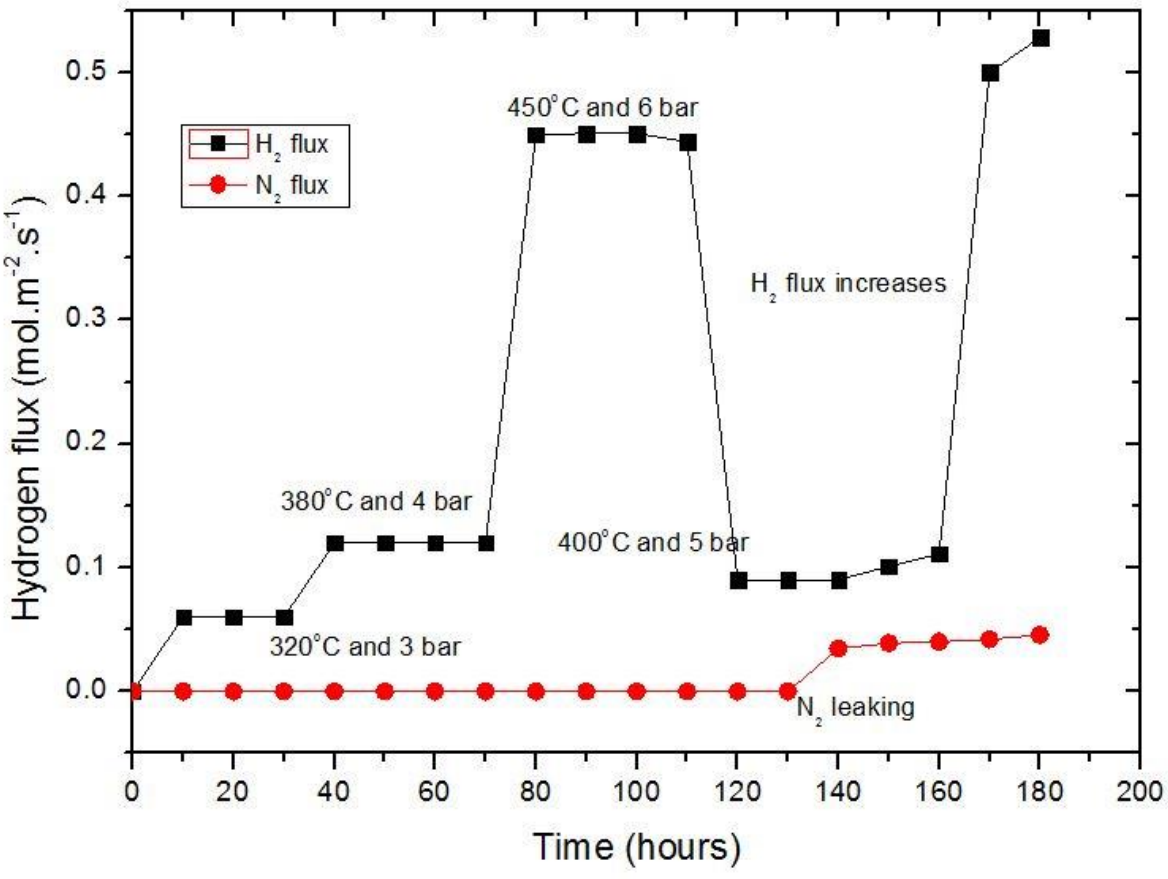

Figure 4.9 Long term permeability of pure hydrogen gas on Pd-Ag at 350^{o}C and 4 bars

After exposing hydrogen on the membrane, within 2 minutes hydrogen started permeating through the membrane. A steady state of hydrogen permeation was observed after an hour. Hydrogen gas continued permeating at a stable rate (0.053 $mol.m^{-2}.s\text{-}^{1}.pa\text{-}^{n}$) for 40 hours at 320°C and 3 bars. The nitrogen leak test was conducted before changing the process variables (temperature and pressure). No nitrogen gas (zero flux measurement) permeated the membrane after 40 hours. The temperature of the system was changed to 380°C and 5 bars. The permeation of hydrogen increased as expected, a stable permeation was observed for 40 hours. The process conditions were varied again; the temperature was increased to 450°C and 6 bars. The membrane showed a stable permeation at 450°C for 50 hours. The membrane was cooled down to 400°C, and at time equal to 150 hours, unusual behaviour was observed. The hydrogen flux started to increase gradually at fixed process parameters. Nitrogen was applied to the system through the entire process. After 160 hours, nitrogen gas started permeating through the membrane, which was an indication of defects (pinholes and cracks) on the surface of membrane.

Alexander (2013) investigated the long term selectivity between helium and hydrogen over time, with a 10 µm thick Pd-Ag membrane at temperatures between 350-450°C. The membrane failed due to three different types of leak growth mechanism which were reported to have occurred. Firstly, the membrane failed instantly at higher temperatures when there was a switch of gases between hydrogen and helium. Secondly slow leak growth was also observed over time, the membrane did not show stable permeation for the entire period tested. For this current work, the membrane failed due to continuous loading of hydrogen on the membrane. The membrane suffered from hydrogen attack due to the transportation of hydrogen through the membrane. Evidence of this is presented by XRD data that shows that lattice expansion (from 3.804Å to 3.880Å) occurred within the crystals, which resulted in the membrane cracking and forming spaces which allowed nitrogen to permeate through the membrane. It was highlighted by Basile *et al*. (1996b) that the nitrogen flux increased as the temperature increased, since the thermal expansion increases the diameter of pinholes thereby reducing the nitrogen permeation through the cracks and pinholes. Similar results were obtained for this present work, as time progress the flux of the inert gas (nitrogen) continued increasing as indicated by figure 4.9.

Some studies (Chein *et al*. 2013; Abdollahi *et al*. 2012; Cooney *et al.* 2014; Tosti *et al*. 2006; Criscuoli *et al*. 2000) reported the mechanical failure of the membrane was due to heat treatment and high pressure stress, because membranes were mostly thin. The mechanical failure occurred between the support material which is substrate and the deposited Pd- layer.

The Pd-Ag used in this work was supported by PSS, the membrane was exposed to nitrogen at high temperatures and pressures, but cracks and leaks were not observed. Therefore, this suggested that the hydrogen was responsible for damaging the membrane. Palladium cracks and membrane deformation were also observed at high pressures and temperature ranges of 830°C and 900°C by Morreale *et al.* (2003) due to continuous loading of hydrogen at higher temperature. As encountered from this work, the membrane failed quicker at higher temperatures.

Remarkable hydrogen permeation stability was observed by Edlund & McCarthy (1995) for 100 hours. However, the membrane suffered from leaks, leak growth occurred after 110 hours. Pre-existing defects from membrane fabrication were re-opened and the membrane failed. A significant obstacle in understanding the occurrence and mechanisms of leak growth in Pd-membranes was the lack of work presented in the literature dealing with the subject matter of leak mechanism of inert gases.

In order to increase the life span of a membrane, the thickness of the Pd foil can be increased, even though the feasibility studies by Criscuoli *et al.* (2001) recommend a thickness of 20µm for membrane reactors to be economically feasible. Although the membrane has been pointed out to have a potential to replace the multi-stage WGS reaction process, they have failed to show durability and complete selectivity over time at various process conditions under continuous exposure of hydrogen.

Section C

This section discusses the production and performance of the Pd-Ag membrane reactor. The performance of the membrane reactor was evaluated based on the recovery of hydrogen and the carbon monoxide conversion ability. Process variables such as temperature, steam to carbon monoxide ratio, Gas Hourly Space Velocity (GHSV) and feed composition were evaluated.

4.9 Pd-Ag membrane reactor for Water Gas Shift reaction

The Pd-Ag membrane reactor was used to produce hydrogen from the WGS reaction in the presence of a ferro-chrome catalyst. The Pd-Ag membrane showed the ability to produce

ultrapure hydrogen that surpasses equilibrium limitations of traditional packed bed reactors currently being used for industrial WGS reaction. The performance of the membrane reactor was evaluated based on the recovery of hydrogen and CO conversion ability. The following equations were used to evaluate the Pd-Ag membrane performance.

$$X_{co} = \frac{F_{co_{inlet}} - F_{co_{outlet}}}{F_{co_{inlet}}} \times 100\% \ldots\ldots\ldots \text{....equation 4.5}$$

Equation 4.5 represents the formula used to calculate the conversion of CO denoted as $X_{co.}$ $F_{coinlet,}$ represents the flow rate of CO entering the reactor and $F_{cooutlet}$ the outlet flow rate of CO on the reject stream.

The hydrogen recovery was calculated based on equation 4.6

$$H_{recovey} = \frac{H_{2\ Perm} - H_{2\ reject}}{H_{2\ perm}} \times 100\% \ldots\ldots\ldots \text{equation 4.6}$$

Based on equation 4.6 the hydrogen recovery was expressed in terms of the percentage of hydrogen on the permeate side ($H_{2\ perm}$) relative to hydrogen in the reject stream ($H_{2\ reject}$) .The Pd-Ag membrane reactor was operated at various conditions. A commercial catalyst for the high temperature -WGS reaction, ferro-chrome (Fe_2O_3-Cr_2O_3), purchased from REB was loaded in the catalyst channel before all reactions for WGS were conducted. The reactor was operated at temperatures ranging from 300-450°C. The pressure had no effect on the equilibrium conversion of CO, because of the equimolar on either side of the reaction. But it was also varied in order to determine the effect on hydrogen recovery rate. The Gas Hourly Space Velocity (GHSV) was also varied by changing the flow rate of the feed in order to investigate the optimum flow rate to achieve higher CO conversion and hydrogen production. The effect of varying the CO content at a fixed steam ratio was also investigated. Additionally, the effect of temperature was investigated.

4.9.1 Effect of temperature on the WGS reaction

A change in temperature occurs when heat is added or removed on a system. A change in temperature has two general opposite effects on membrane reactors used for this work. Firstly, an increase in temperature induces a positive effect on the permeability of hydrogen through the membrane, since the enthalpy of hydrogen adsorption and diffusion is greater at higher temperatures as illustrated by the pure permeability of hydrogen earlier on section 4.3. On the other hand, the WGS reaction is mildly exothermic; therefore the reaction is favoured by low

temperatures. The relationship between temperature, CO conversion and H_2 recovery at a constant catalyst loading is depicted by Figure 4.10.

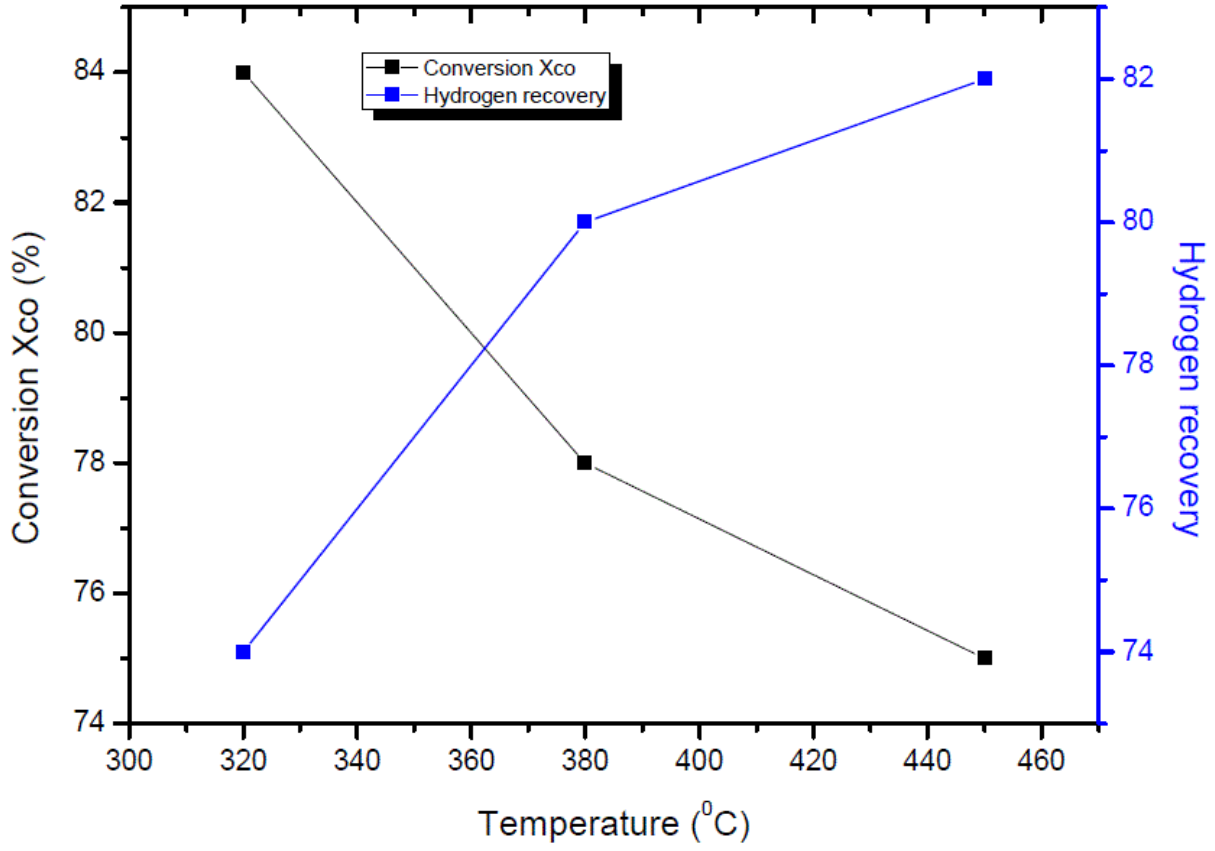

Figure 4.10 the effect of temperature on CO conversion and hydrogen recovery

From figure 4.10, the highest achieved conversion of CO was 84% at 320°C and 4 bars. At same conditions for the highest conversion, the lowest hydrogen recovery of 74 % was achieved. It can be observed from Figure 4.10 that an inverse relationship exists between the hydrogen recovery and the conversion of CO. As the temperature increases, the conversion of CO declined. The inverse relationship can be explained by Le Chatelier's principle for a reaction at equilibrium. An increase in temperature favours an endothermic reaction. In the case of the WGS reaction, the reverse reaction has been favoured since the forward reaction is exothermic. Therefore, with the increase in temperature the reverse reaction is favoured and the net rate of the WGS reaction decreases sharply.

However, higher temperatures favour reaction kinetics and the permeability of hydrogen. The highest hydrogen recovery of 82 % was attained at 450°C. At 320°C and 2 bars the lowest hydrogen was recovered from the product. Furthermore, the permeation rate for hydrogen produced from the reaction was low at 320°C in comparison to the permeation rate for pure

hydrogen in section 4.3 ; therefore the presence of steam and CO at low temperatures affected the permeation rate of the produced hydrogen. A study by Abdollahi *et al*. (2012) reported 99.9% and 90% CO conversion and H_2 recovery respectively at 300°C and 4.4 bars. The recovery was higher due to high pressure and the usage of sweep gas, which increased the driving force for hydrogen permeation relative to the current study. Furthermore, Diogo (2010) investigated the performance of a Pd-based membrane reactor, with the configuration of a shell & tube design. The reactor was loaded with a low temperature shift catalyst ($CuO/ZnO/Al_2O_3$) and N_2 was used as a sweep gas. The reaction was conducted between 200-300°C and a space velocity of 1200 $L_N \cdot k_{gcat}^{-1} \cdot h^{-1}$ was used. Almost 100% conversion was achieved with 80% of hydrogen recovery. The obtained conversion by Diogo (2010) is higher than for this current work because the reaction was carried out at lower temperatures favoring the equilibrium conversion to the right, and more hydrogen was produced. The hydrogen recovery was lower than for current work, even though an external driving force (sweep gas) was used to enhance the permeation rate. The recovery of hydrogen is lower because at temperatures below 300^{o}C the carbon monoxide presents on the feed side blocks the surface of the membrane which inhibits hydrogen permeation. A study by Augustine (2013) also investigated the performance of a membrane reactor and the effect of temperature on CO conversion and hydrogen recovery. Ferro-chrome was used as the catalyst. 98% and 81 % conversion and hydrogen recovery respectively were achieved at 400°C without the presence of a sweep gas. For this study, a higher permeation rate of hydrogen was achieved without the presence of a sweep gas. The higher permeation rate of hydrogen was achieved because of the higher temperature. The conversion of CO attained at higher temperatures was also higher than for normal traditional packed bed reactors. The continuous removal of hydrogen during the cause of the reaction made it possible to exceed the equilibrium limitations encountered in packed bed reactors used for the WGS reaction. Therefore, this suggested that the equilibrium shift effect described by Le Chatelier's principle played an important role in terms of achieving higher conversion at higher temperatures in comparison to traditional packed bed reactors.

4.9.2 Effect of steam ratio on WGS reactor performance

From the kinetics of the WGS reaction, the reaction occurs by following a mechanism known as redox (reduction-oxidation) as earlier explained in chapter 2. The quantity of hydrogen produced depends on the amount of steam supplied during the reaction. Industrial process that involves the WGS reaction are operated in an excess of steam, in order to favour the equilibrium shift (Diogo ,2010). However, the presence of excess steam in membrane reactors while conducting

WGSR has been reported to affect the hydrogen permeation rate negatively (Hwang *et al*. , 2013). A series of experiments were conducted to evaluate the effect of steam for a fixed carbon monoxide ratio at 350°C and 450°C. Figure 4.11 represents the relationship between H_2O/ CO and conversion at different temperatures.

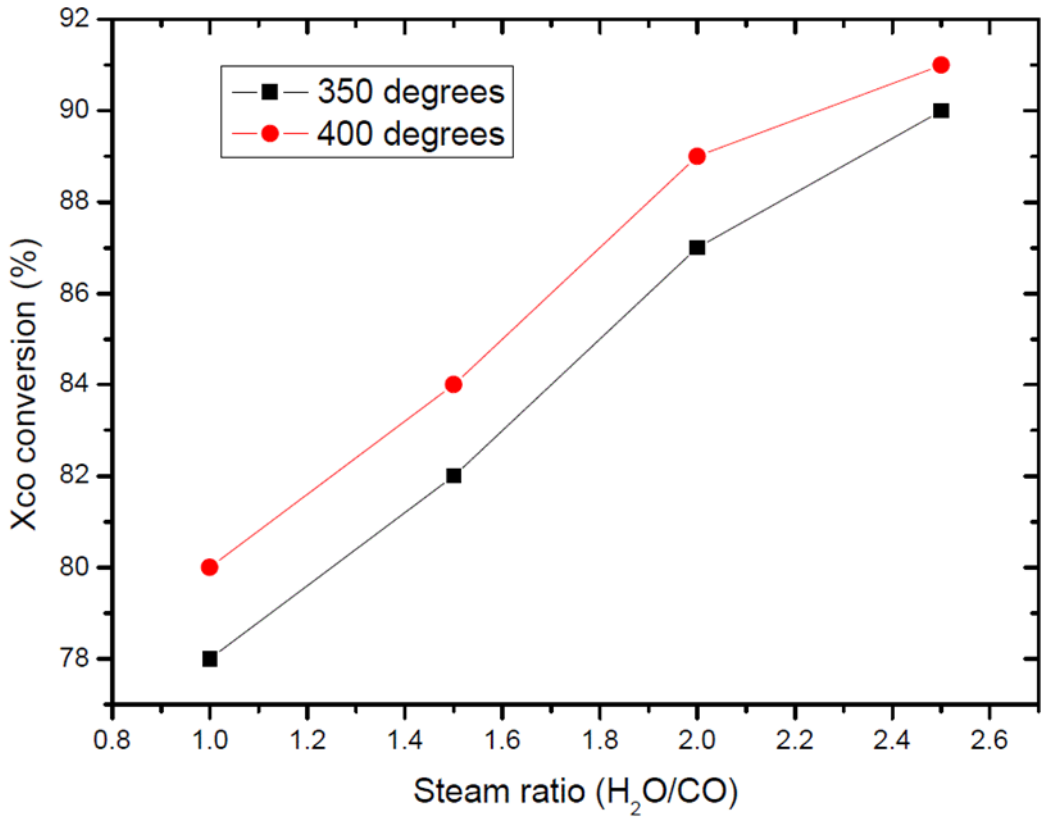

Figure 4.11 The effect of steam /CO ratio on conversion at different temperatures

The effect of the H_2O/CO ratio was investigated at 350°C and 400°C at 8 bars, the steam ratio was varied from 1:1 to 2.5:1 as indicated by figure 4.11. Linearity was observed between the conversion and H_2O/CO in figure 4.11. As the amount of steam supplied in a reactor is increased, the conversion also increases. This occurs due to Le Chatelier's principle, "an increase in the concentration of the reactants for a reaction in equilibrium, the forward reaction will be favoured in order to re-establish a new equilibrium"; therefore more products will be formed. Therefore, as more was hydrogen was being formed, more CO and steam were reacting, which resulted in higher conversion of CO when there is excess steam supplied.

It can also be noted for the same H_2O/CO ratio, but different temperatures, the conversion is greater at 350°C as compared to 450°C as depicted by figure 4.11. This occurs due to forward reaction is exothermic and is favoured by low temperatures. For same temperature as packed bed reactors, but changing the amount of steam supplied in the reaction, also induced a positive effect on the conversion of CO into CO_2.

The shift effect of equilibrium described by Le Chatelier's principle played a role in achieving higher conversion at higher temperature while using the membrane reactor. The conversion for current traditional packed bed reactors being used for industrial application of the WGS reaction is below 50% at temperatures above 320°C.This occurs because the reaction is equilibrium-limited in packed bed reactors. However, for a membrane reactor, the conversion is higher in comparison to packed bed reactors, because products are continuously removed at equilibrium (continuous permeation of hydrogen through the membrane), even though the reverse reaction was endothermic and favoured. But due to higher recovery rate (permeability) of hydrogen at higher temperature the conversion becomes greater. A similar relationship was also observed by (Diogo, 2010; Alexander , 2013; Iyoha *et al*. , 2007; Bi *et al*. 2009). A study by Basile *et al.* (1996b) reported 99.1% CO conversion at equilibrium with a steam to CO ratio (H_2O/CO) of 3.86 at 320°C, which is higher compared to the obtained value of 90 % conversion at H_2O/CO of 2.5 at 350°C for this work.

Figure 4.12 represents the hydrogen recovery as a function of steam/CO ratio at the same conditions used to study the effect of steam/CO ratio on the conversion of CO at different temperatures. According to a study by Tosti *et al*. (2006) the excess of steam has a greater negative effect on the permeation rate of hydrogen in comparison to CO content. If the steam is adsorbed on the surface of the palladium membrane, the adsorbed water dissociates according to equation 4.8 and 4.9 and recombines to form H_2O which hinders the permeation site for H_{ads} to diffuse through the membrane.

$$H_2O_{ads} \rightarrow OH_{ads} + H_{ads} \quad or \quad H_2O \rightarrow O_{ads} + 2H_{ads} \qquad \text{Equation 4.8}$$

$$2OH_{ads} \rightarrow H_2O + O_{ads} \quad or \quad O_{ads} + 2H_{ads} \rightarrow H_2O \qquad \text{Equation 4.9}$$

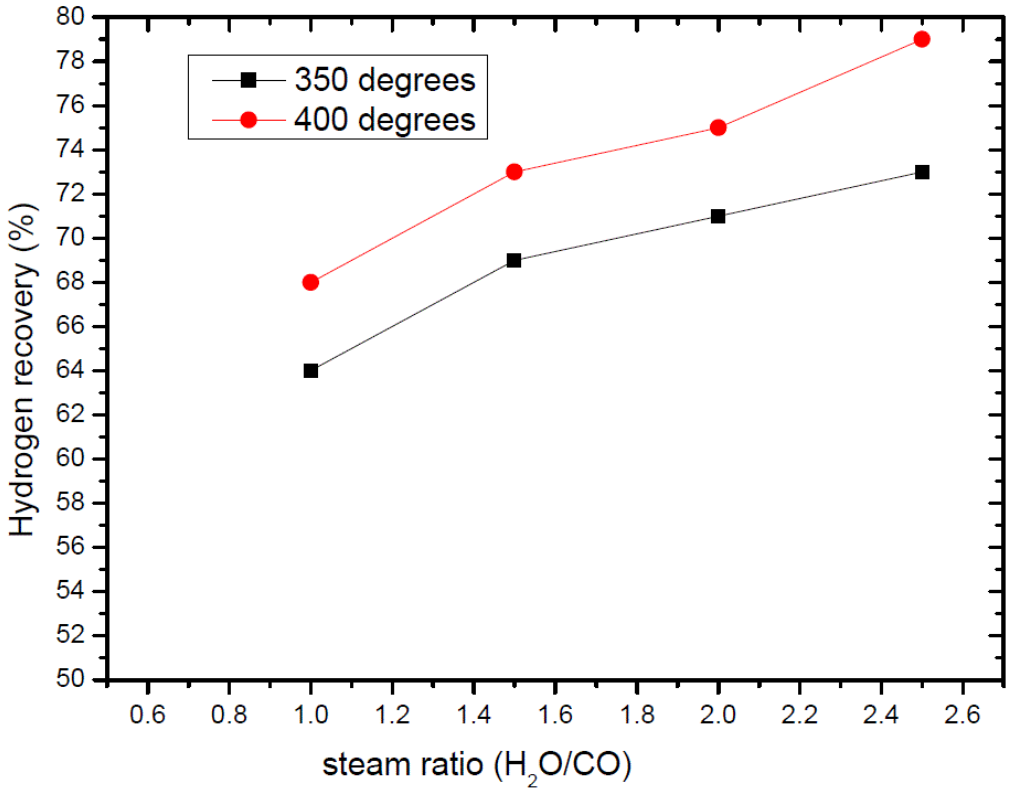

Figure 4.12 effect of steam/CO on hydrogen recovery at different temperature

From figure 4.12, the recovery of H_2 was higher at the higher temperature (400°C) as expected from literature. With a steam ratio of 2.5:1, 79% of the produced hydrogen was recovered. The hydrogen recovery partially increases as the steam ratio increases, since there is more hydrogen to be recovered from the steam. However, it is reported in literature that the higher steam content for a membrane reactor affects the permeation rate due to competitive adsorption. But the competitive adsorption was found to be limited at temperatures greater than 350°C earlier in this work for binary mixtures. It can be suggested that the competitive adsorption was suppressed at 400°C, since the hydrogen recovery is greater than for 350^{o}C for equal steam ratio. It can be observed that the CO has less effect in comparison to H_2O in relation to competitive adsorption. But increasing the steam ratio has a greater positive effect on the produced hydrogen, since the industrial process of WGS reaction is carried on excess steam.

However, a study by Osemwengie (2007) reported that a higher steam ratio lowers the CO conversion, due to the reason that the extraction rate of hydrogen declines as competitive adsorption occurs. However, within this work, the decline in conversion due to competitive adsorption was not observed in both temperatures of 350°C and 400°C.

A study by Augustine *et al.* (2011) investigated the effect of the higher steam ratio on membrane reactors. They indicated that a higher steam ratio leads to higher conversion. However, excess steam ratio causes hydrogen dilution on the membrane surface and the hydrogen recovery will decrease. In this work, the recovery did not decrease relative to an increase on the steam ratio. It was only found to be lower in comparison to pure hydrogen permeation rate. Therefore, the presence of excess steam causes a decline on permeation rate of hydrogen at low temperatures due to competitive adsorption between the steam and hydrogen. The permeation rate declined about 28% relative to the permeation of pure hydrogen.

4.9.3 Effect of Gas Hourly Space Velocity on conversion

It is generally known that the time reactants spent inside a reactor determines the degree of conversion for the reactants. For a batch reactor, conversion is expressed as a function of time. However, for this work, a Plug Flow R (PFR) reactor loaded with catalyst is assumed. Initially, the experiments were conducted by varying the total feed flowrate at fixed temperature and pressure of 380°C and 4 bar respectively. Figure 4.13 represents the relationship between the conversion and hydrogen recovery as a function of gas hourly space velocity.

.

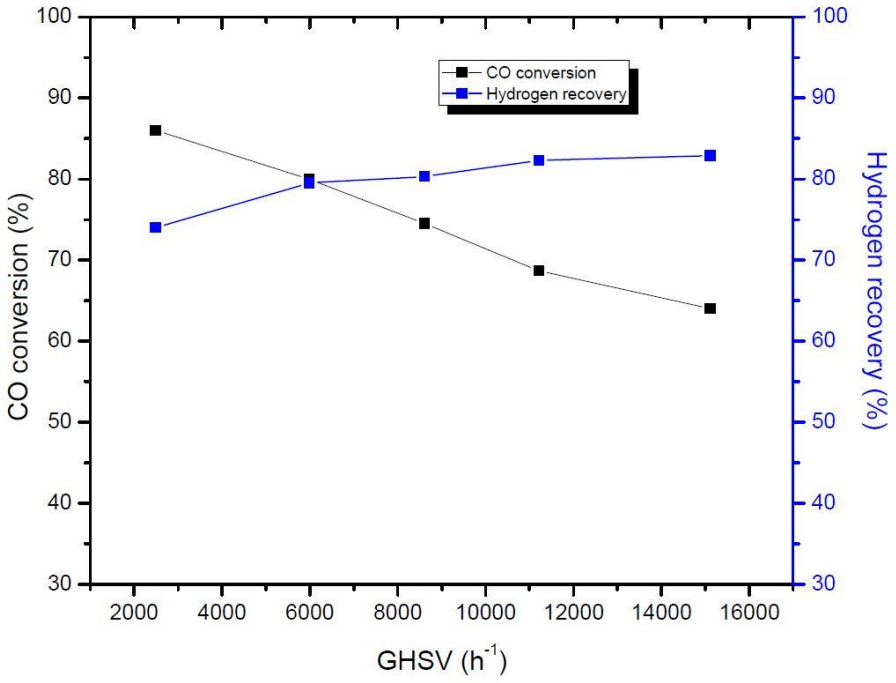

Figure 4.13 The conversion of CO and H_2 recovery versus GHSV at 350°C and 4 bars

The GHSV is defined as the volumetric flow rate per space volume. For this work, the GHSV was calculated based on equation 4.9, where V_o and V are the volumetric flow rate of the feed gas and the volume of the reactor based on the catalyst channel respectively.

$$GHSV = \frac{V_o}{V} \text{.....equation 4.9}$$

From figure 4.13, an inverse relationship was observed between the GHSV and the conversion of CO. As the GHSV increased, the conversion decreased. This is because the contact time between the reactants and catalyst loaded in the reactor is lower at the higher space velocity. The contact time is related to resident time, residence time is defined as the amount of time reactants spent inside a reactor. Mathematically, residence time is the reciprocal of the GHSV as represented by equation 4.10 where r_t denote the residence time.

$$r_t = \frac{1}{GHSV} \qquad \text{Equation 4.10}$$

The highest CO conversion of 86% was achieved at 2560 gh^{-1} with 75%hydrogen recovery. However, at higher GHSV there is limited time for hydrogen generation, since the contact time between the reactants and the catalyst is compromised, since the residence time is the reciprocal of the space velocity.

Higher GHSV implies short contact time between catalyst and reactants; As reported by Cooney *et al*. (2014) the recommended optimal space velocity for packed bed reactors is $4000h^{-1}$.On the other hand, the hydrogen recovery is favoured at higher GHSV, as the driving force is increased at higher flow rate because of the pressure which is partially increased which results in higher permeation rate for hydrogen. According to Bernard (1996) the Fe-Cr catalyst loaded in this reaction experiments is not suitable for small scale, because of the restriction in volume and their pyrophoricity and the requirement of the lengthy pre conditions steps before the reaction.

4.9.4 Effect of CO content on WGS reactor performance

The main goal of WGS reaction is to convert CO into CO_2 while converting H_2O into H_2. It is of importance to investigate the effect of CO content in the feed, since reformate comes in different compositions depending on the feed stock of the steam reforming. The extent of CO conversion is governed by different process variables such as catalyst type, residence time, steam ratio and temperature. However, the CO content affects the recovery rate of hydrogen during the WGS

reaction through membrane reactors. Figure 4.14 represents the effect of CO concentration on hydrogen permeation rate during the reaction and separation for different feed compositions of CO.

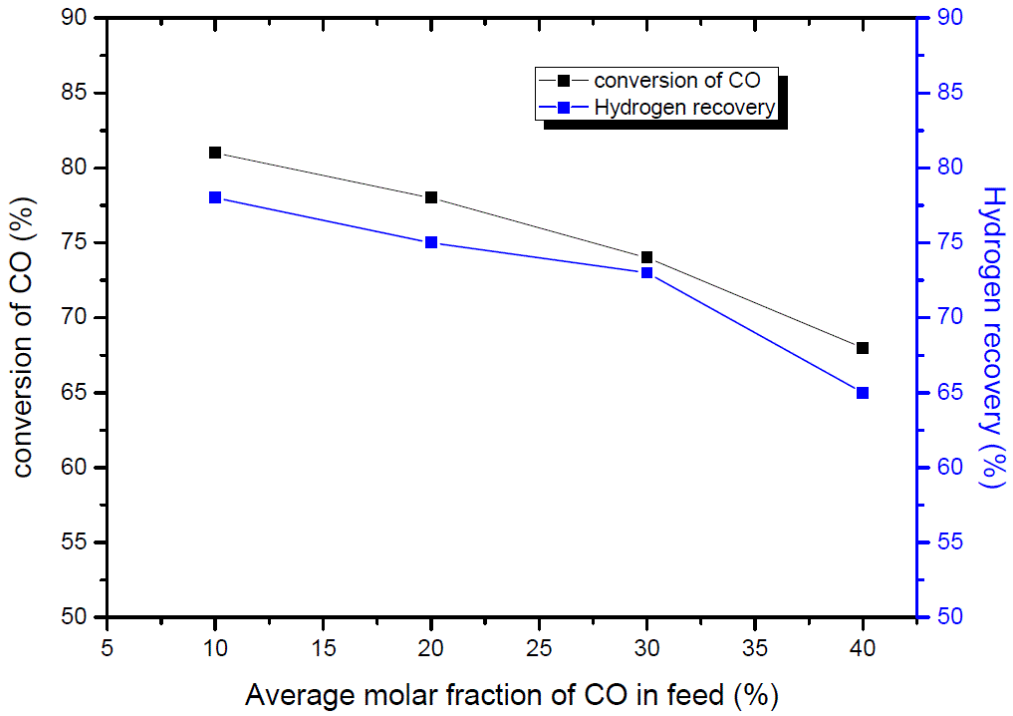

Figure 4.14 The effect of CO content on hydrogen recovery and Conversion at fixed steam ratio

The effect of CO was measured as the function of molar fraction of CO content at a constant temperature of 350°C.The composition of CO in the feed stream was investigated in the range of 10%-40%, to investigate the effect on conversion and hydrogen recovery. According to (Hou and Hughes, (2002) the presence of steam, CO, and CO_2 reduces the hydrogen permeation rate due to competitive adsorption. From figure 4.14, the conversion of CO decreased as the concentration of CO was increased. The decrease in the conversion of CO is due competitive adsorption of CO on the surface which results into a lower the recovery rate of hydrogen. The surface of Pd-Ag for hydrogen dissociation becomes limited when the concentration of CO is increased. Therefore, competitive adsorption between hydrogen and CO occurred strongly. The presence of CO displayed a negative effect on the permeation rate of hydrogen, but the effect is less in comparison to steam as previously observed. The difference in the effect exists because of different adsorption capabilities. The temperature of 350°C was chosen because the conversion and permeability was found to be optimal from previous sections, and the effect of CO is suppressed at higher temperatures for a minimum concentration of CO.

Barbieri *et al* (2008) described the presence of CO and H_2S in a feed stream as inhibitors and poisonous gases which do not only negatively affect the permeation rate, but also the life span of the membrane.

A review of by Gallucci *et al*. (2013) reported that CO affects the permeation rate of hydrogen, because there is a preferential adsorption of CO molecules on the same site used for hydrogen adsorption. From figure 4.14, the conversion is higher when the CO content is low. As the content of CO increases in the feed stream, the permeation of hydrogen rate also declines at the same proportion, and this effect is observed because the CO is adsorbed on the surface of the Pd- Ag, which hinders the diffusion of hydrogen through the surface. The adsorbed CO on the surface causes the hydrogen to diffuse slowly.

Basile *et al*. (2011) indicated that the presence of CO on the feed could cause a decline in the hydrogen permeation flux, due to the adsorbed CO displacing the adsorbed hydrogen and further blocking the adsorption site. However, these phenomena are more effective at temperatures below 150°C or if the concentration of CO is higher. However the effect of CO was observed to have less of an effect on hydrogen recovery as compared to Basile's work, since the temperature in this current research is above 150°C,

As outlined from literature the presence of CO in a feed stream acts as an inhibitor during the permeation of hydrogen through the palladium membrane due to higher energy adsorption. Inhibitors are strongly adsorbed on the membrane surface (Barbieri *et al*. , 2008) .The presence of H_2S and CO decreases membrane efficiency in terms of permeation. Work done by Hwang *et al*., (2013) with a similar reactor design configuration to the current work, similarly reported that the presence of CO affects the permeation rate of hydrogen since CO is an inhibitor.

Li *et al*., (2000a) conducted a similar study evaluating the effect of CO on hydrogen permeation. Lie and co-workers studies showed that CO affects the permeation rate of hydrogen negatively. However, the researcher did not indicate full operating details. A study by Unemoto *et al*. (2007) argued that the presences of non-permeable gases has no effect on the permeation rate of hydrogen, the work was carried at a temperature range of 500-600^{o}C. Relative to the finding for current work, the effect of non-permeable species is minimal at temperatures above 350^{o}C. A prior study by Abdollahi *et al.* (2012) highlighted that CO affects the permeation rate of hydrogen due to competitive adsorption at lower temperatures. This study has shown similar effects to those observed in literature; however, the effect can be suppressed by increasing temperatures which is not favourable for CO conversion at equilibrium.

4.9.5 Effect of feed composition on WGS reaction

The presence of non-permeating species has been reported to have a negative effect on the performance and life span of a membrane. For practical applications, the reformate products from steam reforming process does not only contained the desired species to be separated during the WGS reaction The presence of H_2O, CO ,N and CO_2 was investigated. Three different mixtures were investigated at constant pressure and temperature under the presence of a fixed amount of catalyst. Table 4.2 details the composition of feed investigated for the three mixtures.

Table 4.1 different feed compositions

	Components	%			
	H_2	CO	CO_2	H_2O	N_2
Mixture A	20	10	20	15	35
Mixture B	20	15	25	25	15
Mixture C	20	20	10	30	20

Figure 4.15 represents the conversion of CO as a function of temperature for three different mixtures. The conversion of CO declined as the temperature increases as expected, since the forward reaction is exothermic. It can also be observed that the conversion of CO declined as the concentration of CO increases. On the other hand, the presence of CO also causes membrane deactivation.

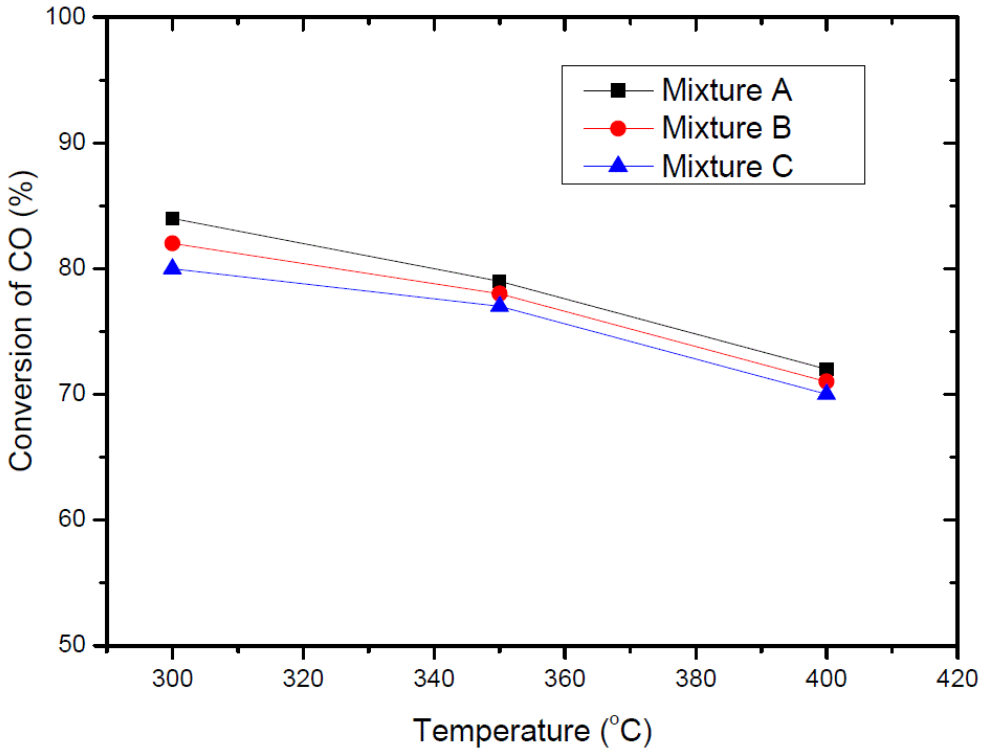

Figure 4.15 Effect of feed composition on CO conversion

From table 4.1 and figure 4.15, it can be observed that doubling the concentration of CO, caused the conversion of CO to decline by 5%.The decline in CO conversion due to an increase in concentration, suggests that the fixed amount of catalyst load was not active enough to convert the CO into CO_2. Additionally, the presence of higher concentration of non-permeating species also hinders the rate of hydrogen recovery. Therefore, the conversion of CO will also suffer, since the equilibrium shift effect of continuous products removal become minimised due to competitive adsorption between hydrogen and non-permeating species. A similar relationship was reported by Hou & Hughes, (2002) it was indicated that the competitive adsorption between CO and H_2 is more significant when the temperature is below 350°C.

Figure 4.16 represents the hydrogen recovery for different mixtures as a function of temperature. The rate of hydrogen recovery is temperature dependent, since as the temperature increases, the permeation rate also increases. However, an unusual result was observed for mixture C at 300°C. The recovery rate was equal to that of mixture A. this unusual behaviour may have occurred during gas system flashing, the system may have failed to flash all gases, therefore the mixture was affected negatively.

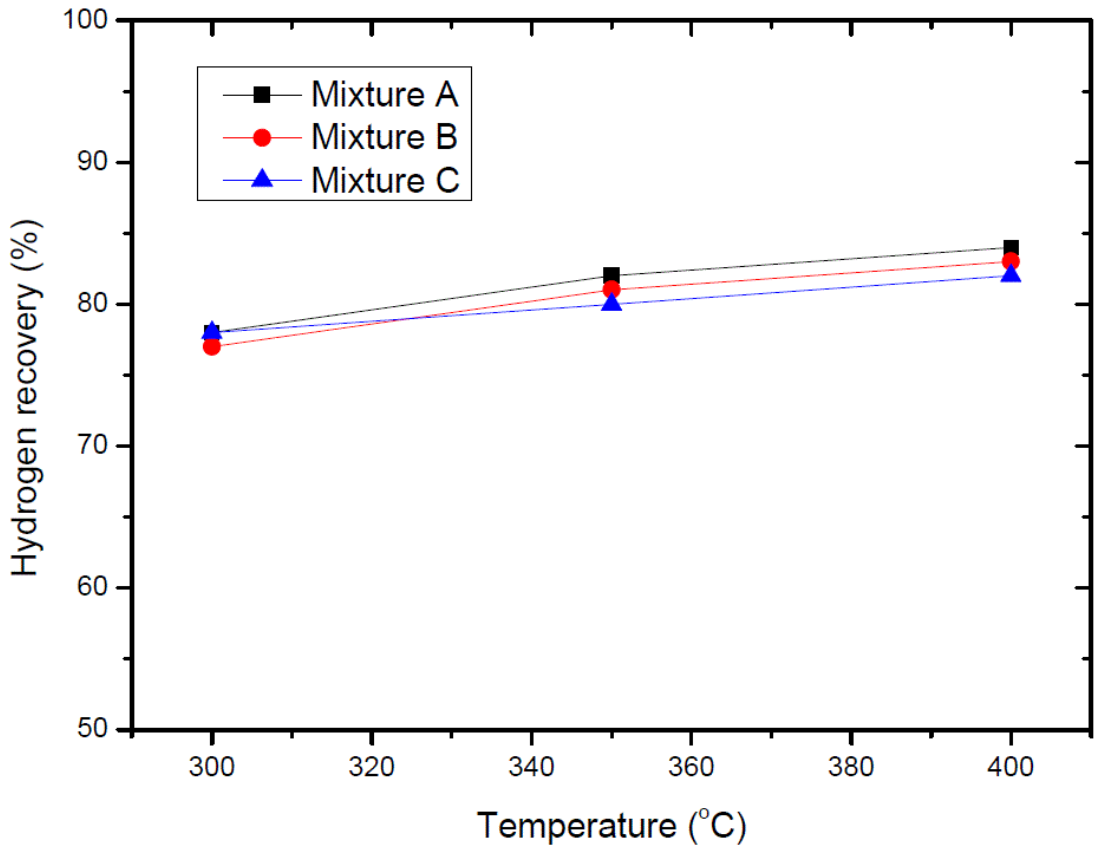

Figure 4.16 Effect of different feed composition on hydrogen recovery

The different effect on hydrogen permeation by these different species can be explained by the different adsorption capability on the metallic membrane due to their properties. It was highlighted by Byron *et al*. (2011) that The CO has higher adsorption capacity on the membrane surface relative to CO_2. From this work it was observed that with an increase in temperature the negative effect (adsorption and absorption capacities) is reduced. A study by Liguori *et al*.(2012) evaluated the performance of a PSS-supported Pd-based membrane reactor, reported a similar effect of the presence of CO, CO_2 and H_2O reducing the hydrogen flux through the membrane.

4.9.6 Water gas shift reaction Membrane stability

The main objective of this work was to produce high purity hydrogen through the use of a Pd-Ag membrane supported by PSS material. A long term (100 hours) study for producing hydrogen at fixed temperature and pressure of 4 bar 380 °C was conducted, with the objective of understanding the gradual change of membrane performance. The membrane performance was evaluated based on conversion of CO and recovery of H_2 respectively. Figure 4.17 represents

the conversion of CO and hydrogen recovery over time. It can be observed from figure 4.17 that the conversion and recovery deteriorated over time at fixed process conditions.

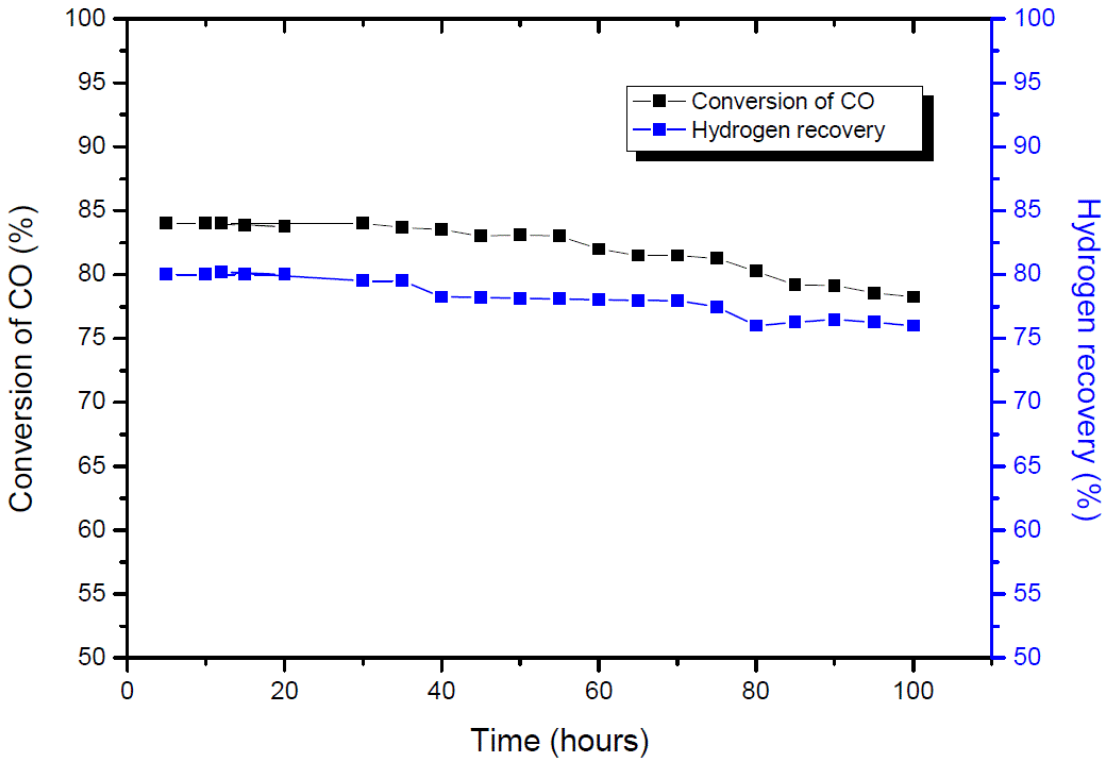

Figure 4.17 long term performance of Pd-Ag membrane for WGSR

From figure 4.17, the conversion of CO remained stable at approximately 83% for the first 40 hrs. However, after 55 hrs the conversion started declining, and fell to 79% at 100 hrs. Furthermore, the hydrogen recovery also declined by 5% from initial permeance levels. It was reported in literature by Ciocco *et al.*(2005) that continuous exposure of gases (CO) to the Pd membrane surface can cause membrane deactivation. The deactivation occurs when coke is formed on the membrane surface which will result in decreasing the permeance of H_2. The hydrogen permeance declined possibly due to coke formation on the surface of the membrane, which blocks the active site for hydrogen to dissociate and diffuse through the membrane.

Another important factor concerning Pd membrane reactors is to produce high degree purity of hydrogen. The produced hydrogen was 99.99% pure, as observed from GC results. A study by Augustine *et al.(*2010) investigated the performance of a WGS membrane reactor under industrial process conditions over time. The tested membrane showed stable permeation of hydrogen for the first few days, as time prolongs, the selectivity of the membrane declined due to

leaks which occurred within the membrane. In a prior study by Basile *et al.* (1996) a Pd-Ag membrane reactor was operated for 8 days and showed stable results and a conversion of 99.89% at fixed conditions. However, for the first 3 days, the membrane failed due to welding, and at day 6, the membrane started leaking due to leak growth as reported by the author.

The long term test for hydrogen production through the use of Pd membrane based is fewer. in literature. Lin & Rie (2001) tested the permeability of hydrogen under reforming conditions for methanol at 350°C for 900 hours using a 20 µm Pd-based membrane. Their study revealed stable permeation and selectivity for the entire period. A study by Torkelson *et al*. (2008) tested the WGS reactor for 70 hours using 6 µm Pd-based membrane, and they reported that the selectivity and permeation declined by 20% due to regeneration adsorption of H_2O..

Unfortunately, the existing body of literature offers no examples of selectivity decline in supported Pd-membranes as a result of extended exposure to mixed gases or WGS reaction conditions. The possible reason behind the decline may be because of membrane deactivation due to exposure to CO for an extended period of time.

Section D

This section discusses the characterisation of the Pd-Ag membrane films before and after hydrogen exposure for different process conditions. SEM analysis was conducted for surface morphological changes, EDS was also performed for analysis of the composition of the Pd-Ag membrane. Lastly XRD was also conducted for crystal lattice analysis. Figure 4.18 represent the schematic overview of a membrane film.

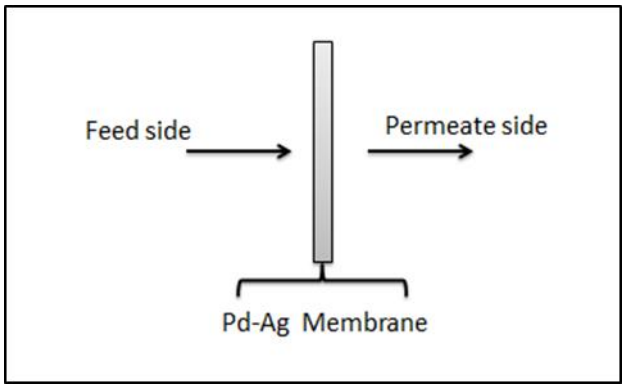

Figure 4.18 schematic overview of a membrane film

Figures 4.18 Schematic of membrane, showing the feed and permeate sides.

4.10 Post Characterization of the Pd-Ag membrane film

4.10.1 Scanning Electron Microscopy (SEM) analysis

4.10.1.1 SEM analysis for Pd-Ag exposed to pure hydrogen

To investigate the degradation mode of the membrane, the membranes were examined using a Scanning Electron Microscope (SEM) to investigate surface morphological changes after exposure of the Pd-Ag membrane to hydrogen. Figure 4.19 represents four different membranes under different process conditions, (A) the pure Pd-Ag membrane (B) the membrane exposed with nitrogen, (C) the feed section of thermal cycle membrane and (D) the membrane tested for thermal stability under hydrogen.

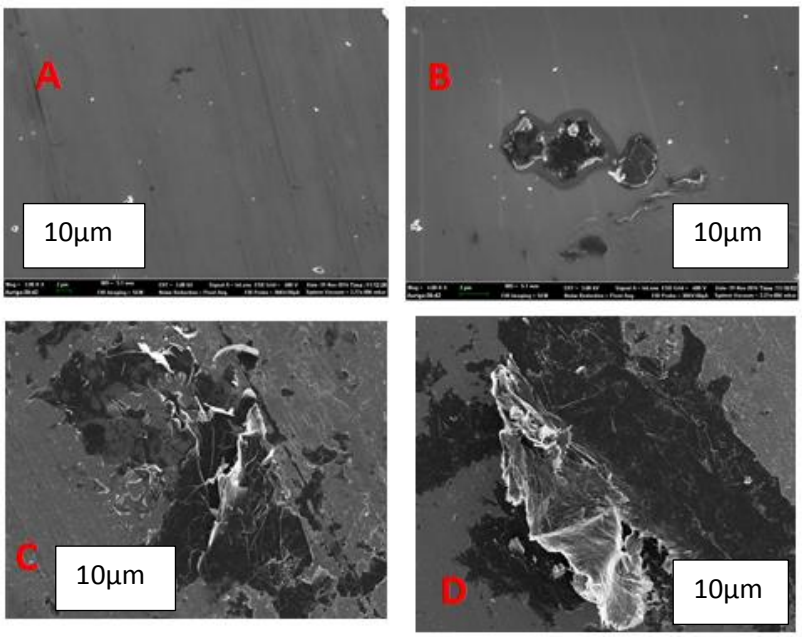

Figure 4.19 SEM images (a) pure Pd membrane (b) membrane exposed to nitrogen (c) feed section for thermal cycling (d) Permeate side for thermal stability

Figure 4.19 (a) shows the Pd-Ag film before hydrogen exposure. The film showed a smooth uniform surface without cracks. Image (b) shows the Pd-Ag membrane feed side under nitrogen cycles. There are minor differences between image (A) and image (B), on image B, there are r debris, which may have possibly resulted from handling of the Pd-Ag film during stage of assembling the membrane reactor. This debris which is observed on image may represent the graphite which was used to seal the two plates during the process of assembling the membrane reactor. The membrane on image B, did not leak nor to allow nitrogen gas to pass through, therefore, these debris does not reflect a defect membrane. The thermal cycling of Pd-Ag under nitrogen loading did not cause any structural changes on the film surface, except a colour change due to thermal treatment.

Figure 4.19 (C) shows the feed side of the Pd-Ag membrane after continuous exposure to hydrogen. A significant structural change can be seen between the Pd-Ag film before (a) and after (c) hydrogen exposure. Major cracks and surface changes were observed after hydrogen exposure. These cracks were formed due to thermal stress and the hydrogen atoms which were diffusing through the membrane. Hydrogen have contributed significantly towards the formation of these cracks, since there were not observed on Image (B) under nitrogen cycle for same process conditions (temperature and pressure). A study by Mcleod (2008), reported the

formation of pinholes under hydrogen loading which enabled non-permeable gases to pass through the membrane. The transport of hydrogen through the membrane maybe the potential cause of this encountered cracks. A study by Suleiman *et al.,* (2003) reported that a continuous loading of hydrogen causes lattice dilation, which results in cracks of the membrane. The absorption and de-sorption of hydrogen atoms on the Pd-membrane based has been reported to form P_nH_n hydride depending on the concentration of hydrogen and the temperature at which the gas is exposed at (Cabrera *et al.* 1994). The formation of Pd-hydride has a potential of causing cracks in membrane films, depending on the phase of the hydride. The phase change of Pd-hydride is detailed under XRD, Figure 4.19 image (d) shows the permeate side of the membrane after hydrogen exposure. Major cracks and structural changes were also observed on the permeate side of the membrane. This shows a serious hydrogen attack on the membrane. These cracks were responsible for allowing nitrogen to permeate through the membrane. A membrane allowing non permeate species such as nitorgen to pass through the it is considered to have failed, since the non permeate species are not the desired products. One of the purposes of a Pd-Ag membrane reactor is to produce a high purity hydrogen, therefore non permeable species should not pass through the membrane.

4.10.1.2 SEM for Pd-Ag film used for Water Gas Shift reaction

Scanning electron microscope (SEM) was also performed to investigate surface changes on the membrane films used to produce hydrogen from the WGS reaction. Figure 4.20 shows the feed and permeate side of the Pd-Ag films after producing hydrogen from WGS reaction.

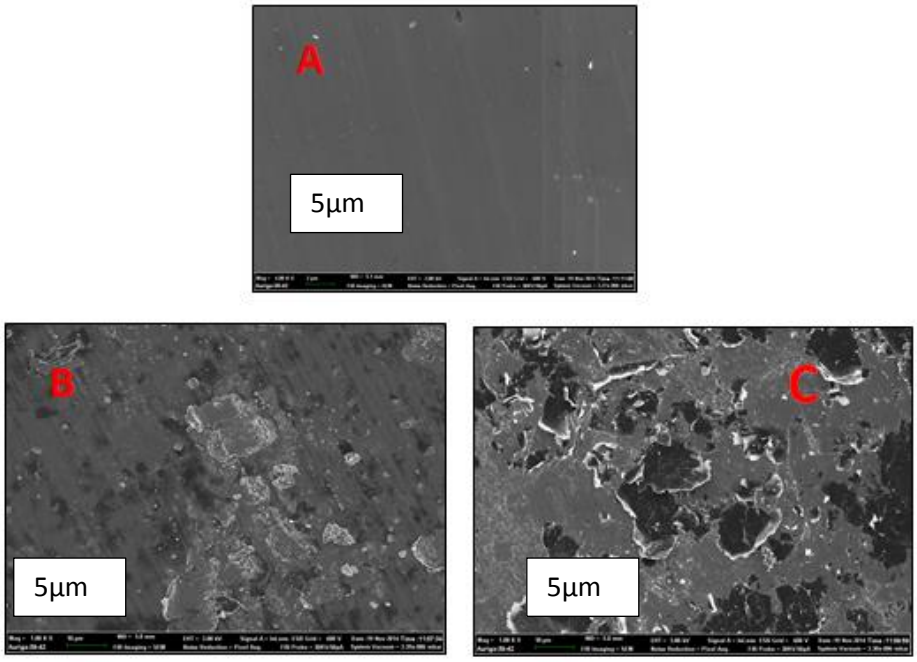

Figure 4.20 SEM for (a) Pure membrane reactor before WGS reaction (b) Feed section of the membrane (C) Permeate site of the membrane film

From figure 4.20 represents SEM images for Pd-Ag membrane films used for WSG reaction. It can be observed from the SEM images that major surface changes occurred after the reaction or during the reaction. The membrane film showed cracks and flaky residue on the permeate side, which allowed the non-permeate gases to pass through the membrane and reduced the degree of purity of the hydrogen. These cracks allowed CO, N_2 and CO_2 to permeate through the membrane, which negatively affected the degree of purity of the hydrogen. The feed section showed the formation of debris, surface has been etched due to mixed gases. Major cracks only exist on the permeate side of the membrane, which was caused by the transportation of hydrogen which resulted in a phase change due to hydrogen concentration polarization. The membrane exposed to pure hydrogen showed larger cracks relative to films used to produce hydrogen. A major crack on exposure of Pd-Ag film to pure hydrogen suggests high degree of concentration polarisation under pure exposure of hydrogen.

4.10.2 Energy Dispersive Spectroscopy (EDS)

The original and pure hydrogen exposed Pd-Ag membrane films were examined using energy dispersive spectroscopy (EDS). EDS was performed to identify the possible occurrence of intermetallic diffusion at 420^{o}C temperatures under hydrogen exposure. Figure 4.21 shows the

EDS results for a pure Pd-Ag film before hydrogen exposure. The EDS results confirmed the manufacture's specifications of 77% Pd and 23% Ag.

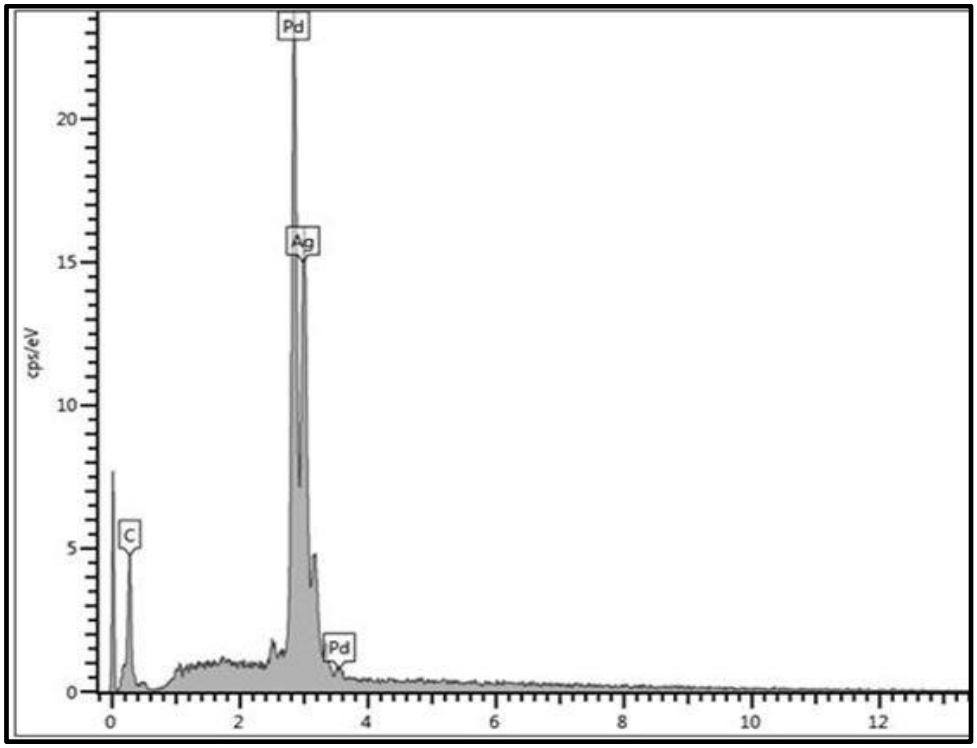

Figure 4.21 EDS results for un exposed Pd-Ag membrane film

The EDS analysis showed 77% Pd and 23% Ag. Carbon was depicted on the membrane film since the material was coated with carbon before ED's analysis.

It is well established that supported Pd-based membrane reactors can suffer from intermetallic diffusion when operated at temperatures above 450^{o}C (Gauzzone & Ma, 2008). The migration of atoms from support material (PSS) to Pd-Ag films results in a decline in hydrogen permeation rate. Intermetallic diffusion mostly occurs at temperature above 500^{o}C, when there is no oxide layer between the support material and the Pd film. An oxide layer on formed on the support material acts as a barrier for ions migration from the support material into the Pd-Ag membrane. The decline in hydrogen permeation observed in section B for this work at high temperature may suggested that intermetallic diffusion may have occurred. Outlined by Gauzzone *et al*. (2006) the presence of (Fe, Cr and Ni) affects the permeance of the membrane.

Therefore, EDS was performed to investigate the cause of the decline of hydrogen permeation. The hydrogen flux declined at higher temperatures (430°C), and the process of intermetallic diffusion between the support and the Pd film is mostly cited by scholars Ma *et al*.(2004), Guazzone *et al*.(2006) and Hara *et al*. (2012) as the reason for the decline of hydrogen flux. Figure 4.22 depicts the EDS analysis of a membrane after hydrogen expsoure at 450^{o}C. It can be observed from the graph that foreign atoms have migrated from the support material to the surface of Pd-Ag film.

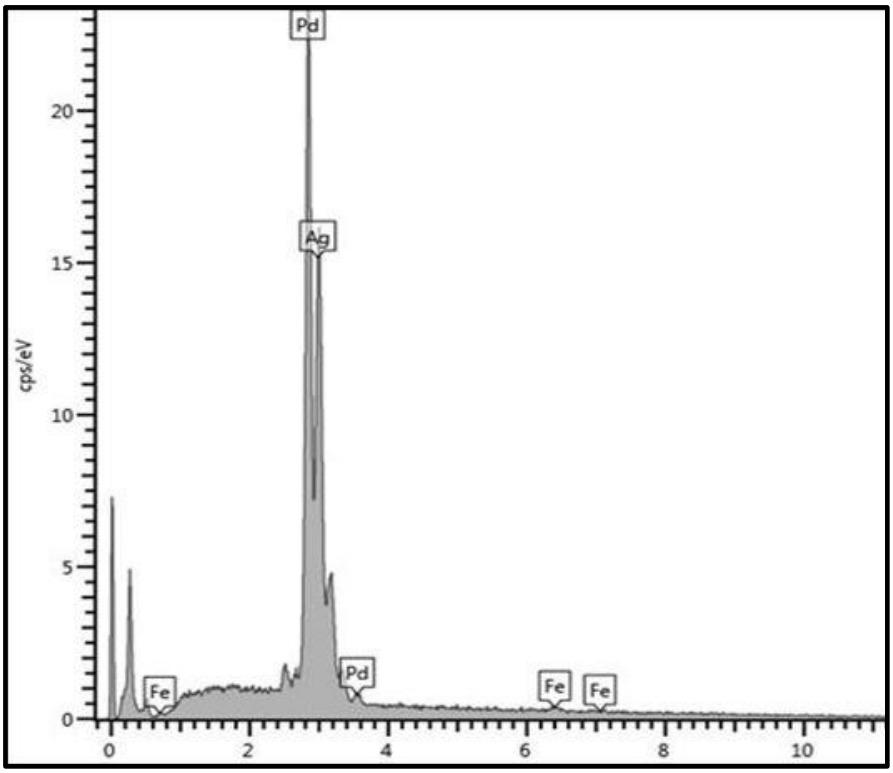

Figure 4.22 EDS after hydrogen exposure

From figure 4.22, the EDS results showed the presences of foreign atoms on the metal film. The Iron (Fe) atoms have migrated from the support to the membrane. The presences of foreign atoms on the Pd-Ag film are responsible for the decline in hydrogen flux at higher temperatures. A study by Gauzzone *et al*.(2006) reported 30% content of Fe which migrated into the Pd membrane. The presences of Fe atoms reduce active site for hydrogen molecules to dissociate in order to be transported through the metal. The EDS results indicated that the Fe atoms on the surface of the membrane film was not evenly distributed on the surface, some parts of the

membrane film had higher Fe (15%) content and other side lower content of Fe (5%). As outlined earlier, the presences of an oxide layer is to act as a barrier for ions migration from the support material into the Pd membrane. However, for this current work the ions migrated from the PSS support material into the surface of Pd-Ag membrane. Therefore, this migration of the Fe atoms from the support material to the Pd-Ag surface suggested that the oxide layer formed to prevent intermetallic diffusion was not sufficient enough.

The part of Pd-Ag membrane which had the higher Fe content hindered the permeation rate of hydrogen more in comparison to the other part which had less Fe content. The presence of non-uniform concentration of Fe atoms on the Pd material also suggest that the oxide layer was not uniformly formed between the support and Pd-Ag metal. A study by Hawa *et al.* (2015) conducted a thermal stability effect of Pd based membranes at 500^{o}C. However, the study did not observe the intermetallic diffusion problem, which suggests that the oxide layer was thick enough to prevent the process. Afterwards, a thicker layer was developed before conducting WGS reaction experiments to prevent the intermetallic diffusion. For WGS reaction, no intermetallic diffusion occurred based on EDS results, therefore, it can be suggested that the newly formed oxide layer on the support material was improved relative to the first one.

4.11 **X-Ray Diffraction Analysis (XRD)**

4.11.1 hydrogen exposed Pd-Ag membrane reactor

The X-ray diffraction patterns for the used Pd-Ag films during the experiments were obtained by using PAN analytical X'pert pro diffractometer with a CuKα radiation source. The Pd-Ag films were analysed before and after being exposed to hydrogen to investigate the effect of absorption and desorption on the metal crystal lattice. Figure 4.23 shows the diffraction patterns for pure Pd-Ag membrane films, long term hydrogen-exposed Pd-Ag membrane and the Pd-Ag film used for thermal stability under hydrogen exposure which was discussed in section 4.7 and 4.8. XRD provides information about crystal size, size distribution and crystal dislocation.

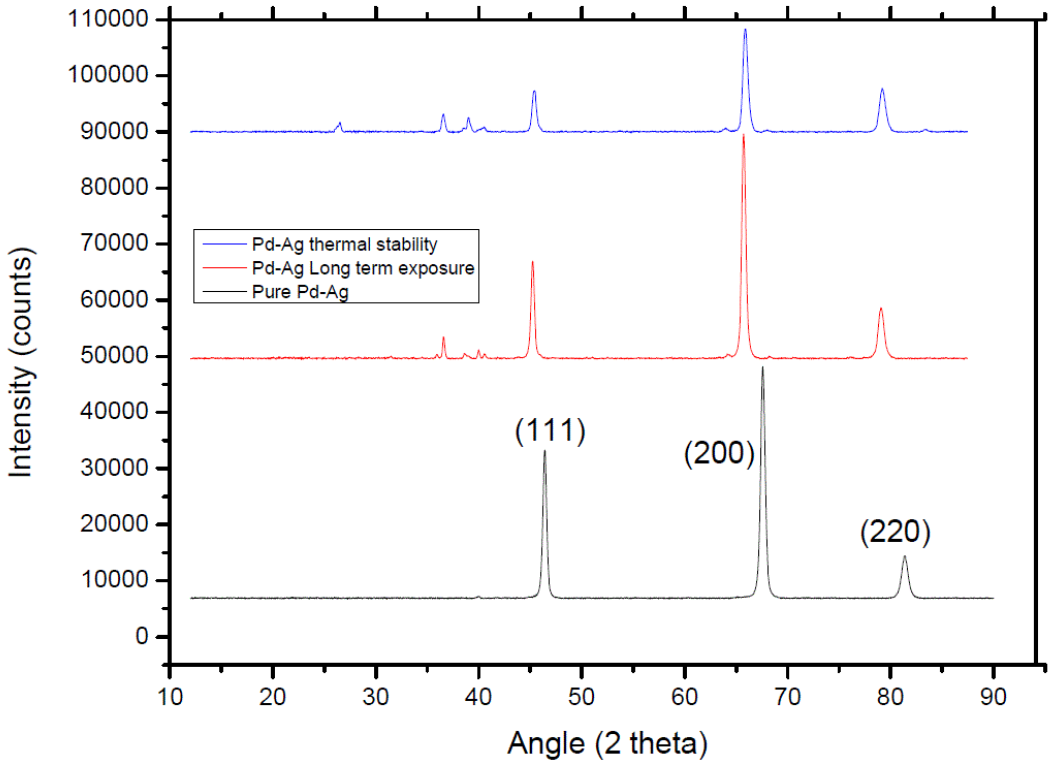

Figure 4.23 X-ray diffraction patterns for used Pd-Ag membrane

The unexposed Pd-Ag film, which was analysed for benchmarking purposes, shows three major peaks with the corresponding Miller indices 45^{o} (111), 68^{o} (200) and at 82^{o}. These Miller Indices represent the direction and the plane within a crystal lattice. Identical diffraction patterns for a composite Pd based membrane with different composition were reported by other researchers (Basile *et al*. (2004). Iyoha., *et al.* (2005)., Xie *et al*., (2009)). For the long term hydrogen exposed membrane film, the peak intensities were reduced and little bit shifted relative to the unexposed Pd-Ag film, and new peaks were formed as shown in figure 4.23. The shifting of peaks reveals the presences of internal stress, twining, faults stacking and chemical heterogeneities (Ungar, 2004). The peaks for long term hydrogen exposure shifted to lower angles, therefore stress was exerted on the material due to hydrogen adsorption and de-sorption. A study by Ungar (2004) outlined the broadening of peaks due to crystal dislocation, micro stress and crystal smallness. However, peak broadening was not observed within this work.

New peaks were observed in the long term exposed and the thermal stability membrane film between 35-42^{o}. The newly formed peaks on the long term exposed films were more intense in comparison to the peaks form for the membrane tested for thermal stability, but within the same

range of angle. The XRD data for the long term hydrogen-exposed membrane started showing minor peaks from 25^{o} -39^{o}. The formation of these new peaks and broadening may be due to the crystal size change and the effect Pd ligament size change could cause significant peak broadening as observed from figure 4.23.

The diffusion of hydrogen through Pd-Ag material has a potential of causing distortion of the material structure. The instant exposure and diffusion of hydrogen through the metal causes the lattice structure to expand from 3.89 Á to 3.895 Á. The exposure of transactional metals, especially PGMs, to hydrogen leads to a reversible metal hydride formation. For this work, the possible metal hydride to be formed is Pd_nH_n. The metal hydrides can exist in two different phases, depending on the stoichiometric coefficient of the hydrides.

The two possible phases of palladium hydride are formed on a non-stoichiometric basis, $Pd\text{-}H_{0.-0.02}$ known as the α phase and the $Pd\text{-}H_{>0.58}$ known as the β-phase. In the range between $Pd\text{-}H_{0.02\text{-}0.58}$ both phases co-exist. The β-phase is more brittle than α phase. A study by Johansson *et al*., (2010) reported that "the lattice constant of palladium is increased by 3.5% once the β-phase is formed, the β phase cause tensile strain on lattice.

The stored hydrogen in the β phase causes micro-structural changes in the host matrix. The failure mode of the membrane under long term and high thermal stability exposure of hydrogen could possibly have been due to the phase change. The complete de-sorption of the absorbed hydrogen atoms on the octahedral side palladium matrix takes time (Isaeva *et al*., 2011). The adsorption and de-sorption of hydrogen through the Pd membrane has a potential of forming a defect phase known as Pd_3VacH_4, the formation of this phase affects the stability of the membrane (Isaeva *et al*., 2011).

A study by Kulprathipanja *et al*.(2004) investigated the effect of hydrogen stress caused by hydrogen adsorption and de-sorption through a metal. The stress exerted within the Pd material when loaded with hydrogen at temperatures ranges of (25-627^{o}C) was investigated. The study revealed that when to the hydrogen concentration was increased, the stress level on the Pd also increased. However, after reducing the concentration of hydrogen to zero, the material does not go back to its original normal stress, there was about 4-5% permanent stress exerted on the Pd foil. In Pd hydrides, H atoms occupy octahedral interstitial sites in the Pd matrix. Hydrogenation and dehydrogenation causes reversible transformation between pure Pd and hydride phases which results in lattice expansion and contraction. This leads to stress changes in the film that can be used to track hydrogen adsorption and desorption. Since the membrane failed under hydrogen exposure, it can be suggested that hydrogen caused stress on the

material which resulted in cracks and resulted in allowing non permeable species to pass through the membrane.

4.11.2 Pd-Ag films used Water gas shift reaction

An x-ray diffraction pattern was also generated for membrane films used for production of hydrogen in the WGS reaction. Figures 4.24 represents the diffraction patterns for feed and permeate side of the film under exposure of different gases. The intensity of the peaks was reduced relative to the pure film after exposure with different gases. New peaks which were less intense were formed between 34-39^{o} with miller indices of (100). The formation of new peaks was an indication of structural changes for the membrane.

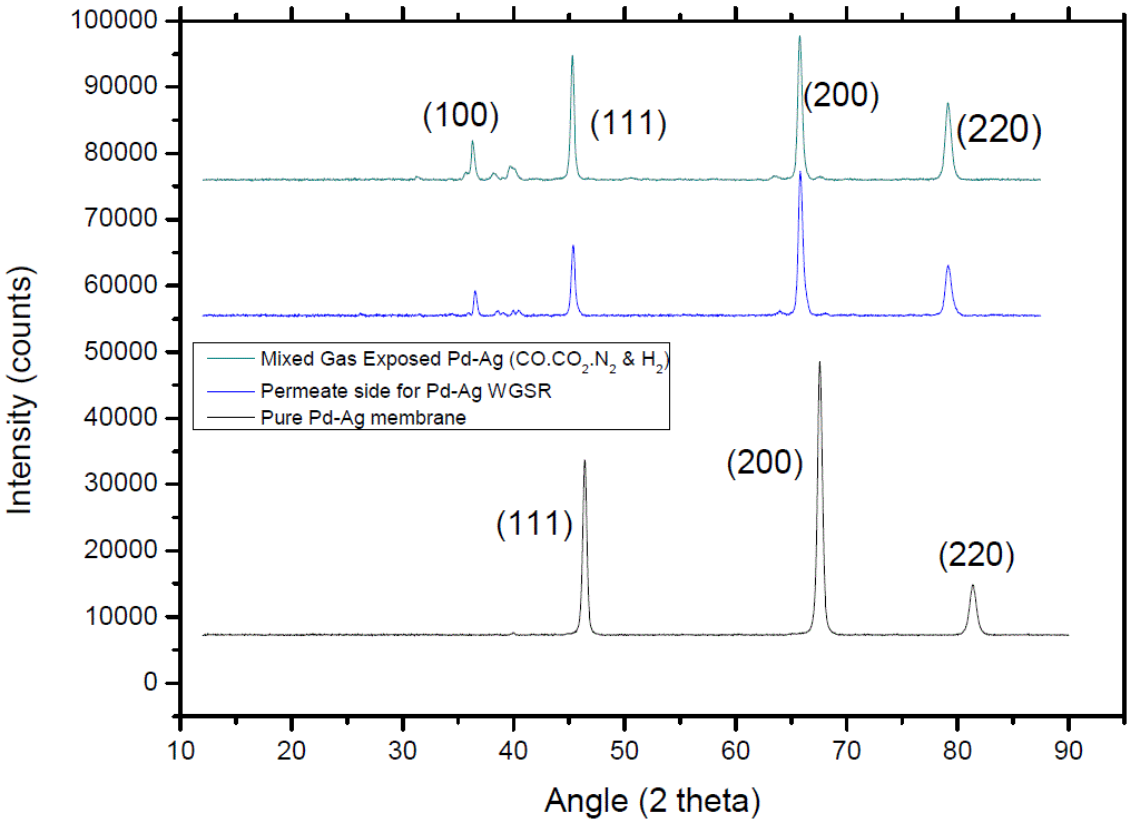

Figure 4.24 X-ray diffraction for WGRS film

From the XRD data obtained, lattice parameters were identified by using general structure analysis system (GSAS) software for data refinement. Table 4.3 details the lattice parameters for Pd-Ag films under different process conditions. From table 4.3 it can be seen that the lattice size of the crystal before and after hydrogen exposure changed. There has been lattice expansion on

the membrane film used for hydrogen separation; therefore phase transition took place from α phase to β-phase. Therefore, the existence of β-phase on a Pd membrane is likely to cause fractures since the crystals are distorted once β phase formed due to higher hydrogen concentration.

Table 4.2 Lattice parameter's for Pd-Ag

Process conditions	**a (Å)**	**d (Å)**	**references**
Pd-Ag (pure)	3.980	5.8083	Current work
Pd-Ag (mixed gas)	3.984	5.8801	Current work
Pd-Ag (Thermal stability)	3.989	5.8441	Current work
Pd-Ag (Durability)	3.994	5.8745	Current work
Pd	3.895	5.8084	(Cabrera *et al*. , 1994)
Pd-Ag16 (exposed to H_2)	3.925	5.5508	(Iseava *et al*.,2008)

The lattice expansion of the Pd-Ag film due to hydrogen exposure has led to a membrane failure. A study by Isaeva *et al*., (2010) showed that the positions of hydrogen atoms in the defect phase strongly affect its stability and may be a reason for further phase transitions in the defect phase.

Summary

This chapter discussed the permeability of Pd-Ag membrane reactor at different temperatures; tested the long term permeability at different process condition under hydrogen exposure. The thermal stability and cyclibility of Pd-Ag membrane reactor exposed with hydrogen was investigated. The production of hydrogen from WGS reaction through the use of Pd-Ag membrane reactor was conducted, the performance of membrane reactor for potential replacement of the current two stage process of WGS reaction was measured based on the conversion and recovery of carbon monoxide and hydrogen respectively. Lastly, different analytical techniques (SEM, XRD and EDS) have been used to investigate the degradation mode of the membrane after exposed with hydrogen.

CHAPTER FIVE

5 Conclusions and Recommendations

This chapter concludes the work done and suggests future research to be undertaken for improving the membrane durability or life span and to overcome the encountered challenges related to membrane reactors for hydrogen production.

5.1 Conclusions

The purchased Pd-Ag film (20µm thick) was used to construct a membrane reactor for producing high degree purity of hydrogen through the Water Gas Shift reaction. This research has yielded the following conclusions;

- The Pd-Ag membrane reactor has displayed the ability of being able to diffuse hydrogen with infinite selectivity (provided the membrane is defect free). The Pd-Ag membrane has shown to have higher permeability towards hydrogen in comparison to pure a Pd-membrane.
- The rate limiting step for hydrogen flux permeating through the membrane was found to be different at each temperature; at 320°C bulk diffusion of hydrogen atoms was the rate limiting step. At 380°C and 420°C surface contamination and hydrogen dissociation was the rate limiting step for hydrogen flux. These rate limiting steps were predicted based on the “n” value from Sieverts plot.
- The Mixed gas experiments were conducted to investigate the effect of surface inhibition. The presence of non-permeate species (CO, CO_2 and H_2O) have been shown to affect the hydrogen flux through the membrane. The presence of CO at temperatures below 350°C caused a decline in hydrogen flux. The presence of CO has a greater negative effect in comparison to CO on the permeation rate, but this effect can be suppressed by increasing temperature. The presence of nitrogen (inert gas) in the feed does not affect the permeation rate of hydrogen.
- The presence of excess steam has shown to be the major species responsible for competitive adsorption. Excess steam causes dilution of the H_2 and decreases the permeance rate of H_2. However, this negative effect can be mitigated by increasing temperature.

- The Pd-Ag membrane film showed poor thermal cycling (heating and cooling) under hydrogen exposure at 320°C. The Pd-Ag film failed after 10 cycles due to continuous loading of hydrogen which caused phase change which resulted in lattice expansion. The failure of Pd-Ag was not due to thermal stress, but it was rather due to the adsorption and desorption of hydrogen. Since the membrane was cycled for 10 times without failure or structural changes under nitrogen. Therefore, it can be concluded the adsorption and de-sorption of hydrogen caused membrane failure.
- The membrane was tested for long term thermal stability at high (450^{o}C) and low (300°C) temperature for 230 hours under hydrogen exposure. The membrane failed earlier at the higher temperature (after 150 hours) with cracks being formed due to hydrogen diffusion through the membrane. The membrane also failed at low temperatures after 190 hours. From SEM images, it was seen that cracks were formed on the surface of the membrane film after hydrogen exposure. Therefore, non-permeating species passed through the membrane which was an indication for membrane failure.
- The Pd-Ag membrane showed poor durability over time and the selectivity declined over time. Micro surface defects were observed due to hydrogen adsorption and desorption. XRD data showed lattice expansion, the phase transition of α phase to β phase caused lattice expansion which resulted in a membrane failure.
- During the WGS reaction, different process conditions such as temperature, GHSV, steam ratio and external species were investigated for the optimal conversion of carbon monoxide and recovery of hydrogen. At higher temperatures, the permeability of the produced hydrogen is greater; the equilibrium conversion of CO was not limited at higher temperatures as compared to traditional packed bed reactors. For membrane reactor, the equilibrium shift effect of Le Chatelier's principle played an important role for achieving higher conversion for exothermic reaction at high temperatures. Operating the membrane reactor at low GHSV results in higher conversion of CO with a low recovery of hydrogen. Recommended by the catalyst manufacturer, using the catalyst at higher GHSV reduces the catalyst effectiveness towards conversion.
- The performance of the Pd-Ag membrane reactor during WGS reaction was measured based on hydrogen recovery (ability to select only hydrogen) and conversion of carbon monoxide respectively. The membrane reactor successfully achieved 84% hydrogen recovery and 88% carbon monoxide conversion under the presence of Iron oxide catalyst. High purity hydrogen (infinite selectivity towards hydrogen) was produced before membrane failed.

- The Pd-Ag membrane was tested for the long term production of hydrogen. It was found that the performance of the membrane declines as time elapses. This suggests that the membrane was losing its catalytic activity (ability to dissociate hydrogen) towards hydrogen permeation.
- XRD analyses revealed lattice expansion due to phase change which was caused by the continuous loading of hydrogen in the membrane reactor. Therefore, it can be deduced that the loading hydrogen in Pd-Ag film caused crystal defects which resulted in membrane failure over time.

5.2 **Recommendations**

There are several factors that still need to be addressed for the adoption of Pd-Ag membrane based reactors for producing high degree purity of hydrogen from water gas shift reaction.

- The present work on the durability, thermal stability of Pd based membranes should be extended and further explored, especially the effect of hydrogen concentration through the membrane, since there is a phenomena called concentration polarisation. The effect of the transport of hydrogen through the membrane structure needs to be further explored, since long term exposure to hydrogen caused phase transition which resulted in lattice expansion and crystals distortion and defects to appear in the membrane.

- The long term stability for a Pd membrane WGS reactor should be tested under practical conditions by using reformate from an actual industrial process that has been scrubbed and de-sulphurized.
- The challenge of phase transition and inability of Pd-Ag membrane reactor to show stable hydrogen permeation at higher temperatures needs to be furthered explored.

•

6 References

Abdollahi, M., Yu, J., Liu, P.K.T., Ciora, R., Sahimi, M. & Tsotsis, T.T., 2012. Ultra-pure hydrogen production from reformate mixtures using a palladium membrane reactor system. *Journal of Membrane Science,* 391(10), pp. 32-42.

Adesina, A., Meeyoo, V. & Foulds, G., 1995. Thermolysis of hydrogen sulphide in an open tubular reactor. *International Journal of Hydrogen Energy*, 20(10), pp. 777-783.

Alexander Sullivan Augustine, 2013. *Supported Pd and Pd/Alloy Membranes for Water-Gas Shift Catalytic Membrane Reactors* , PhD thesis, Department of Chemical Engineering, Worcester Polytechnic Institute.

Amadeo, N. & Laborde, M., 1995. Hydrogen production from the low-temperature water-gas shift reaction: kinetics and simulation of the industrial reactor. *International Journal of Hydrogen Energy,* **20**(12), pp. 949-956.

Amandusson, H., Ekedahl, L. & Dannetun, H., 2001. Hydrogen permeation through surface modified Pd and PdAg membranes. *Journal of Membrane Science,* **193**(1), pp. 35-47.

Armor, J.N., 1989. Catalysis with permselective inorganic membranes. *Applied Catalysis,* **49**(1), pp. 1-25.

Augustine, A.S., Ma, Y.H. & Kazantzis, N.K., 2011. High pressure palladium membrane reactor for the high temperature water–gas shift reaction. *International Journal of Hydrogen Energy,* **36**(9), pp. 5350-5360.

Augustine, A.S., Mardilovich, I.P., Kazantzis, N.K. & Hua Ma, Y., 2012. Durability of PSS-supported Pd-membranes under mixed gas and water–gas shift conditions. *Journal of Membrane Science,* **415–416**(0), pp. 213-220.

Barbieri, G., Scura, F., Lentini, F., De Luca, G.& Drioli, E., 2008. A novel model equation for the permeation of hydrogen in mixture with carbon monoxide through Pd–Ag membranes. *Separation and Purification technology,* **61**(2), pp. 217-224.

Baschuk, J. & Li, X., 2001. Carbon monoxide poisoning of proton exchange membrane fuel cells. *International Journal of Energy Research,* **25**(8), pp. 695-713.

Basile, A., Iulianelli, A., Longo, T., Liguori, S. & De Falco, M., 2011. Pd-based Selective Membrane State-of-the-Art. *Membrane Reactors for Hydrogen Production Processes.* pp. 21-55.

Basile, A., Criscuoli, A., Santella, F. & Drioli, E., 1996a. Membrane reactor for water gas shift reaction. *Gas Separation & Purification,* **10**(4), pp. 243-254.

Basile, A., Drioli, E., Santell, F., Violante, V., Capannelli, G. & Vitulli, G., 1996b. A study on catalytic membrane reactors for water gas shift reaction. *Gas Separation & Purification,* **10**(1), pp. 53-61.

Basile, A., Chiappetta, G., Tosti, S. & Violante, V., 2001. Experimental and simulation of both Pd and Pd/Ag for a water gas shift membrane reactor. *Separation and Purification Technology,* **25**(1–3), pp. 549-571.

Baykara, S., 2004. Experimental solar water thermolysis. *International Journal of Hydrogen Energy,* **29**(14), pp. 1459-1469.

Bi, Y., Xu, H., Li, W. & Goldbach, A., 2009. Water–gas shift reaction in a Pd membrane reactor over Pt/Ce0.6Zr0.4O2 catalyst. *International Journal of Hydrogen Energy,* **34**(7), pp. 2965-2971.

Brown, B.B., Yiridoe, E.K. & Gordon, R., 2007. Impact of single versus multiple policy options on the economic feasibility of biogas energy production: Swine and dairy operations in Nova Scotia. *Energy Policy,* **35**(9), pp. 4597-4610.

Byron Smith, R.J., Muruganandam, L. & Murthy Shekhar, S., 2011. CFD analysis of water gas shift membrane reactor. *Chemical Engineering Research and Design,* **89**(11), pp. 2448-2456.

Cabrera, A., Morales-Leal, E., Hasen, J. & Schuller, I.K., 1994. Changes in crystallographic orientation of thin foils of palladium and palladium alloys after the absorption of hydrogen. *Catalysis letters,* **30**(1-4), pp. 11-23.

Callaghan, C.A., 2006. Kinetics and catalysis of the water-gas-shift reaction: A microkinetic and graph theoretic approach, Master's thesis, Department of applied chemistry Worcester Polytechnic Institute

Caravella, A., Scura, F., Barbieri, G. & Drioli, E., 2010. Sieverts law empirical exponent for Pd-based membranes: critical analysis in pure H2 permeation. *The Journal of Physical Chemistry B,* **114**(18), pp. 6033-6047.

Chein, R., Chen, Y. & Chung, J.N., 2013. Parametric study of membrane reactors for hydrogen production via high-temperature water gas shift reaction. *International Journal of Hydrogen Energy,* **38**(5), pp. 2292-2305.

Chiappetta, G., Clarizia, G. & Drioli, E., 2008. Theoretical analysis of the effect of catalyst mass distribution and operation parameters on the performance of a Pd-based membrane reactor for water–gas shift reaction. *Chemical Engineering Journal,* **136**(2–3), pp. 373-382.

Chicas, .O.S., 2013. Development of a novel catalytic membrane reactor: application in wastewater treatment, PhD Thesis, Dept of Chemical Engineering, University of rovira i virgil

Chotirach, M., Tantayanon, S., Tungasmita, S. & Kriausakul, K., 2012. Zr-based intermetallic diffusion barriers for stainless steel supported palladium membranes. *Journal of Membrane Science,* **405**, pp. 92-103.

Ciocco, M., Morreale, B., Rothenberger, K., Howard, B., Killmeyer, R., Enick, R. & Bustamante, F., 2005. Water-Gas Shift Membrane Reactor Studies. *Report available on DOE/NETL website,* .

Cooney, D.A., Way, J.D. & Wolden, C.A., 2014. A comparison of the performance and stability of Pd/BCC metal composite membranes for hydrogen purification. *International Journal of Hydrogen Energy,* **39**(33), pp. 19009-19017.

Criscuoli, A., Basile, A. & Drioli, E., 2000. An analysis of the performance of membrane reactors for the water–gas shift reaction using gas feed mixtures. *Catalysis Today,* **56**(1–3), pp. 53-64.

Criscuoli, A., Basile, A., Drioli, E. & Loiacono, O., 2001. An economic feasibility study for water gas shift membrane reactor. *Journal of Membrane Science,* **181**(1), pp. 21-27.

Davidson, O.R., 2004. Energy for Sustainable Development: Department of Energy .South African Profile.

Deveau, N.D., Ma, Y.H. & Datta, R., 2013. Beyond Sieverts' law: A comprehensive microkinetic model of hydrogen permeation in dense metal membranes. *Journal of Membrane Science,* **437**(0), pp. 298-311.

Mendes,D.M.P., 2010. *Use of Pd-Ag Membrane Reactors in the Water-Gas Shift Reaction for Producing Ultra-Pure Hydrogen*, PhD thesis, Department of Chemical Engineering. University of Porto.

Drnevich, R.F. And Papavassiliou, V., 2006. *Steam methane reforming method,* US Patent 7,037,485,

Edlund, D.J. & Mccarthy, J., 1995. The relationship between intermetallic diffusion and flux decline in composite-metal membranes: implications for achieving long membrane lifetime.*Journal of Membrane Science,* **107**(1), pp. 147-153.

.

Figueroa, J.D., Fout, T., Plasynski, S., Mcilvried, H. & Srivastava, R.D., 2008. Advances in CO 2 capture technology—the US Department of Energy's Carbon Sequestration Program. *International journal of greenhouse gas control,* **2**(1), pp. 9-20.

Fishtik, I. & Datta, R., 2002. A UBI–QEP micro kinetic model for the water–gas shift reaction on Cu (111). *Surface Science,* **512**(3), pp. 229-254.

Ford, P.C., 1981. The water gas shift reaction: homogeneous catalysis by ruthenium and other metal carbonyls. *Accounts of Chemical Research,* **14**(2), pp. 31-37.

Fogler,H.S., 2005. Elements of Chemical Reaction Engineering. 4 edn. New York: Pearson Education International.

Gade, S.K., Thoen, P.M. & Way, J.D., 2008. Unsupported palladium alloy foil membranes fabricated by electroless plating. *Journal of Membrane Science,* **316**(1), pp. 112-118.

Gallucci, F., Fernandez, E., Corengia, P. & Van Sint Annaland, M., 2013. Recent advances on membranes and membrane reactors for hydrogen production. *Chemical Engineering Science,* **92**(0), pp. 40-66.

Guazzone, F., Engwall, E.E. & Ma, Y.H., 2006. Effects of surface activity, defects and mass transfer on hydrogen permeance and n-value in composite palladium-porous stainless steel membranes. *Catalysis Today,* **118**(1), pp. 24-31.

Guazzone, F. & Ma, Y.H., 2008. Leak growth mechanism in composite Pd membranes prepared by the electroless deposition method. *AIChE Journal,* **54**(2), pp. 487-494.

Hara, S., Caravella, A., Ishitsuka, M., Suda, H., Mukaida, M., Haraya, K., Shimano, E. & Tsuji, T., 2012. Hydrogen diffusion coefficient and mobility in palladium as a function of equilibrium pressure evaluated by permeation measurement. *Journal of Membrane Science,* **421–422**(0), pp. 355-360.

Hawa,l E.I, Hani,W.A.,, Paglieri, S.N., Morris, C.C., Harale, A. & Way, J.D., 2014. Identification of thermally stable Pd-alloy composite membranes for high temperature applications. *Journal of Membrane Science,* **466**, pp. 151-160.

Hawa, E.I., Hani .W. A., Paglieri, S.N., Morris, C.C., Harale, A. & Way, J.D., 2015. Application of a Pd–Ru composite membrane to hydrogen production in a high temperature membrane reactor. *Separation and Purification Technology,* **147**, pp. 388-397

Holladay, J.D., Hu, J., King, D.L. & Wang, Y., 2009. An overview of hydrogen production technologies. *Catalysis Today,* **139**(4), pp. 244-260.

Holleck, G.L., 1970. Diffusion and solubility of hydrogen in palladium and palladium--silver alloys. *The Journal of physical chemistry,* **74**(3), pp. 503-511.

Hou, K. & Hughes, R., 2003. Preparation of thin and highly stable Pd/Ag composite membranes and simulative analysis of transfer resistance for hydrogen separation. *Journal of Membrane Science,* **214**(1), pp. 43-55.

Hou, K. & Hughes, R., 2002. The effect of external mass transfer, competitive adsorption and coking on hydrogen permeation through thin Pd/Ag membranes. *Journal of Membrane Science,* **206**(1–2), pp. 119-130.

Hurlbert, R. & Konecny, J., 1961. Diffusion of hydrogen through palladium. *The Journal of chemical physics,* **34**, pp. 655.

Israni, S.H. & Harold, M.P., 2010. Methanol steam reforming in Pd− Ag membrane reactors: effects of reaction system species on transmembrane hydrogen flux. *Industrial & Engineering Chemistry Research,* **49**(21), pp. 10242-10250.

Iyoha, o., Enick, r., Killmeyer, r., Howard, b., Ciocco, m. & Morreale, b., 2007. H2 production from simulated coal syngas containing H2S in multi-tubular Pd and 80 wt% Pd–20 wt% Cu membrane reactors at 1173 K. *Journal of Membrane Science,* **306**(1–2), pp. 103-115.

Iyoha, O., Enick, R., Killmeyer, R., Howard, B., Morreale, B. & Ciocco, M., 2007. Wall-catalyzed water-gas shift reaction in multi-tubular Pd and 80 wt%Pd–20 wt%Cu membrane reactors at 1173 K. *Journal of Membrane Science,* **298**(1–2), pp. 14-23.

Jansen, D., Dijkstra, J.W., Van Den Brink, R.W., Peters, T.A., Stange, M., Bredesen, R., Goldbach, A., Xu, H.Y., Gottschalk, A. & Doukelis, A., 2009. Hydrogen membrane reactors for CO2 capture. *Energy Procedia,* **1**(1), pp. 253-260.

Kajiwara, M., Uemiya, S. & Kojima, T., 1999. Stability and hydrogen permeation behavior of supported platinum membranes in presence of hydrogen sulfide. *International Journal of Hydrogen Energy,* **24**(9), pp. 839-844.

Koc, R., Kazantzis, N.K. & Ma, Y.H., 2011. Process safety aspects in water-gas-shift (WGS) membrane reactors used for pure hydrogen production. *Journal of Loss Prevention in the Process Industries,* **24**(6), pp. 852-869.

Kulprathipanja, A., Alptekin, G.O., Falconer, J.L. & Way, J.D., 2004. Effects of water gas shift gases on Pd-Cu alloy membrane surface morphology and separation properties.*Industrial & Engineering Chemistry Research,* **43**(15), pp. 4188-4198.

Laurendeau, N.M., 1978. Heterogeneous kinetics of coal char gasification and combustion. *Progress in energy and combustion science,* **4**(4), pp. 221-270.

Lester Li, Amanda E. Young, 2009. *Composite Pd membranes for hydrogen separtion.*

Lewis, A.E., Kershner, D.C., Paglieri, S.N., Slepicka, M.J. & Way, J.D., 2013. Pd–Pt/YSZ composite membranes for hydrogen separation from synthetic water–gas shift streams. *Journal of Membrane Science,* **437**(0), pp. 257-264.

Li, A., Liang, W. & Hughes, R., 2000a. The effect of carbon monoxide and steam on the hydrogen permeability of a Pd/stainless steel membrane. *Journal of Membrane Science,* **165**(1), pp. 135-141.

Li, A., Liang, W. &Hughes, R., 2000b. Fabrication of dense palladium composite membranes for hydrogen separation. *Catalysis Today,* **56**(1), pp. 45-51.

Liguori, S., Pinacci, P., Seelam, P., Keiski, R., Drago, F., Calabrò, V., Basile, A. & Iulianelli, A., 2012. Performance of a Pd/PSS membrane reactor to produce high purity hydrogen via WGS reaction. *Catalysis Today,* **193**(1), pp. 87-94.

Liguori, S., Iulianelli, A., Dalena, F., Pinacci, P., Drago, F., Broglia, M., Huang, Y. & Basile, A., 2014. Performance and long-term stability of Pd/PSS and Pd/Al2O3 membranes for hydrogen separation. *Membranes,* **4**(1), pp. 143-162.

Lin, Y. & Rei, M., 2001. Study on the hydrogen production from methanol steam reforming in supported palladium membrane reactor. *Catalysis Today,* **67**(1), pp. 77-84.

Louthan, M., Caskey, G., Donovan, J. & Rawl, D., 1972. Hydrogen embrittlement of metals. *Materials Science and Engineering,* **10**, pp. 357-368.

Ma, Y.H., Engwall, E.E. & Mardilovich, I.P., 2003. Composite palladium and palladium-alloy membranes for high temperature hydrogen separations. *Fuel Chem Division Preprints,***48**, pp. 333-334.

Ma, Y.H., Akis, B.C., Ayturk, M.E., Guazzone, F., Engwall, E.E. & Mardilovich, I.P., 2004. Characterization of intermetallic diffusion barrier and alloy formation for Pd/Cu and Pd/Ag porous stainless steel composite membranes. *Industrial & Engineering Chemistry Research,* **43**(12), pp. 2936-2945.

Ma, Y.H., Akis, B.C., Ayturk, M.E., Guazzone, F., Engwall, E.E. & Mardilovich, I.P., 2004. Characterization of intermetallic diffusion barrier and alloy formation for Pd/Cu and Pd/Ag porous stainless steel composite membranes. *Industrial & Engineering Chemistry Research,* **43**(12), pp. 2936-2945.

Maleka,E.M., Mashimbye,L., & Goyns .P., 2010. *Energy Information Management, Process Design and Publications South African Energy Synopsis 2010.* ISBN: 978-1-920435-4. Pretoria, South Africa: The Department of Energy of the Republic of South Africa.

Mardilovich, P.P., She, Y., Ma, Y.H. & Rei, M., 1998. Defect-free palladium membranes on porous stainless-steel support. *American Institute of Chemical Engineers.AIChE Journal,***44**(2), pp. 310.

Marín, P., Díez, F.V. & Ordóñez, S., 2012. Fixed bed membrane reactors for WGSR-based hydrogen production: Optimisation of modelling approaches and reactor performance. *International Journal of Hydrogen Energy,* **37**(6), pp. 4997-5010.

Mcleod, L.S., Degertekin, F.L. & Fedorov, A.G., 2009. Non-ideal absorption effects on hydrogen permeation through palladium–silver alloy membranes. *Journal of Membrane Science,* **339**(1–2), pp. 109-114.

Mendes, D., Mendes, A., Madeira, L., Iulianelli, A., Sousa, J. & Basile, A., 2010. The water-gas shift reaction: from conventional catalytic systems to Pd-based membrane reactors—a review. *Asia-Pacific Journal of Chemical Engineering,* **5**(1), pp. 111-137.

Mendes, D., Sá, S., Tosti, S., Sousa, J.M., Madeira, L.M. & Mendes, A., 2011. Experimental and modelling studies on the low-temperature water-gas shift reaction in a dense Pd–Ag packed-bed membrane reactor. *Chemical Engineering Science,* **66**(11), pp. 2356-2367.

Morreale, B.D., Ciocco, M.V., Enick, R.M., Morsi, B.I., Howard, B.H., Cugini, A.V. & Rothenberger, K.S., 2003. The permeability of hydrogen in bulk palladium at elevated temperatures and pressures. *Journal of Membrane Science,* **212**(1), pp. 87-97.

Nakamura, J., Campbell, J.M. & Campbell, C.T., 1990. Kinetics and mechanism of the water-gas shift reaction catalysed by the clean and Cs-promoted Cu (110) surface: A comparison with Cu (111). *J.Chem.Soc., Faraday Trans.,* **86**(15), pp. 2725-2734.

National Treasury, 2013. *Carbon Tax Policy Paper.* South Africa: Department of national treasury of Republic of South Africa.

Okazaki, J., Tanaka, D.A.P., Tanco, M.A.L., Wakui, Y., Mizukami, F. & Suzuki, T.M., 2006. Hydrogen permeability study of the thin Pd–Ag alloy membranes in the temperature range across the α–β phase transition. *Journal of Membrane Science,* **282**(1), pp. 370-374.

Okazaki, J., Ikeda, T., Tanaka, D.A.P., Sato, K., Suzuki, T.M. & Mizukami, F., 2011. An investigation of thermal stability of thin palladium–silver alloy membranes for high temperature hydrogen separation. *Journal of Membrane Science,* **366**(1–2), pp. 212-219.

Ovesen, C., Clausen, B., Hammershøi, B., Steffensen, G., Askgaard, T., Chorkendorff, I., Nørskov, J.K., Rasmussen, P., Stoltze, P. & Taylor, P., 1996. A microkinetic analysis of the water–gas shift reaction under industrial conditions. *Journal of catalysis,* **158**(1), pp. 170-180.

Ovesen, C., Stoltze, P., Nørskov, J. & Campbell, C., 1992. A kinetic model of the water gas shift reaction. *Journal of catalysis,* **134**(2), pp. 445-468.

Pan, X., Stroh, N., Brunner, H., Xiong, G. & Sheng, S., 2003. Pd/ceramic hollow fibers for H< sub> 2</sub> separation. *Separation and purification technology,* **32**(1), pp. 265-270.

Peters, T., Tucho, W., Ramachandran, A., Stange, M., Walmsley, J., Holmestad, R., Borg, A. & Bredesen, R., 2009. Thin Pd–23% Ag/stainless steel composite membranes: long-term stability, life-time estimation and post-process characterisation. *Journal of Membrane Science,* **326**(2), pp. 572-581.

Pinacci, P., Broglia, M., Valli, C., Capannelli, G. & Comite, A., 2010. Evaluation of the water gas shift reaction in a palladium membrane reactor. *Catalysis Today,* **156**(3–4), pp. 165-172.

Rei, M., Yeh, G., Tsai, Y., Kao, Y. & Shiau, L., 2011. Catalysis-spillover-membrane. III: The effect of hydrogen spillover on the palladium membrane reactor in the steam reforming reactions. *Journal of Membrane Science,* **369**(1–2), pp. 299-307.

Rhodes, C., Hutchings, G. & Ward, A., 1995. Water-gas shift reaction: finding the mechanistic boundary. *Catalysis Today,* **23**(1), pp. 43-58.

Romero, E.L. & Wilhite, B.A., 2012. Composite catalytic-permselective membranes: Modeling analysis for H2 purification assisted by water–gas-shift reaction. *Chemical Engineering Journal,* **207–208**(0), pp. 552-563.

Rossi, A., Lamonaca, G., Pinacci, P. And Drago, F., 2012. Development of a Dynamic Model of a Palladium Membrane Reactor for Water Gas Shift. *Energy Procedia,* **23**(0), pp. 161-170.

Sánchez, J.M., Barreiro, M.M. & Maroño, M., 2011. Hydrogen enrichment and separation from synthesis gas by the use of a membrane reactor. *Biomass and Bioenergy,* **35,** Supplement 1(0), pp. S132-S144.

Santucci, A., Borgognoni, F., Vadrucci, M. & Tosti, S., 2013. Testing of dense Pd–Ag tubes: Effect of pressure and membrane thickness on the hydrogen permeability. *Journal of Membrane Science,* **444**(0), pp. 378-383.

Schumacher, N., Boisen, A., Dahl, S., Gokhale, A.A., Kandoi, S., Grabow, L.C., Dumesic, J.A., Mavrikakis, M. & Chorkendorff, I., 2005. Trends in low-temperature water–gas shift reactivity on transition metals. *Journal of Catalysis,* **229**(2), pp. 265-275.

Shaw, E., The Effect Of H2s On The Long-Term Stability Of Pd/Cu Membranes And The Characterisitics of H_2S Poisoning Of Electroless Deposited Pd. Chemical Engineering journal,206-209 (2).pp.226-237

Smith, R., Loganathan, M. & Shantha, M.S., 2010. A review of the water gas shift reaction kinetics. *International Journal of Chemical Reactor Engineering,* **8**(1),.

Straczewski, G., Völler-Blumenroth, J., Beyer, H., Pfeifer, P., Steffen, M., Felden, I., Heinzel, A., Wessling, M. & Dittmeyer, R., 2014. Development of thin palladium membranes supported on large porous 310L tubes for a steam reformer operated with gas-to-liquid fuel. *Chemical Engineering and Processing: Process Intensification,* **81**, pp. 13-23.

Suleiman, M., Jisrawi, N., Dankert, O., Reetz, M., Bähtz, C., Kirchheim, R. & Pundt, A., 2003. Phase transition and lattice expansion during hydrogen loading of nanometer sized palladium clusters. *Journal of Alloys and Compounds,* **356**, pp. 644-648.

Thoen, P.M., Roa, F. & Way, J.D., 2006. High flux palladium–copper composite membranes for hydrogen separations. *Desalination,* **193**(1), pp. 224-229.

Tong, H.D., Gielens, F., Gardeniers, J., Jansen, H., Van Rijn, C., Elwenspoek, M. & Nijdam, W., 2004. Microfabricated palladium-silver alloy membranes and their application in hydrogen separation. *Industrial & Engineering Chemistry Research,* **43**(15), pp. 4182-4187.

Tosti, S., Basile, A., Bettinali, L., Borgognoni, F., Chiaravalloti, F. & Gallucci, F., 2006. Long-term tests of Pd–Ag thin wall permeator tube. *Journal of Membrane Science,* **284**(1), pp. 393-397.

.

Uemiya, S., Matsuda, T. & Kikuchi, E., 1991. Hydrogen permeable palladium-silver alloy membrane supported on porous ceramics. *Journal of Membrane Science,* **56**(3), pp. 315-325.

Unemoto, A., Kaimai, A., Sato, K., Otake, T., Yashiro, K., Mizusaki, J., Kawada, T., Tsuneki, T., Shirasaki, Y. & Yasuda, I., 2007. The effect of co-existing gases from the process of steam reforming reaction on hydrogen permeability of palladium alloy membrane at high temperatures. *International Journal of Hydrogen Energy,* **32**(14), pp. 2881-2887.

Ward, T.L. & Dao, T., 1999. Model of hydrogen permeation behavior in palladium membranes. *Journal of Membrane Science,* **153**(2), pp. 211-231.

Xue, E., O'keeffe, M.O. & Ross, J.R.H., 1996. Water-gas shift conversion using a feed with a low steam to carbon monoxide ratio and containing sulfur. **30**(107), pp. 141.

Yun,.L., 2005. *Novel Fe2O3-Cr2O3 Catalyst For High Temperature Water Gas Shift Reaction*,PhD thesis, Department of Chemical Engineering. University of New South Wales.

Zhang, K., Gade, S.K., Hatlevik, Ø. & Way, J.D., 2012. Absorption rate hypothesis for the increase in H 2 permeability of palladium-silver (Pd–Ag) membranes caused by air oxidation. *International Journal of Hydrogen Energy,* **37**(1), pp. 583-593.

Zhao, H., Hu, Y. & Li, J., 1999. Reduced rate method for discrimination of the kinetic models for the water–gas shift reaction. *Journal of Molecular Catalysis A: Chemical,* **149**(1), pp. 141-146.

7 Appendix

7.1 Research output

7.1.1 Poster Presentation

- A poster was presented by Liberty Ntshuxeko Baloyi at *the South African Chemical Institute Inorganic Chemistry Conference (SAIIC)*, held at Rhodes University, 28-2 July 2015. Title of poster: “Permeability*, stability and durability of Pd-Ag membrane exposed to hydrogen*”.
- A journal Paper was submitted to South African Journal of Chemical Engineering, titled

“The production of Hydrogen through the use of a 77wt%Pd 23wt%Ag Membrane Water Gas Shift Reactor”